

TRANSPORTATION RESEARCH RECORD 712

Bituminous Materials and Skid Resistance

TRANSPORTATION RESEARCH BOARD

*COMMISSION ON SOCIOTECHNICAL SYSTEMS
NATIONAL RESEARCH COUNCIL*

*NATIONAL ACADEMY OF SCIENCES
WASHINGTON, D.C. 1979*

Transportation Research Record 712
Price \$3.80
Edited for TRB by Mary McLaughlin

mode

1 highway transportation

subject areas

24 pavement design and performance
31 bituminous materials and mixes
33 construction
35 mineral aggregates

Transportation Research Board publications are available by ordering directly from TRB. They may also be obtained on a regular basis through organizational or individual affiliation with TRB; affiliates or library subscribers are eligible for substantial discounts. For further information, write to the Transportation Research Board, National Academy of Sciences, 2101 Constitution Avenue, N.W., Washington, DC 20418.

Notice

The papers in this Record have been reviewed by and accepted for publication by knowledgeable persons other than the authors according to procedures approved by a Report Review Committee consisting of members of the National Academy of Sciences, the National Academy of Engineering, and the Institute of Medicine.

The views expressed in these papers are those of the authors and do not necessarily reflect those of the sponsoring committee, the Transportation Research Board, the National Academy of Sciences, or the sponsors of TRB activities.

Library of Congress Cataloging in Publication Data

National Research Council. Transportation Research Board. Bituminous materials and skid resistance.

(Transportation research record; 712)

Reports prepared for the 58th annual meeting of the Transportation Research Board.

1. Pavements, Bituminous—Addresses, essays, lectures. 2. Pavements—Skid resistance—Addresses, essays, lectures. I. Title. II. Series.

TE7.H5 no. 712 [TE270] 625.8'5 79-21732
ISSN 0361-1981 ISBN 0-309-02959-7

Sponsorship of the Papers in This Transportation Research Record

GROUP 2—DESIGN AND CONSTRUCTION OF TRANSPORTATION FACILITIES

Eldon J. Yoder, *Purdue University, chairman*

Bituminous Section

Moreland Herrin, *University of Illinois at Urbana-Champaign, chairman*

Committee on Characteristics of Bituminous Materials

J. Claine Petersen, *Laramie Energy Technical Center, chairman*
E. Keith Ensley, *Laramie Energy Research Center, secretary*
James R. Couper, Richard L. Davis, Robert L. Dunning, Jack N. Dybalski, William H. Gotolski, Woodrow J. Halstead, C. W. Heckathorn, Prithvi S. Kandhal, Willis C. Keith, L. C. Krchma, Robert P. Lottman, Richard E. Merz, James J. Murphy, C. A. Pagen, Rowan J. Peters, Charles F. Potts, Vytautas P. Puzinauskas, Donald Saylak, Charles G. Schmitz, J. York Welborn, Richard M. White, Leonard E. Wood

Committee on Characteristics of Nonbituminous Components of Bituminous Paving Mixtures

Gene R. Morris, *Arizona Department of Transportation, chairman*
Richard W. Smith, *National Asphalt Pavement Association, secretary*

Oliver E. Briscoe, J. T. Corkill, John J. Emery, Bob M. Galloway, John M. Gibbons, William H. Gotolski, Richard H. Howe, Bobby J. Huff, John E. Huffman, L. C. Krchma, Dah-Yinn Lee, Donald W. Lewis, Robert P. Lottman, Charles R. Marek, Charles F. Potts, Vytautas P. Puzinauskas, James M. Rice, Russell H. Schnormeier, Garland W. Steele, Egons Tons, Richard D. Walker, Leonard E. Wood

Committee on Characteristics of Bituminous-Aggregate Combinations to Meet Surface Requirements

Leonard E. Wood, *Purdue University, chairman*
Sabir H. Dahir, Richard L. Davis, Rudolf A. Jimenez, Bernard F. Kallas, Prithvi S. Kandhal, Larry L. Kole, Dah-Yinn Lee, G. W. Maupin, Jr., James A. Scherocman, Stewart R. Spelman, E. A. Whitehurst

Committee on Characteristics of Bituminous Paving Mixtures to Meet Structural Requirements

Bernard F. Kallas, *The Asphalt Institute, chairman*
Grant J. Allen, Charles W. Beagle, Oliver E. Briscoe, H. W. Busching, J. T. Corkill, Jon A. Epps, Charles R. Foster, William O. Hadley, Erling Henrikson, R. G. Hicks, Rudolf A. Jimenez, Ignat V. Kalcheff, Thomas W. Kennedy, Charles V. Owen, Charles F. Parker, David W. Rand, R. M. Ripple, Donald R. Schwartz, Jack E. Stephens, Ronald L. Terrel, David G. Tunnickliff, James D. Zubiena

Construction Section

David S. Gedney, *Federal Highway Administration, chairman*

Committee on Flexible Pavement Construction

Val Worona, *Pennsylvania Department of Transportation, chairman*
Verdi Adam, R. W. Beaty, James A. Cechetini, Charles R. Foster, William E. Gehman, Myron Geller, C. S. Hughes III, Richard C. Ingberg, Cyrus S. Layson, Edward T. Lynch, Duncan A. McCrae, James J. Murphy, W. L. Salmon, Jr., W. H. Shaw, Harrison S. Smith, Richard W. Smith, R. R. Stander, Gerald S. Triplett, David G. Tunnickliff

General Materials Section

Roger V. LeClerc, *Washington State Department of Transportation, chairman*

Committee on Mineral Aggregates

T. C. Paul Teng, *Mississippi State Highway Department, chairman*
Grant J. Allen, Gordon W. Beecroft, John C. Cook, J. T. Corkill, Ludmila Dolar-Mantuani, Karl H. Dunn, Stephen W. Forster, Richard D. Gaynor, Donn E. Hancher, Robert F. Hinshaw, William W. Hotaling, Jr., Richard H. Howe, Eugene Y. Huang, William B. Ledbetter, Donald W. Lewis, Charles R. Marek, John E. McChord, Jr., Andy Munoz, Jr., Jerry G. Rose, N. Thomas Stephens, Hollis N. Walker, Richard D. Walker

Bob H. Welch and William G. Gunderman, *Transportation Research Board staff*

Sponsorship is indicated by a footnote at the end of each report. The organizational units and officers and members are as of December 31, 1978.

Contents

EVALUATION OF SIX AC-20 ASPHALT CEMENTS BY USE OF THE INDIRECT TENSILE TEST Prithvi S. Kandhal	1
IMPLEMENTATION OF STRIPPING TEST FOR ASPHALTIC CONCRETE G. W. Maupin, Jr.	8
ENGINEERING CHARACTERISTICS OF DRYER-DRUM ASPHALT MIXTURES (Abridgment) Thomas W. Kennedy and Adedare S. Adedimila	12
EVALUATION OF OREGON'S FIRST PROJECT IN HOT-MIX ASPHALT RECYCLING William G. Whitcomb, Gordon Beecroft, and James E. Wilson	15
EFFECT OF PORTLAND CEMENT ON CERTAIN CHARACTERISTICS OF ASPHALT-EMULSION- TREATED MIXTURES Ahmed Atef Gadallah, Leonard E. Wood, and Eldon J. Yoder	23
FATIGUE PERFORMANCE OF A BITUMINOUS ROAD MIX UNDER REALISTIC TEST CONDITIONS L. Francken	30
EFFECT OF LABORATORY CURING AND COMPACTION METHODS ON THE STRESS-STRAIN BEHAVIOR OF OPEN-GRADED EMULSION MIXES R. G. Hicks, Ronald Williamson, and L. E. Santucci	37
EFFECTS OF TEXTURES AND THE AGGREGATES THAT PRODUCE THEM ON THE PERFORMANCE OF BITUMINOUS SURFACES J. J. Henry and S. H. Dahir	44
SKID RESISTANCE OF BITUMINOUS- PAVEMENT TEST SECTIONS: TORONTO BY-PASS PROJECT J. Ryell, J. T. Corkill, and G. R. Musgrove	51
SYNTHETIC AGGREGATES FOR SKID-RESISTANT SURFACE COURSES D. A. Anderson and J. J. Henry	61

Evaluation of Six AC-20 Asphalt Cements by Use of the Indirect Tensile Test

Prithvi S. Kandhal, Bureau of Materials, Testing, and Research,
Pennsylvania Department of Transportation

In a 1976 research project on pavement durability in northern Pennsylvania, six AC-20 asphalt cements from different sources were used in the construction of test pavements. Two test pavements developed extensive low-temperature-associated shrinkage cracking during the first winter. The indirect tensile test is used to characterize asphaltic concrete mixes that contain the six asphalt cements. Basic mix properties, such as stiffness modulus, Poisson's ratio, tensile strength, and tensile strain at failure, are determined. The effect of temperature and asphalt rheology on these measured mix properties is evaluated. Within the temperature range used in the study [4°C to 60°C (39.2°F to 140°F)], both temperature and asphalt penetration correlate very well with mix tensile strength and stiffness modulus. Mix tensile strength and stiffness modulus increase as temperature or penetration decreases. The two cracked test pavements have much higher stiffness moduli than the other test pavements, as indicated by measurements at 25°C (77°F) or lower temperatures. The stiffness moduli of the asphaltic concrete, which are computed by two indirect methods (Heukelom and McLeod modifications of the van der Poel method), compare reasonably well with the measured values in the 4°C to 25°C temperature range.

Six test pavements were constructed on US-219 in Elk County, Pennsylvania, in September 1976. AC-20 asphalt cements from different sources were used. Penetration of the AC-20 asphalt cements ranged from 42 to 80. The research project consisted of 38-mm (1.5-in) thick, dense-graded asphaltic concrete resurfacing of the existing structurally sound pavement so that the performance of each test pavement could be studied on a comparative basis. Mix composition and compaction levels were held reasonably consistent. The only significant variable is the type or source of asphalt.

Visual observation of the six test pavements after the severe winter of 1976 and 1977 revealed that two pavements had developed extensive, low-temperature-associated transverse (shrinkage) cracking. A pavement temperature as low as -23°C (-10°F) was recorded during that winter. The stiffness moduli of the asphalts and asphaltic concrete were indirectly determined at low temperatures by using modified van der Poel charts and taking into consideration the temperature susceptibility of the asphalts used in the research project. The higher stiffness moduli of the asphaltic concrete (at low service temperatures) that contained the two asphalts were determined to be the primary cause of the non-load-associated transverse cracking. Complete details of this research project and test data are given elsewhere (1).

It was desired to determine the stiffness moduli of the asphaltic concrete by using the same six asphalts and by taking direct measurements in the laboratory. The indirect tensile test has been used to characterize asphalt paving mixtures by obtaining basic properties such as stiffness modulus, Poisson's ratio, and tensile strength (2, 3). Stiffness modulus, as used in this paper, is the relation between stress and strain as a function of time of loading and temperature. In many applications of asphaltic concrete, the stiffness characteristics of the material must be known not only to assess the behavior of the mix itself but also to evaluate the per-

formance of an engineering structure of which the mix is a part, such as a highway pavement (4). At very short times of loading and/or low temperatures, the behavior of asphaltic concrete is almost elastic in the classical sense, and stiffness S_T is analogous to an elastic modulus E .

TEST PROCEDURE AND CALCULATIONS

The indirect tensile test involves loading a cylindrical specimen with compressive loads that act parallel to and along the vertical diametrical plane. Marshall specimens 101.6 mm (4 in) in diameter and 63.5 mm (2.5 in) in height were used in this study. To distribute the load and maintain a constant loading area, the compressive load was applied through a 12.7-mm (0.5-in) wide steel loading strip that was curved at the interface with the specimen and had a radius equal to that of the specimen.

This loading configuration develops a relatively uniform tensile stress perpendicular to the direction of the applied load and along the vertical diametrical plane that ultimately causes the specimen to fail by splitting or rupturing along the vertical diameter. By measuring the applied load at failure and by continuously monitoring the loads and the horizontal and vertical deformations of the specimens, one can estimate mix tensile strength S_T , Poisson's ratio ν , and stiffness modulus S_F . The equipment and test procedure are described elsewhere (5). A relatively high deformation rate of 0.84 mm/s (2 in/min) was used.

The theoretical relations used in calculating S_T , ν , and S_F are complex and require integration of various mathematical functions. However, by assuming a specimen diameter, one can make the required integrations and simplify the relations (3, 5). These simplified relations for calculating S_T , ν , S_F , and total tensile strain at failure ϵ_T for a 10.2-cm (4-in) diameter specimen with a 1.3-cm (0.5-in) wide curved loading strip are as follows (since the equations are formulated in U.S. customary units of measurement, no SI equivalents are given):

$$S_T = 0.156 (P_{fail}/h) \quad (1)$$

$$\nu = (0.0673 DR - 0.8954)/(-0.2494 DR - 0.0156) \quad (2)$$

$$S_F = (SH/h) (0.9976\nu + 0.2692) \quad (3)$$

$$\epsilon_T = X_{TF} (0.1185\nu + 0.03896)/(0.2494\nu + 0.0673) \quad (4)$$

where S_T and S_F are given in pounds force per square inch and

P_{fail} = total load at failure (lb),

h = height of specimen (in),

DR = deformation ratio (Y_T/X_T) = slope of the line of best fit between vertical deformation Y_T and the corresponding horizontal deformation X_T

in the linear portion only,
 S_H = horizontal tangent modulus (P/X_T) = slope of
the line of best fit between load P and X_T in the
linear portion only, and
 X_{Tr} = total horizontal deformation at failure.

The line of best fit was determined by the least-
squares method. It was felt that a stiffness value ob-
tained from the linear portion of the stress-strain rela-
tion would be more meaningful than the failure stiffness.
Typical load-deformation curves are shown in Figure 1.

Figure 1. Typical load-deformation curves.

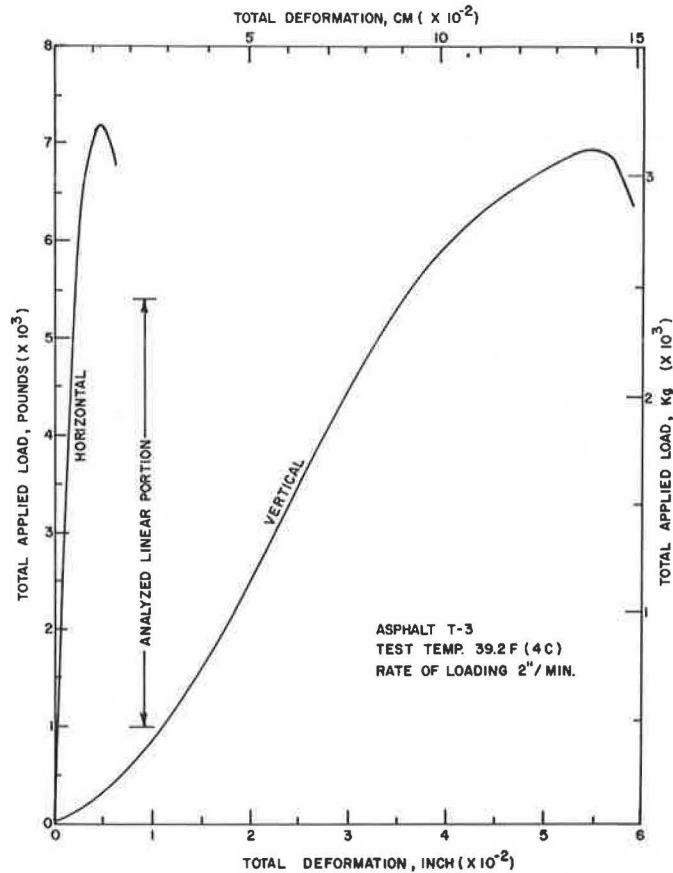


Table 1. Sources of crude and methods of refining.

Asphalt	Source	Method of Refining
T-1	49 percent Sahara, 21 percent West Texas, 21 percent Montana, 9 percent Kansas	Vacuum distillation and propane deasphalting
T-2	66.6 percent Texas Mid-Continent, 33.3 percent Arabian	Steam distillation
T-3	85 percent Light Arabian, 15 percent Bachaquero	Vacuum distillation
T-4	75 percent West Texas Sour, 25 percent Texas and Louisiana Sour	Vacuum distillation
T-5	49 percent Sahara, 21 percent West Texas, 21 percent Montana, 9 percent Kansas	Vacuum distillation and propane deasphalting
T-6	Blend of Heavy Venezuelan and Middle East crude	Vacuum distillation

Table 2. Properties of original AC-20 asphalt cements.

Test	Asphalt					
	T-1	T-2	T-3	T-4	T-5	T-6
Penetration (100 g, 5 s)						
At 4°C	2.0	7.4	6.2	6.7	3.4	7.5
At 15.6°C	11.2	25.0	24.5	23.0	16.0	29.0
At 25°C	42	64	72	65	54	80
Dynamic viscosity at 60°C (Pa·s)	270	228.4	176.4	170.5	175.9	198.2
Kinematic viscosity at 135°C (cm ² /s)	4.2	4.02	3.93	3.55	3.56	4.06
Penetration index	-2.77	-0.71	-1.51	-1.05	-2.23	-1.29
Penetration-viscosity number	-1.04	-0.70	-0.61	-0.86	-1.03	-0.45
Thin film oven residue						
Penetration at 25°C (100 g, 5 s)	26	38	45	38	37	44
Dynamic viscosity at 60°C (Pa·s)	550.1	683.5	398.2	469.4	324.8	572.1
Kinematic viscosity at 135°C (cm ² /s)	5.63	5.69	5.56	5.27	4.64	5.75
Ductility (cm)						
At 4°C, 1 cm/min	3.5	3.5	4.6	5.2	8.6	12.4
At 15.6°C, 5 cm/min	11.6	7.0	95.2	12.8	90.6	33.0

Note: $t^{\circ}C = (t^{\circ}F - 32)/1.8$; 1 Pa·s = 10 poises; 1 cm²/s = 100 centistokes; 1 cm = 0.39 in.

Since the asphalt properties were determined at 4°C, 15.6°C, 25°C, and 60°C (39.2°F, 60°F, 77°F, and 140°F), these temperatures were used to conduct the indirect tensile test on the Marshall specimens. All reported test data are based on an average of three specimens.

MIX COMPOSITION AND ASPHALT PROPERTIES

The mix consisted of gravel coarse aggregate and natural sand. Mix composition data are given below (1 mm = 0.039 in):

Sieve Size (mm)	Percentage Passing
12.5	100
9.5	93
4.75	62
2.36	45
1.18	33
0.6	22
0.3	12
0.15	9
0.075	5

Asphalt content by weight of mix was 7.5 percent. The Marshall design data for the mix were as follows: theoretical maximum specific gravity (ASTM D 2041) = 2.326, specimen specific gravity = 2.278, percentage

voids in mineral aggregate = 18.8, percentage air voids = 2.1, stability = 943 kg (2075 lb), and flow = 3.3 mm (0.13 in). This mix was also used on the Elk County project.

AC-20 asphalt cements were supplied by five refineries. Asphalts T-1 and T-5 came from the same refinery. Details of crude sources and methods of refining are given in Table 1.

The properties of original AC-20 asphalt cements are given in Table 2. Asphalts were recovered from the road cores taken from the six test sections just after construction. The properties of these asphalts are given in Table 3. Asphalts were also recovered from the Marshall specimens used in the indirect tensile test. The properties of these asphalts are given in Table 4. It can be observed that the asphalts (except T-1) generally hardened more on the roadway than in the laboratory. In evaluating the indirect tensile test data, only the properties of asphalts recovered from the Marshall specimens are used.

INDIRECT TENSILE TEST DATA

Tables 5 and 6 give mix test data on tensile strength, total tensile failure strain, and stiffness modulus for the six asphalts at four temperatures. In reviewing the test data, it should be kept in mind that pavements T-1 and T-5 developed excessive transverse shrinkage

Table 3. Properties of recovered AC-20 asphalt cements (roadway).

Test	Asphalt					
	T-1	T-2	T-3	T-4	T-5	T-6
Penetration (100 g, 5 s)						
At 4°C	1.5	4.5	4.5	4.0	2.0	5.8
At 15.6°C	7	17	16	13	9	20
At 25°C	24	40	43	34	29	49
Dynamic viscosity at 60°C (Pa·s)	552.6	572.9	378.9	382.9	401.9	461.1
Kinematic viscosity at 135°C (cm ² /s)	5.65	5.69	5.26	4.87	4.88	5.76
Ductility (cm)						
At 4°C, 1 cm/min	0.2	4.6	13.9	5.9	0.6	14.9
At 15.6°C, 5 cm/min	8.3	7.2	48.5	10.0	15.5	34
At 25°C, 5 cm/min	≥150	80	≥150	≥150	≥150	≥150
Penetration index	-2.24	-0.80	-0.99	-0.65	-2.03	-0.64
Penetration-viscosity number	-1.13	-0.68	-0.72	-1.03	-1.16	-0.47

Note: $t^{\circ}\text{C} = (t^{\circ}\text{F} - 32)/1.8$; 1 Pa·s = 10 poises; 1 cm²/s = 100 centistokes; 1 cm = 0.39 in.

Table 4. Properties of recovered AC-20 asphalt cements (Marshall specimens).

Test	Asphalt					
	T-1	T-2	T-3	T-4	T-5	T-6
Penetration (100 g, 5 s)						
At 4°C	2.2	6.9	5.0	5.0	3.6	7.2
At 15.6°C	6.2	21.4	20.7	19.7	9.8	25.7
At 25°C	22	48.2	56	49	30.4	59.3
Dynamic viscosity at 60°C (Pa·s)	659.7	349.1	266.7	268.9	401.1	281.8
Kinematic viscosity at 135°C (cm ² /s)	5.90	4.64	4.67	4.22	4.72	4.69
Ductility (cm)						
At 4°C, 1 cm/min	0	17.3	31	28	0	12.3
At 15.6°C, 5 cm/min	3.5	13.0	144.3	20.3	3.2	120.3
Penetration index	-1.08	+0.14	-1.44	-1.11	-0.54	-0.61
Penetration-viscosity number	-1.16	-0.81	-0.63	-0.89	-1.16	-0.57

Note: $t^{\circ}\text{C} = (t^{\circ}\text{F} - 32)/1.8$; 1 Pa·s = 10 poises; 1 cm²/s = 100 centistokes; 1 cm = 0.39 in.

Table 5. Tensile strength S_T and total tensile failure strain ϵ_T .

Asphalt	S_T (kPa)				ϵ_T (mm)			
	4°C	15.6°C	25°C	60°C	4°C	15.6°C	25°C	60°C
T-1	3847	2923	1193	139	0.0234	0.1173	0.1814	0.2428
T-2	2875	1269	641	114	0.0752	0.1994	0.2624	0.3708
T-3	3061	1455	690	118	0.0579	0.1821	0.2545	0.3693
T-4	3075	1420	627	117	0.0607	0.1661	0.2624	0.3589
T-5	3882	2124	1145	114	0.0279	0.1661	0.2098	0.3378
T-6	2999	1282	655	125	0.0881	0.1880	0.2350	0.3589

Note: 1 kPa = 0.145 lbf/in²; $t^{\circ}\text{C} = (t^{\circ}\text{F} - 32)/1.8$; 1 mm = 0.039 in.

cracking during the first winter. The modified cracking indexes (I) for pavements T-1 and T-5 were determined to be 51 and 38, respectively. The remaining four pavements have not developed such cracking so far.

Tensile Strength

The tensile strength of the asphaltic concrete increased as the test temperature was decreased from 60°C to 4°C (140°F to 39.2°F). Excellent correlation was found between temperature T and log S_T for all asphalts, as indicated below:

Asphalt	Correlation Coefficient	Relation
T-1	-0.992	Log S _T = 3.408 - 0.0149 T
T-2	-0.995	Log S _T = 3.095 - 0.0136 T
T-3	-0.995	Log S _T = 3.149 - 0.0138 T
T-4	-0.992	Log S _T = 3.135 - 0.0138 T

Table 6. Stiffness modulus (tensile test).

Asphalt	Stiffness Modulus (MPa)			
	4°C	15.6°C	25°C	60°C
T-1	7517	1172	579	80
T-2	1793	558	255	63
T-3	2690	814	248	63
T-4	2138	841	248	65
T-5	7172	1000	552	48
T-6	2207	648	227	86

Note: t°C = (t°F - 32)/1.8; 1 MPa = 145 lbf/in².

Asphalt	Correlation Coefficient	Relation
T-5	-0.999	Log S _T = 3.386 - 0.0153 T
T-6	-0.993	Log S _T = 3.092 - 0.0133 T

As shown in Figure 2, the rate of increase of tensile strength with decreasing temperatures is higher for asphalts T-1 and T-5 than for the other four asphalts. The penetration and viscosity of these two asphalts show that they are highly susceptible to temperature.

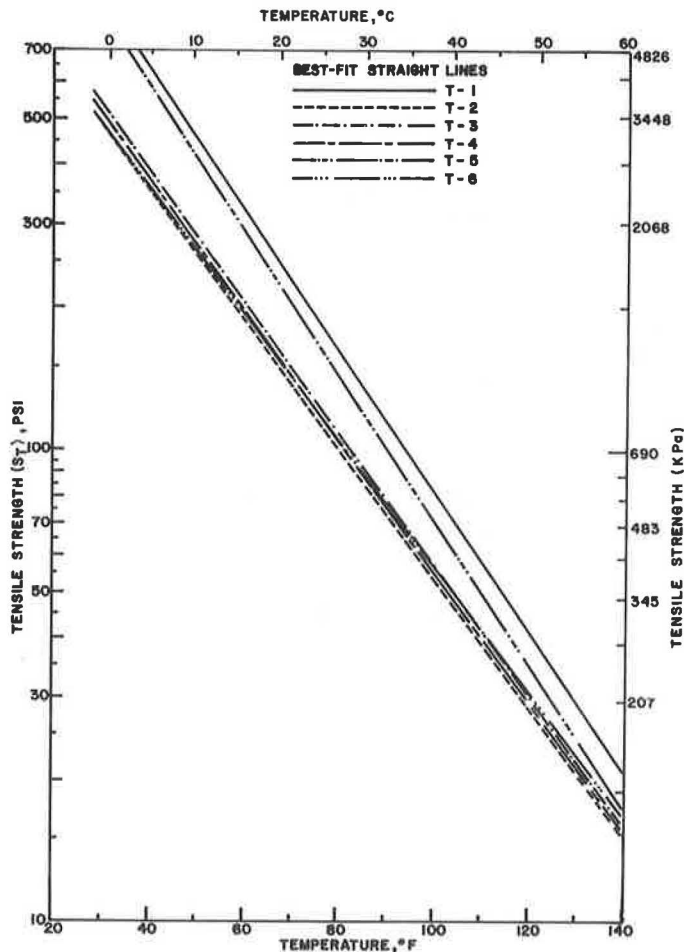
Figure 3 shows the effect of penetration of recovered asphalt on mix tensile strength. The regression analysis of log penetration and log tensile strength gives a correlation coefficient of -0.981. As penetration is decreased, tensile strength increases at a faster-than-linear rate. Ninety-six percent of the tensile strength values are attributable to the change in penetration as measured by the coefficient of determination (r²).

Poisson's Ratio

The data indicate that the average Poisson's ratio is temperature dependent and increases as the temperature increases [t°C = (t°F - 32)/1.8]:

Test Temperature (°C)	Average Poisson's Ratio for All Asphalts
4	0.10
15.6	0.31
25	0.41
60	0.92

Figure 2. Temperature versus mix tensile strength.



At 60°C (140°F), the specimen begins to develop hair-line cracks well before total failure, and these tension cracks cause an apparent increase in volume that explains the value greater than 0.5. Vila and Terrel (6) chose to use the term "strain ratio" rather than Poisson's ratio,

which seems appropriate at higher temperatures.

Tensile Strain at Failure

Figure 4 shows the plot of temperature versus tensile

Figure 3. Penetration versus mix tensile strength.

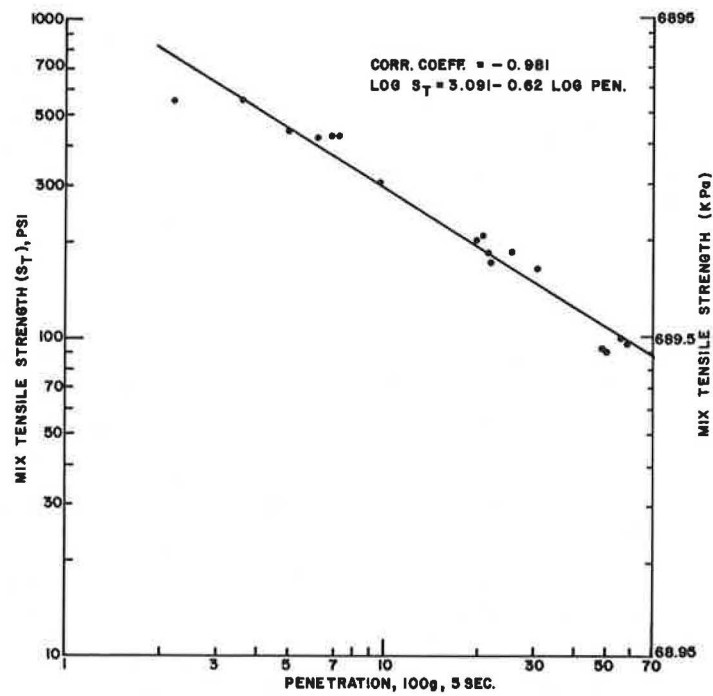
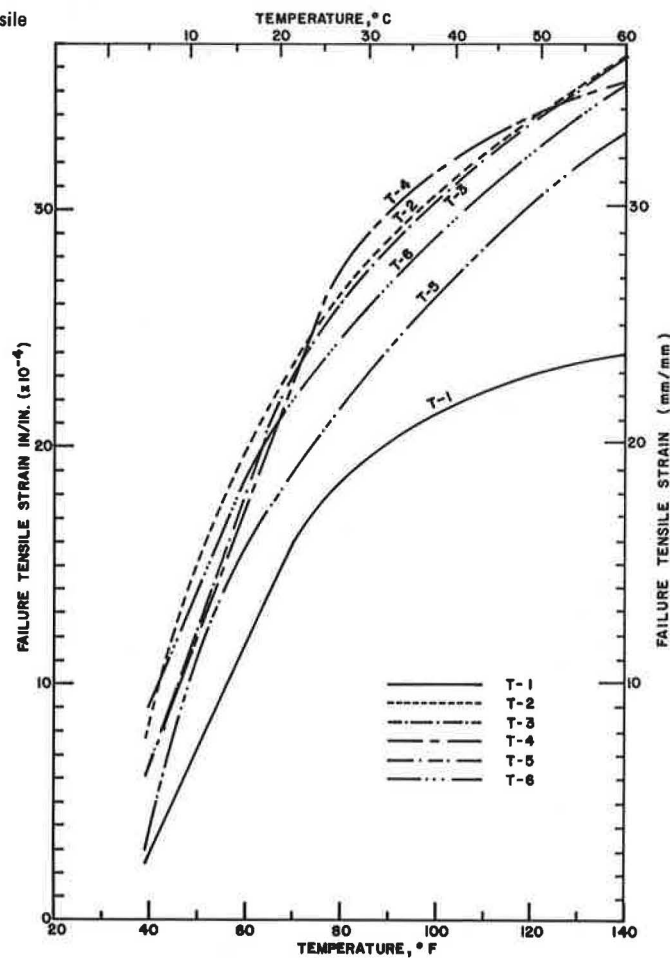


Figure 4. Temperature versus failure tensile strain.



strain at failure. At all temperatures, asphalts T-1 and T-5 failed at tensile strains lower than those for the remaining four asphalts. This trend should continue at temperatures lower than 4°C (39.2°F). Anderson and Hahn (7) consider failure strain the most significant parameter. The occurrence of cracking was found to increase as failure strain decreased.

Stiffness Modulus

As would be expected, the stiffness modulus of the asphaltic concrete increased as the temperature was decreased from 60°C to 4°C (140°F to 39.2°F). Excellent correlation was found between temperature T and $\log S_F$ for all asphalts in the temperature range 4°C to 25°C (39.2°F to 77°F), as given below:

Asphalt	Correlation Coefficient	Relation
T-1	-0.981	$\log S_F = 3.147 - 0.0297 T$
T-2	-0.998	$\log S_F = 2.284 - 0.0224 T$
T-3	-0.998	$\log S_F = 2.686 - 0.0272 T$
T-4	-0.991	$\log S_F = 2.486 - 0.0245 T$
T-5	-0.971	$\log S_F = 3.116 - 0.0298 T$
T-6	-0.999	$\log S_F = 2.531 - 0.0260 T$

Figure 5 shows that asphalts T-1 and T-5 have much higher stiffness moduli than the other asphalts. The greater the stiffness modulus, the greater is the thermal stress developed in the pavement by temperature change (8). This explains the low-temperature-associated shrinkage cracking in pavements T-1 and T-5.

Figure 6 shows the influence of recovered asphalt penetration on the stiffness modulus of the mix. As the penetration is lowered, the stiffness modulus increases at a faster-than-linear rate. Ninety-four percent of the stiffness moduli values show this trend, as measured by r^2 .

Comparison with Past Use of Indirect Methods

Indirect methods of estimating the stiffness moduli of asphalt and asphaltic concrete have been used in the past. Two methods that are modifications of the original van der Poel method (9) were used in this study:

1. The Heukelom method (10) uses penetration at two or three temperatures, "corrected" softening point T_{B00} penetration, and penetration index. The original van der Poel nomograph is used for determining the asphalt stiffness modulus.
2. The McLeod method (11) uses penetration at 25°C (77°F), viscosity at 135°C (275°F), base temperature, and penetration-viscosity number.

The stiffness modulus of a paving mixture can be determined from the stiffness modulus of asphalt and C_v^1 , a factor for volume concentration of aggregate, by using the chart developed by van der Poel (12). The stiffness moduli of Marshall specimens were determined by these indirect methods at 4°C, 15.6°C, and 25°C (39.2°F, 60°F, and 77°F). A loading time of 2 s was used to correspond with the average loading time of the indirect tensile test. Based on the Marshall density data, C_v^1 was determined to be 0.84.

Figure 7 indicates that the stiffness moduli values computed by the indirect methods compare reasonably well with the measured values. It should be noted that 80 percent of these values are within the accuracy that van der Poel attributes to the nomograph for stiffness determinations on the asphalts—that is, a factor of two (shown by the dotted lines in Figure 7).

At 60°C (140°F), the stiffness moduli computed by indirect methods were considerably lower than the measured values.

Figure 5. Temperature versus mix stiffness modulus.

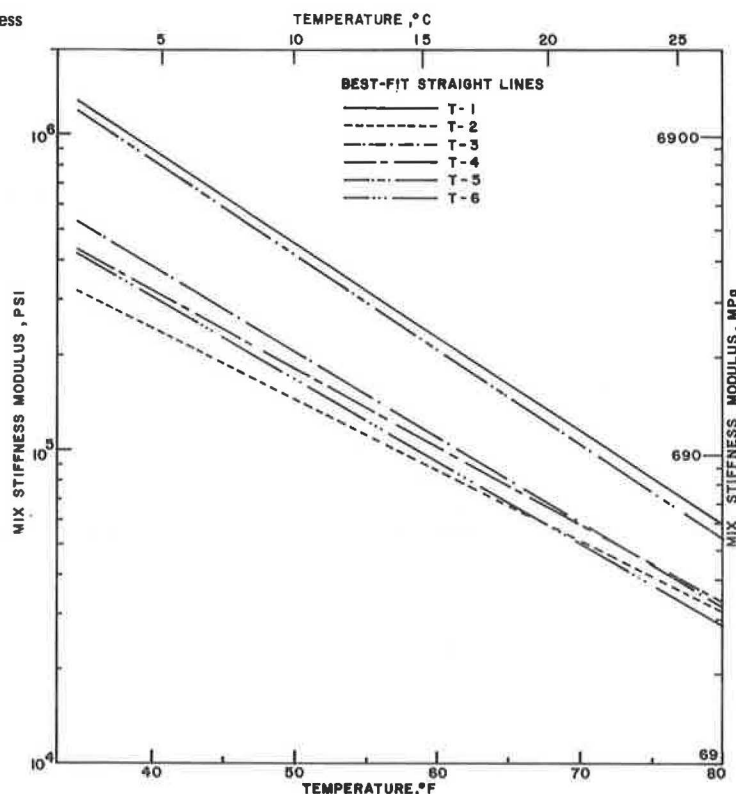


Figure 6. Penetration versus mix stiffness modulus.

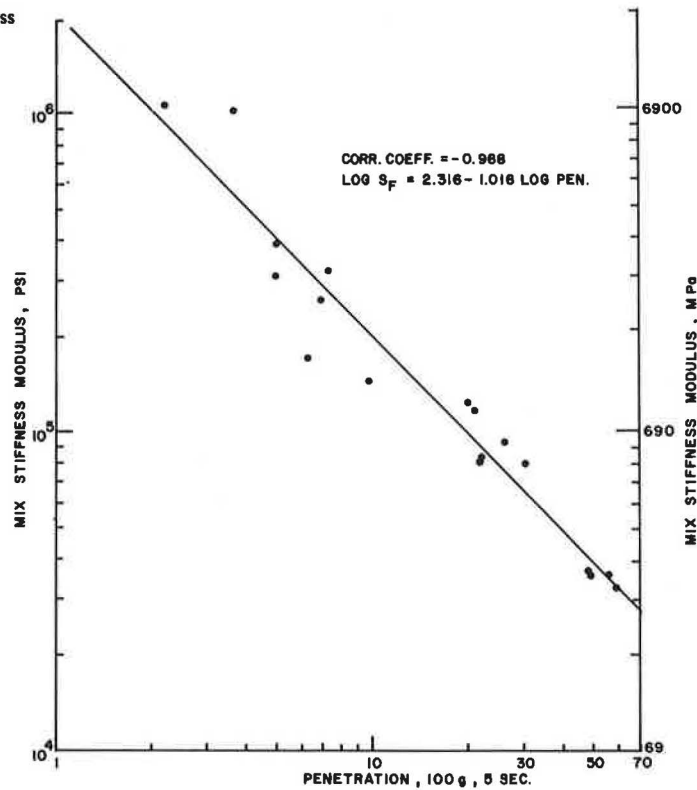
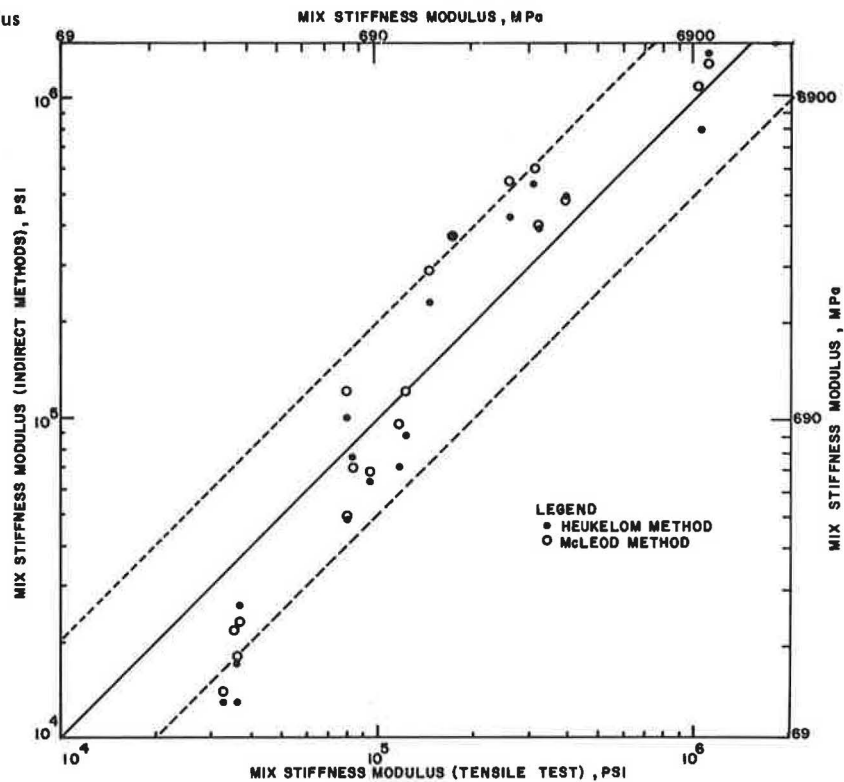


Figure 7. Measured mix stiffness modulus versus results from indirect methods.



SUMMARY AND CONCLUSIONS

This study was limited to one mix composition, six asphalt cements, and a temperature range from 4°C to 60°C (39.2°F to 140°F). The following conclusions can be drawn:

1. The indirect tensile test can be used to determine the tensile strength, Poisson's ratio, tensile strain at failure, and stiffness modulus of asphaltic concrete. These data can be used (a) to design the pavement structure and (b) to indicate the potential of low-temperature shrinkage cracking.
2. The reported test data are of major significance

since the same six AC-20 asphalt cements and the same mix composition were used on the Elk County research project, which has been evaluated periodically since September 1976. Two of the six test sections developed low-temperature-associated shrinkage cracking during the first winter. It should be realized, however, that the 0.84-mm/s (2-in/min) rate of loading that was used is much higher than the rate of loading at which such cracking actually takes place.

3. Within the temperature range used in this study, both temperature and recovered asphalt penetration showed excellent correlation with mix tensile strength. Mix tensile strength increased as temperature or penetration decreased.

4. Both temperature and asphalt penetration correlated very well with mix stiffness modulus. Mix stiffness modulus increased as temperature or penetration decreased.

5. The asphaltic concrete stiffness moduli computed by the two indirect methods (the Heukelom and McLeod modifications of the van der Poel method) compare reasonably well with the measured values in the temperature range from 4°C to 25°C (39.2°F to 77°F).

ACKNOWLEDGMENT

This research project was undertaken by the Pennsylvania Department of Transportation with the cooperation of the Federal Highway Administration, U.S. Department of Transportation. The opinions, findings, and conclusions expressed here are mine and not necessarily those of the Pennsylvania Department of Transportation or the Federal Highway Administration.

The encouragement given by Leo D. Sandvig and William C. Koehler of the Bureau of Materials, Testing, and Research, Pennsylvania Department of Transportation, is appreciated. Richard Basso, Ivan Myers, Edgar Moore, Paul Kaiser, and Steve Fulk assisted in evaluation and in obtaining test data. Edward Macko prepared the original illustrations, and Karen Ford assisted in the preparation of the original manuscript.

REFERENCES

1. P. S. Kandhal. Low Temperature Shrinkage Cracking of Pavements in Pennsylvania. Paper

presented at Annual Meeting, AAPT, Lake Buena Vista, FL, Feb. 13-15, 1978.

2. G. W. Maupin, Jr. Results of Indirect Tests Related to Asphalt Fatigue. HRB, Highway Research Record 404, 1972, pp. 1-7.
3. T. W. Kennedy. Characterization of Asphalt Pavement Materials Using the Indirect Tensile Test. Proc., AAPT, Vol. 46, Feb. 1977.
4. F. N. Finn. Factors Involved in the Design of Asphalt Pavement Surfaces. NCHRP, Rept. 39, 1967.
5. Test Procedures for Characterizing Dynamic Stress-Strain Properties of Pavement Materials. TRB, Special Rept. 162, 1975.
6. J. M. Vila and R. L. Terrel. Influence of Accelerated Climatic Conditioning on Split Tension Deformations of Asphalt Concrete. Proc., AAPT, Vol. 44, Feb. 1975, pp. 119-142.
7. K. O. Anderson and W. P. Hahn. Design and Evaluation of Asphalt Concrete with Respect to Thermal Cracking. Proc., AAPT, Vol. 37, Feb. 1968, pp. 1-31.
8. E. O. Busby and L. F. Rader. Flexural Stiffness Properties of Asphalt Concrete at Low Temperatures. Proc., AAPT, Vol. 41, Feb. 1972, pp. 163-187.
9. C. van der Poel. A General System Describing the Viscoelastic Properties of Bitumens and Its Relationship to Routine Test Data. Journal of Applied Chemistry, Vol. 4, May 1954.
10. W. Heukelom. An Improved Method of Characterizing Asphaltic Bitumens with the Aid of Their Mechanical Properties. Proc., AAPT, Vol. 42, Feb. 1973, pp. 67-98.
11. N. W. McLeod. Asphalt Cements: Pen-Vis Number and Its Application to Moduli of Stiffness. Journal of Testing and Evaluation, ASTM, Vol. 4, No. 4, July 1976.
12. C. van der Poel. Time and Temperature Effects on the Deformation of Asphaltic Bitumens and Bitumen-Mineral Mixtures. Journal of Society of Plastics Engineers, Vol. 2, No. 7, 1955.

Publication of this paper sponsored by Committee on Characteristics of Bituminous Materials.

Implementation of Stripping Test for Asphaltic Concrete

G. W. Maupin, Jr., Virginia Highway and Transportation Research Council, Charlottesville

Laboratory data were gathered by using a stripping test that is being developed and evaluated under NCHRP Project 4-8(3)/1 and is expected to be adopted for use in the state of Virginia. The testing program included a determination of the significant influences of different brands of asphalt cement and antistripping additives on the susceptibility to stripping of asphaltic concrete. Aggregates from eight sources, three asphalt cements, and two antistripping additives were used in various combinations. The results indicate that the new test method measured no significant differences in the stripping susceptibility of mixes with different asphalts. In one of the three mixes in which the effect of the type of additive was

determined, a significant difference was found. Results of supplementary tests with a modified version of the test method indicate a good correlation with those obtained by use of the original method. It is concluded that the new method can probably be simplified to allow the use of equipment now available in district materials laboratories in Virginia.

A means of accurately predicting the stripping susceptibility of an asphaltic concrete has been sought for many

years. The many test methods used to determine the tendency to strip have proved deficient when they are used to predict stripping under today's environmental and traffic conditions. However, a test recently developed under NCHRP Project 4-8(3)/1 appears promising (1).

For the field evaluation phase of the NCHRP project, the Virginia Department of Highways and Transportation was one of seven state agencies selected to install test sections with stripping-susceptible aggregates and to monitor their performance. A 290-m (950-ft) test section was installed in the coastal plains of Virginia in May 1976. The asphaltic concrete mix contained a stripping-susceptible aggregate and no antistripping additive. The stripping test performed on the mix at the time of construction revealed low strength values, and a significant amount of asphalt was observed to be separated from the aggregate surfaces. Quantitatively, the test predicted that significant stripping would occur over a long period of time. Observation and testing of cores performed two years after construction have indicated that stripping damage is occurring and apparently in the manner predicted.

On the basis of preliminary results from the field evaluation, the test method was investigated further to obtain answers to two questions:

1. Does the type of asphalt cement used affect the stripping susceptibility of a mix to such an extent that the test would have to be repeated each time a different asphalt cement was used with a particular aggregate?
2. Does the type of antistripping additive affect stripping susceptibility to such an extent that a mix that requires an additive would have to be retested each time a different additive was used?

PURPOSE AND SCOPE OF THE RESEARCH

The purpose of the investigation was to determine the effect of the type of asphalt cement and antistripping additive on the stripping of several asphaltic concretes as that effect is measured by the newly developed stripping test. It was also desirable to become familiar with the test in preparation for its adoption by the Virginia Department of Highways and Transportation. The test was performed on mixes that were believed to be susceptible to stripping. Three brands of asphalt cement and two brands of antistripping additives were used in various combinations with aggregates from eight sources.

PROCEDURE

Mixes and Materials

The aggregates and mix designs were obtained from each Virginia highway district where the mixes had been used in a pavement installation. All mixes were type S-5 except mix 7, which was a type I-2 mix (2) (1 mm = 0.039 in):

Sieve Size (mm)	Percentage Passing	
	S-5 Mix	I-2 Mix
25.4		100
12.8	100	
9.5		63-77
4.75	53-67	43-57
2.36		
0.6	19-27	
0.3		6-14
0.075	4-8	2-6
	5.0-8.5	4.5-8.0

The percentage asphalt content in the two types of mixes was as follows: 5.0-8.5 percent in the S-5 mix and 4.5-8.0 percent in the I-2 mix. The aggregates from the eight different sources, all of which were thought to be susceptible to stripping, were granite, gravel, quartzite, and diabase.

The properties of AC-20 asphalt cements obtained from the Exxon, Shell, and Chevron companies are given below [$1 \text{ cm}^2/\text{s} = 100 \text{ centistokes}$; $1 \text{ Pa}\cdot\text{s} = 10 \text{ poises}$; $t^\circ\text{C} = (t^\circ\text{F} - 32)/1.8$; $1 \text{ mm} = 0.039 \text{ in}$]:

Asphalt Source	Viscosity		Penetration at 25°C, 0.1 mm
	At 135°C (cm ² /s)	At 60°C (Pa·s)	
Exxon	4.25	215.9	78
Shell	3.90	191.7	63
Chevron	4.08	185.4	75

The antistripping additives used were 0.5 percent No-strip ACRA-500 and 1.0 percent Kling Beta LV by weight of asphalt cement (amounts recommended by the Virginia Department of Highways and Transportation).

The mixes tested are given in Table 1. In test phase 1, eight mixes with Exxon asphalt cement and no additive were tested. Mixes 3, 4, and 7, which yielded the high, medium, and low ratios of tensile strength, respectively, were selected for testing in phase 2 with Shell and Chevron asphalt cements. In phase 3, the antistripping additives were combined with the asphalt cement that produced the lowest tensile-strength ratio in phases 1 and 2.

The procedure suggested by Lottman in the field evaluation phase of NCHRP Project 4-8(3)/1 (3) was used in preparing, preconditioning, and testing the specimens.

Preparation of Specimens

The aggregates were combined according to mix design gradations obtained from district materials engineers. The aggregate was heated in an oven to 149°C (300°F); the asphalt cement was heated to 135°C (275°F) and then mixed with the aggregate in a laboratory mixer for approximately 2 min. The mixture was cooled at room temperature for 2.5 h and then placed in a forced-air oven at 60°C (140°F) for 15 h. The mixture was removed from the forced-air oven and placed in a 121°C (250°F) oven for 2 h before compaction.

Compaction was performed according to section 3.5 of ASTM D 1559-76—Standard Test Method for Resistance to Plastic Flow of Bituminous Mixtures Using Marshall Apparatus. The compactive effort was 50 blows on each side except for mixes 2, 5, and 8, which required only 30, 30, and 25 blows, respectively, to yield a void content representative of in-service pavements.

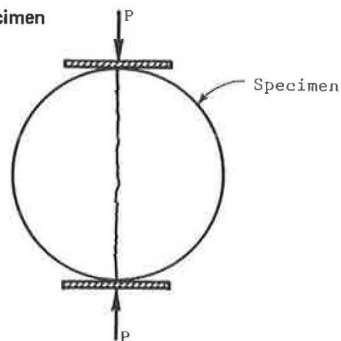
It has been verified by Lottman that voids have a significant influence on the degree of stripping in a mix; it was therefore important for the laboratory mixes to contain void contents similar to those produced in field mixes. One of the mixes known to have a stripping history was initially compacted at a low void content, and the test results indicated no stripping. Specimens were recompacted at a higher void content, and the tests indicated a significant amount of stripping.

Permeable voids (voids saturated with water under vacuum) were determined by the procedure given by Lottman (3). This required weighing the desiccated specimen in air and in water, the surface-dry specimen in air, and the vacuum-saturated specimen in air and in water.

Table 1. Asphalt cements and antistripping additives contained in mixes.

Mix	Aggregate	Test Phase		
		1	2	3
1	Crushed gravel	Exxon asphalt		
2	Quartzite	Exxon asphalt		
3	Crushed gravel	Exxon asphalt	Shell and Chevron asphalts	Shell asphalt, Kling Beta LV and ACRA 500 additives
4	Granite	Exxon asphalt	Shell and Chevron asphalts	Chevron asphalt, Kling Beta LV and ACRA 500 additives
5	Granite	Exxon asphalt		
6	Diabase	Exxon asphalt		
7	Granite	Exxon asphalt	Shell and Chevron asphalts	Shell asphalt, Kling Beta LV and ACRA 500 additives
8	Granite	Exxon asphalt		

Figure 1. Loading of specimen in indirect tensile test.



Preconditioning

Preconditioning is designed to simulate damage that occurs when the pavement is subjected to the environment and to traffic. The two types of preconditioning were (a) vacuum saturation and (b) vacuum saturation plus freezing at -18°C (0°F) for 15 h and thawing in a 60°C (140°F) water bath for 24 h (referred to as freeze-thaw).

Vacuum saturation is achieved by applying a vacuum of about 100 mm (4 in) of mercury for 30 min to the submerged specimens and then allowing them to remain submerged for an additional 30 min. This type of preconditioning simulates short-term damage, whereas freeze-thaw preconditioning simulates long-term damage that may occur over several years.

Testing

The specimens to be tested dry were wrapped in aluminum foil and coated with wax to ensure watertightness and were placed in a 12°C (54°F) water bath 3 h before testing. The preconditioned specimens were placed unwrapped in the water bath 3 h before testing. The direct tensile test was performed by loading the specimen in a diametral direction at a vertical deformation rate of 1.6 mm/min (0.065 in/min) with a hydraulic, closed-loop test system (see Figure 1). The indirect tensile strength S_t (in pascals) was computed as follows:

$$S_t = (S/1.75 \times 10^6) (P/t) \quad (1)$$

where

P = maximum compressive load on specimen (N);

t = thickness of sample (m); and

S = maximum tensile stress (Pa) produced in a 102-mm (4-in) diameter solid cylinder by a load of $P = 1733$ N per millimeter of thickness (10 000 lb per inch of thickness) (S is dependent on flattening of the specimen edge and may be determined by formula or graphic solution).

After testing, the specimens were split apart and examined visually for stripping damage.

Resilient modulus tests were performed on each specimen at 22°C (72°F) and 12°C (54°F) although the results were not used to determine susceptibility to stripping. The specimens were initially placed in a 22°C water bath for 2 h as described above. The resilient modulus test was performed, and then the specimens were placed in the 12°C water bath for 3 h, after which the resilient modulus tests were repeated. After the resilient modulus tests at 12°C , the specimens were treated immediately in indirect tension as previously described.

RESULTS

Phase 1

The stripping test was performed on eight mixes with the same asphalt cement (Exxon AC-20). The tensile strength ratio (TSR)—a ratio of preconditioned strength to dry strength—is used to predict stripping. A TSR of 1.0 indicates no stripping potential, and a TSR of less than 1.0 indicates that there is stripping potential. From experience, a TSR of less than 0.7 was considered unsatisfactory. None of the mixes showed significant damage as a result of preconditioning by vacuum saturation (see Table 2). Six of the eight mixes yielded a TSR of less than 0.7 under freeze-thaw preconditioning; thus, significant stripping over the long term is predicted.

Three mixes were selected for further investigation in phases 2 and 3. The mixes selected as having a high, medium, and low TSR were mixes 3, 4, and 7, respectively. It was impossible to test more than three mixes in phases 2 and 3 because of the excessive number of specimens and tests that would have been required.

Phase 2

Phase 2 involved testing mixes 3, 4, and 7 with two additional asphalt cements to determine if the brand of asphalt cement affected the TSR. The test results are given in Table 3.

The TSR showed no damage to the specimens preconditioned by vacuum saturation. The magnitudes of the TSR values for the mixes with different asphalt cements were similar for the specimens preconditioned by freeze-thaw.

An analysis of variance indicated that the asphalt cement did not have a significant effect on the TSR of the freeze-thaw specimens at a 95 percent level of confidence. The significance of this result is that, after a mix has been tested, it will not have to be retested each time a different asphalt cement is used.

Table 2. Results of phase 1 of indirect tensile test.

Mix	Voids in Total Mix (%)	Average Indirect Tensile Strength (MPa)			Average TSR	
		Dry	Vacuum Saturation	Freeze-Thaw	Vacuum Saturation to Dry	Freeze-Thaw to Dry
1	6.3	0.63	0.64	0.29	1.01	0.46
2	5.4	0.39	0.39	0.20	1.02	0.52
3	3.4	0.62	0.69	0.72	1.11	1.17
4	4.7	0.61	0.62	0.32	1.02	0.52
5	6.1	0.36	0.34	0.28	0.94	0.77
6	8.0	0.42	0.43	0.23	1.02	0.56
7*	6.8	0.41	0.42		1.02	
	6.8	0.53		0.23		0.44
8	7.0	0.44	0.46	0.28	1.03	0.62

Note: 1 MPa = 145 lbf/in².

*Two sets of specimens were required because of testing malfunction.

Table 3. Results of phase 2 of indirect tensile test.

Mix	Asphalt	Voids in Total Mix (%)	Average Indirect Tensile Strength (MPa)			Average TSR	
			Dry	Vacuum Saturation	Freeze-Thaw	Vacuum Saturation to Dry	Freeze-Thaw to Dry
3	Exxon ^a	3.4	0.62	0.69	0.72	1.11	1.17
	Shell	3.4	0.75	0.77	0.61	1.03	0.81
	Chevron	3.9	0.65	0.70	0.65	1.09	1.00
4	Exxon ^a	4.7	0.61	0.62	0.32	1.02	0.52
	Shell	6.0	0.79	0.79	0.37	0.99	0.47
	Chevron	5.3	0.65	0.68	0.27	1.05	0.41
7	Exxon ^a	6.8	0.41	0.42		1.02	
		6.8	0.53		0.23		0.44
	Shell	7.4	0.70	0.71	0.19	1.01	0.26
	Chevron	6.9	0.61	0.61	0.21	0.99	0.35

Note: 1 MPa = 145 lbf/in².^aTest results from phase 1.**Table 4. Results of phase 3 of indirect tensile test.**

Mix	Asphalt	Additive	Voids in Total Mix (%)	Average Indirect Tensile Strength (MPa)			Average TSR	
				Dry	Vacuum Saturation	Freeze-Thaw	Vacuum Saturation to Dry	Freeze-Thaw to Dry
3	Shell	ACRA 500	4.5	0.77	0.77	0.74	1.00	0.96
		Kling Beta LV	4.5	0.78	0.79	0.75	1.02	0.96
		None	3.4	0.75	0.77	0.61	1.03	0.81
4	Chevron	ACRA 500	7.0	0.63	0.67	0.59	1.05	0.92
		Kling Beta LV	7.0	0.63	0.64	0.56	1.01	0.88
		None	5.3	0.65	0.68	0.27	1.05	0.41
7	Shell	ACRA 500	6.7	0.68	0.69	0.45	1.02	0.66
		Kling Beta LV	6.7	0.74	0.74	0.65	1.02	0.90
		None	7.4	0.71	0.71	0.19	1.01	0.26

Note: 1 MPa = 145 lbf/in².**Table 5. Tensile strength ratios determined by two test methods.**

Mix	1.6 mm/min at 12°C		51 mm/min at 25°C	
	Voids in Total Mix (%)	TSR	Voids in Total Mix (%)	TSR
1	6.3	0.46	6.9	0.52
2	5.4	0.52	5.4	0.45
3	3.4	1.17	4.7	1.12
4	4.7	0.52	5.5	0.51
5	6.1	0.77	6.6	0.72
6	8.0	0.56	7.3	0.52
7	6.9	0.44	6.6	0.41
8	7.0	0.62	7.5	0.52

Note: 1 mm = 0.039 in.

Phase 3

In phase 3, mixes 3, 4, and 7 were tested in combination with two antistripping agents. The results are given in Table 4.

The TSR measurements showed no damage to the specimens preconditioned by vacuum saturation. Both

of the antistripping additives caused an increase in TSR over the TSR of the mixes with no additive, and an analysis of variance indicated that the increase was significant. There was also a significant difference between the performances of the two antistripping additives. Therefore, if an aggregate or a mix is tested and found to require an additive, it will probably have to be retested each time a different additive is used. Particular additives may have to be required for particular aggregates.

Modification of Test Method

Materials laboratories in Virginia that would normally be performing the stripping test do not have the equipment to test at a deformation rate of 1.6 mm/min (0.065 in/min) and a temperature of 12°C (54°F). Thus, it would be easier to implement the test method if existing equipment could be used.

To investigate this possibility, the mixes tested in phase 1 were retested at a deformation rate of 51 mm/min (2 in/min) and a test temperature of 25°C (77°F). The Marshall device for testing stability and the 25°C

(77°F) water bath used in the test of asphalt cement penetration, devices that are usually available in materials laboratories, were used in performing the test.

The results of both test methods are given in Table 5. A correlation between the two test methods was obtained in the following form:

$$Y = 0.927X + 0.008 \quad R = 0.976 \quad (2)$$

where Y = TSR at 51-mm/min (2-in/min) deformation rate and 25°C (77°F) test temperature and X = TSR at 1.6-mm/min (0.065-in/min) deformation rate and 12°C (54°F) test temperature.

The t -test indicated that there was no significant difference in the test methods at a 95 percent level of confidence. The methods were equivalent in their ability to predict stripping.

The test conditions selected in NCHRP Project 4-8(3)/1 were developed by using asphalt and aggregate sources representative of the United States; therefore, these test conditions may yield the best overall predictions. However, the modified test results are encouraging and appear to yield comparable predictions of TSR values for Virginia asphalts and aggregates.

Visual Examination of Split Specimens

After the indirect tensile tests were performed, the specimens were split apart and examined visually for stripping damage. Generally, the amount of stripping that was visible was indicative of the relative TSR, especially for the same mix with different properties (such as density) or with and without additives.

CONCLUSIONS

1. None of the mixes showed significant stripping damage after only preconditioning by vacuum saturation; therefore, either pavement damage would not occur in a short period of time or preconditioning by vacuum saturation does not predict the short-term performance of Virginia mixes. This conclusion is supported by observed stripping failures in Virginia.

2. Six of the eight mixes showed significant stripping damage after freeze-thaw preconditioning; therefore, pavements that incorporate these mixes would probably show evidence of stripping over a long period of time.

3. On the basis of results with the three asphalt cements used, asphalt cement does not significantly affect the tensile-strength ratio.

4. There was a significant difference between the performances of antistripping additives for one mix.

5. A modified test method that uses equipment now available in most materials laboratories in Virginia can be used in place of the test method that calls for a 1.6-mm/min (0.065-in/min) deformation rate and a 12°C (54°F) test temperature.

6. The relative magnitude of stripping can be detected by a visual examination of specimens.

ACKNOWLEDGMENT

I wish to express appreciation to the district materials engineers of the Virginia Department of Highways and Transportation for providing mix designs and aggregates. Special thanks also go to R. P. Lottman for his advice throughout the project.

This research was funded by the Virginia Department of Highways and Transportation. The opinions, findings, and conclusions expressed in this paper are mine and not necessarily those of the sponsoring agency.

REFERENCES

1. R. P. Lottman. Final Report—Predicting Moisture-Induced Damage to Asphaltic Concrete. Univ. of Idaho, Moscow, Feb. 28, 1974.
2. Road and Bridge Specifications. Virginia Department of Highways and Transportation, Charlottesville, Jan. 1, 1978.
3. R. P. Lottman. Working Plan and Guidelines to Participating States for NCHRP Research Project 4-8(3)/1. Univ. of Idaho, Moscow, June 10, 1975.

Publication of this paper sponsored by Committee on Characteristics of Bituminous Materials.

Abridgment

Engineering Characteristics of Dryer-Drum Asphalt Mixtures

Thomas W. Kennedy, Department of Civil Engineering, University of Texas at Austin
Adedare S. Adedimila, University of Lagos, Lagos, Nigeria

In recent years, there has been a substantial increase in the use of dryer-drum mixers. Although several investigators have studied some of the properties of the asphalt concrete mixtures produced by using these mixers, tensile strengths, resilient or elastic properties, and fatigue properties for these kinds of mixtures are not readily available. Thus, the Texas State Department of Highways and Public Transportation (TSDHPT) requested that a limited investigation be conducted to determine the char-

acteristics of asphalt mixtures produced by using a dryer drum and to determine whether these mixtures are satisfactory.

EXPERIMENTAL PROGRAM

The objectives of the study summarized in this paper were

1. To evaluate the fatigue and elastic properties of

Table 1. Description of asphalt concrete projects.

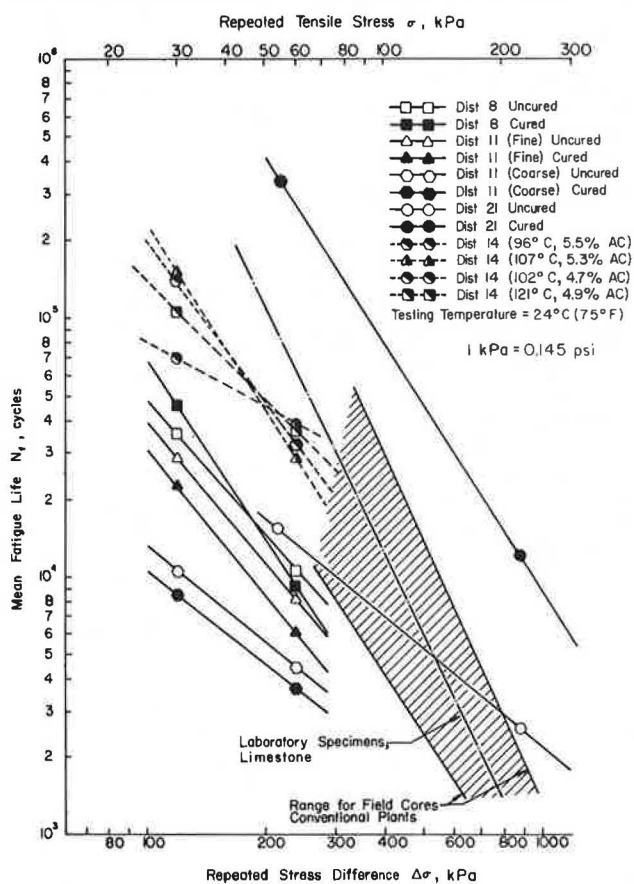
County	District Project	Treatment ^a	Temperature (°C)		Number of Specimens		Asphalt		Aggregate
			Mixing	Compaction	Fatigue	Static	Type	Percentage ^b	
Taylor	8	Cured	-	Same as mixing	9	3	AC-10	8.2	Lightweight
		Uncured	-		10	3			
Shelby	11	Fine Cured	-	121	10	3	AC-10	5.0	Crushed iron ore, fine gradation
		Uncured	-	Same as mixing	12	3			
		Coarse Cured	-	121	4	2	AC-10	5.0	Crushed iron ore, coarse gradation
		Uncured	-	Same as mixing	4	2			
Hidalgo	21	Cured	124-129	121	13	2	AC-20	5.2	Limestone
		Uncured	124-129	124-129	12	2			
Hays	14	Uncured	96	96	7	2	AC-10	5.5	Limestone
		Uncured	107	107	7	2		5.3	
		Uncured	102	102	7	2		4.7	
		Uncured	121	121	7	2		4.9	

Note: $t^{\circ}\text{C} = (t^{\circ}\text{F} - 32)/1.8$.

^aCured specimens were dried to a constant weight at 121°C before compaction. Uncured specimens were compacted at the plant temperature immediately after mixing.

^bBy weight of total mix.

Figure 1. Logarithmic relations between fatigue life and stress.



asphalt mixtures produced by using a dryer-drum plant,

2. To compare the properties of asphalt mixtures produced by using a dryer-drum plant with the properties of asphalt mixtures produced in conventional plants, and

3. To evaluate the effects of curing treatment and mixing temperature on properties of asphalt mixtures produced by using a dryer-drum plant.

Laboratory-prepared specimens of mixtures obtained during construction of five projects in Texas were tested by using the static and repeated-load indirect tensile

tests. A summary of the project information is given in Table 1. Test procedures and specimen preparation are described elsewhere (1, 2).

The properties analyzed were tensile strength, static Poisson's ratio, and resilient modulus of elasticity. Fatigue life was defined as the number of load applications required to completely fracture the specimen.

ANALYSIS AND EVALUATION

Fatigue Properties

Only two stress levels were used. The results of previous studies have shown a linear relation between the logarithm of applied stress and the logarithm of fatigue life for asphalt mixtures. This relation for the repeated-load indirect tensile test (3) can be expressed as

$$N_f = K'_2 (1/\Delta\sigma)^{n_2} \quad (1)$$

where

$$\begin{aligned} N_f &= \text{fatigue life (cycles),} \\ \Delta\sigma &= \text{stress difference} \approx 4\sigma_T \text{ (kPa),} \\ \sigma_T &= \text{applied tensile stress (kPa), and} \\ K'_2 \text{ and } n_2 &= \text{material constants.} \end{aligned}$$

Values of n_2 were fairly constant, ranging from 1.24 to 2.65. These values were low compared with previously reported values for field cores of mixtures produced by conventional plants and for laboratory specimens at optimum asphalt content. Since $1/\sigma$ or $1/\Delta\sigma$ is always less than 1.0 for the normal range of stresses exerted on pavements, lower values of n_2 would generally indicate higher values of fatigue life.

Values of K'_2 ranged from 1.86×10^5 to 2.52×10^8 . These values are small compared with previously reported values of K'_2 for mixtures produced by conventional plants and for laboratory specimens at optimum asphalt content, which should indicate shorter fatigue lives.

The logarithmic relations shown in Figure 1 generally indicate that the dryer-drum mixtures had lower fatigue lives for the range of stress shown. However, as the N_f -values indicate, the reverse would probably occur at very high levels of stress.

The coefficients of variation of fatigue life ranged from 2 to 82 percent; these values are generally lower than those reported by Navarro and Kennedy (4). This

Table 2. Comparison of tensile strength and elastic properties.

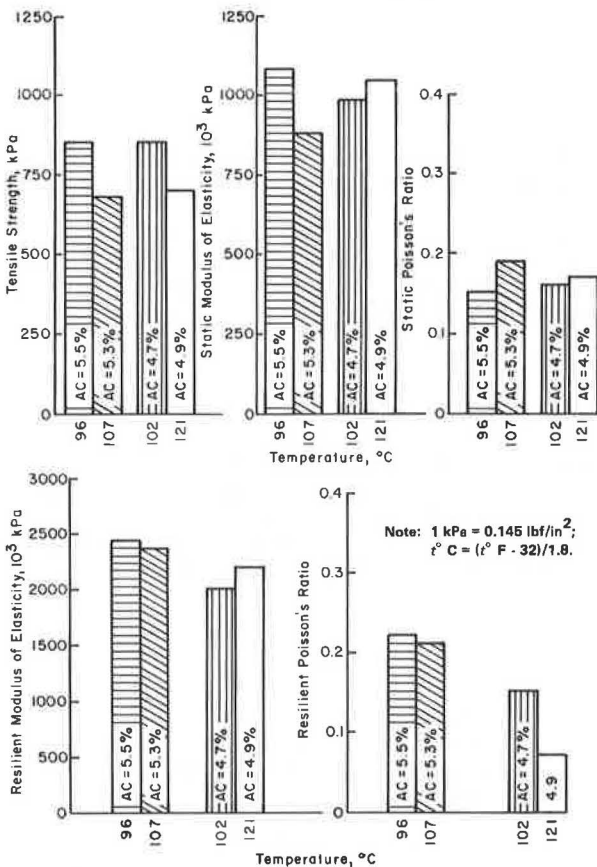
Type	Tensile Strength (kPa)	Static Modulus of Elasticity (MPa)	Static Poisson's Ratio	Resilient Modulus of Elasticity ^a (MPa)	Resilient Poisson's Source Ratio ^c
Dryer-drum specimens	421-1021	558-1827	0.14-0.42	1283-3489	0.05-0.38
In-service cores	421-1089	317-1158	0.03-0.35	1524-4241	0.06-0.58
Laboratory specimens ^b					
Limestone	1000	800	0.08	3262	0.21
Gravel	1000	1358	0.20	2896	0.06

Notes: 1 kPa = 0.145 lbf/in²; 1 MPa = 145 lbf/in²; $t^{\circ} = (t^{\circ}F - 32)/1.8$. Testing temperature = 24°C.

^aAverage of values obtained for cycles corresponding to 30, 50, and 70 percent of fatigue life.

^bAt optimum asphalt content.

Figure 2. Effect of mixing and compaction temperature on engineering properties of mixtures from one project.



is probably partially attributable to the fact that the specimens were compacted in the laboratory.

Strength and Elastic Properties

Values of tensile strength, modulus of elasticity, and Poisson's ratio obtained for dryer-drum mixtures were approximately the same as values previously obtained for conventional mixtures (see Table 2). Thus, in terms of static elastic and strength properties, the dryer-drum mixtures should perform as well as the in-service materials and the laboratory-prepared specimens.

The mean values of the resilient modulus ranged from 1283 to 3489 MPa (186 000-506 000 lbf/in²) (Table 2). The moduli were consistent within each project; therefore, the coefficients of variation for each project were small, ranging from 4 to 25 percent. As the data given in Table 2 show, the resilient moduli obtained for dryer-

drum mixtures tested in this study were slightly smaller than those of conventional mixtures but were within the range of previously reported values.

Effect of Curing Treatment and Moisture Condition

In general, there were no differences in the elastic and fatigue properties of the cured and uncured specimens. The effect of water content, however, could not be evaluated since no appreciable difference in water content was observed between the cured and uncured specimens of any given mixture. In fact, the water contents were approximately equal to those that might be expected in conventional plants.

Effect of Mix Temperature

As Figure 2 shows, an increase in mixing and compaction temperature caused a small decrease in tensile strength. The increments in the mixing and compaction temperature in this study, however, were small, and the mixtures also involved different asphalt contents. Thus, it was concluded that modulus of elasticity and static Poisson's ratio were not affected by changes in mix temperature.

As can be seen in Figure 1, the values of n_2 and K'_2 and, consequently, fatigue life were approximately equal for the group of specimens produced with 5.5 percent asphalt content at 96°C (205°F) and those produced with 5.3 percent asphalt content at 107°C (225°F). Nevertheless, there were differences in the fatigue life for the mixtures that contained 4.7 and 4.9 percent asphalt and were mixed at 102°C (215°F) and 121°C (250°F), respectively.

No consistent change in the value of the resilient modulus was observed with a change in mixing temperature (Figure 2). The resilient Poisson's ratio decreased with an increase in mixing temperature, and the change was significant at the lower asphalt content.

SUMMARY AND CONCLUSIONS

This paper summarizes the findings of a study to evaluate the fatigue and elastic properties of asphalt mixtures produced by using a dryer-drum plant. All specimens were mixed in the field and compacted in the laboratory. The resulting conclusions are summarized below.

1. The engineering properties of the dryer-drum mixtures evaluated in this study—including tensile strength, static and resilient Poisson's ratio, and static and resilient modulus of elasticity—were generally equal to those of previously evaluated in-service and laboratory-prepared mixtures. The one exception was fatigue life, which appeared to be less for the dryer-drum mixtures.

2. Based on the findings of this study and the experience and findings of others, it is felt that satisfactory mixtures can be produced by using the dryer drum. The only question relates to the effect of moisture, and it would appear from previous experience that moisture produces little if any adverse effect.

3. An increase in mixing and compaction temperature caused a decrease in resilient Poisson's ratio but did not have any significant effect on tensile strength, static and resilient modulus of elasticity, and static Poisson's ratio. There was an indication that fatigue life was improved by an increase in mixing temperature up to a certain stress level. However, the asphalt content also varied slightly.

ACKNOWLEDGMENT

This investigation was conducted at the Center for Highway Research, University of Texas at Austin. We wish to thank the sponsors, the Texas State Department of Highways and Public Transportation, and the Federal Highway Administration, U.S. Department of Transportation.

The contents of this paper reflect our views, and we are responsible for the facts and the accuracy of the data presented. The contents do not necessarily reflect the official views or policies of the Federal Highway Admin-

istration. This paper does not constitute a standard, specification, or regulation.

REFERENCES

1. A. S. Adedimila and T. W. Kennedy. Fatigue and Resilient Characteristics of Asphalt Mixtures by Repeated-Load Indirect Tensile Test. Center for Highway Research, Univ. of Texas at Austin, Res. Rept. 183-5, Aug. 1975.
2. M. Rodriguez and T. W. Kennedy. The Resilient and Fatigue Characteristics of Asphalt Mixtures Processed by the Dryer-Drum Mixer. Center for Highway Research, Univ. of Texas at Austin, Res. Rept. 183-8, Dec. 1976.
3. B. W. Porter and T. W. Kennedy. Comparison of Fatigue Test Methods for Asphalt Materials. Center for Highway Research, Univ. of Texas at Austin, Res. Rept. 183-4, April 1975.
4. D. Navarro and T. W. Kennedy. Fatigue and Repeated-Load Elastic Characteristics of Inservice Asphalt-Treated Materials. Center for Highway Research, Univ. of Texas at Austin, Res. Rept. 183-2, Jan. 1975.

Publication of this paper sponsored by Committee on Characteristics of Bituminous Paving Mixtures to Meet Structural Requirements.

Evaluation of Oregon's First Project in Hot-Mix Asphalt Recycling

William G. Whitcomb, Department of Civil Engineering,
Oregon State University, Corvallis
Gordon Beecroft and James E. Wilson, Oregon Department
of Transportation, Salem

Pavement recycling has been suggested as a workable alternative to more conventional methods of pavement rehabilitation and a means of offsetting some of the problems that result from spiraling energy costs and shortages of raw materials. The Woodburn asphalt recycling paving project, Oregon's first experience with using a hot-mix process in large-scale recycling of asphalt concrete, is discussed. The project is described, overlay and mix designs are indicated, the construction program and the specific equipment used are reviewed, the program of materials sampling and testing and data collection is described, and test results are summarized. Special emphasis is given to an investigation of possible changes in material properties through the construction process. A summary is presented of the factors that most affect the production of emissions. Costs and fuel consumption are examined, and possible savings over a similar, conventional paving project are highlighted. Specific recommendations are presented for the benefit of other agencies that are considering similar projects, and future research needs are outlined.

The need to reduce fuel consumption and conserve natural resources has been an item of ever-increasing importance during recent years. In 1976, the highway division of the Oregon Department of Transportation (DOT) was faced with the problem of disposing of nearly 45 000 Mg (50 000 tons) of asphalt concrete pavement placed for temporary purposes in the rehabilitation of I-5 between Salem and Woodburn. Officials of the division recognized the possibility of using this asphalt concrete as raw material for recycling and,

with the assistance of federal funding through Region 15 of the Federal Highway Administration (FHWA), a demonstration project that became known as the Woodburn asphalt pavement recycling project was initiated.

To fulfill the objectives of the national demonstration project program for asphalt pavement recycling, a comprehensive work plan was developed that specified the responsibilities of the highway division through the project's duration. Included in the plan was a program for sampling, testing, and evaluation before and during construction. In addition, provision was made for post-construction testing and evaluation to continue for years to come.

This paper discusses the results of the investigations performed by the highway division of the Oregon DOT in fulfilling its responsibilities through the first year of project evaluation. Specifically, the objectives of this paper are to

1. Present a description of the project, including its location, overlay thickness design, asphalt concrete mix design, and final mix specifications;
2. Indicate the final construction procedure and equipment used;
3. Describe the program of materials sampling and testing and collection of data on weather, pollutant

Figure 1. Typical roadway section from Woodburn project before rehabilitation.

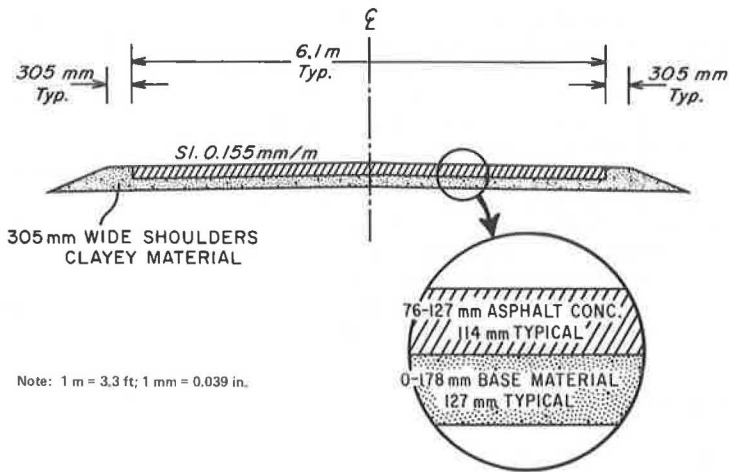


Table 1. Pavement deflection measurements for Woodburn recycling project.

Section Stations	Traffic Lane	Deflection* (mm)		
		Mean	Standard Deviation	Coefficient of Variation
89+00 to 96+50	Eastbound	1.09	0.25	0.23
115+50 to 123+00	Westbound	1.02	0.36	0.35
132+00 to 139+50	Eastbound	0.97	0.23	0.24
166+50 to 174+00	Westbound	1.14	0.30	0.27
192+00 to 199+50	Eastbound	0.69	0.23	0.33
220+50 to 228+00	Westbound	0.97	0.18	0.18
253+00 to 260+50	Eastbound	1.37	0.58	0.43
271+50 to 279+00	Westbound	1.09	0.43	0.40
288+00 to 295+50	Eastbound	1.12	0.330	0.30
318+50 to 326+00	Westbound	1.19	0.46	0.38
358+00 to 365+50	Eastbound	1.22	0.30	0.25
371+50 to 379+00	Westbound	1.27	0.76	0.60
409+00 to 416+50	Eastbound	1.19	0.53	0.45
429+50 to 437+00	Westbound	0.97	0.23	0.24
474+00 to 481+50	Eastbound	1.19	0.28	0.24
481+50 to 489+00	Westbound	1.30	0.45	0.34

Note: 1 mm = 0.039 in; $t^{\circ}\text{C} = (t^{\circ}\text{F} - 32)/1.8$.
*Adjusted to pavement temperature of 21°C.

emissions, costs, and energy use;

4. Present the results of materials tests and highlight any changes in the properties of materials through the construction process;

5. Document the levels of pollutant emissions reported during the project and indicate factors that seemed to affect the increase or decrease of opacity and particulates;

6. Present a summary of the costs and energy consumption of the project and indicate possible savings in comparison with a conventional asphalt concrete paving project; and

7. Present recommendations that may be useful to other agencies that are considering similar projects and draw final conclusions.

DESCRIPTION OF THE PROJECT

Location

The Woodburn recycling project consisted of widening and overlaying a 16-km (10-mile) section between Woodburn and St. Paul on the Hillsboro-Silverton Highway, a state secondary highway located in Marion County, Oregon.

Cross Sections and Overlay Design

Investigations were conducted early in the project to determine the characteristics of the pavement to be overlaid. Before reconstruction, the highway had an asphalt concrete surface 6.1 to 7.3 m (20 to 24 ft) wide. A sample of eight cores was obtained. Results of tests on those cores indicated that the thickness of the surface wearing course ranged from 76 to 127 mm (3 to 5 in) and the thickness of the base course ranged from 0 to 178 mm (0 to 7 in). Average values for surface- and base-course thicknesses were 114 and 127 mm (4.5 and 5 in), respectively, as shown in Figure 1.

In February of 1977, a Benkelman beam inventory was conducted to develop an overlay thickness design and to document any changes in deflection that resulted from the placement of a known thickness of recycled asphalt concrete. The mean and standard deviation of the temperature-corrected deflections for each 228.6-m (750-ft) study section are given in Table 1.

As a result of these investigations, a 152-mm (6-in) thick overlay design was developed. Two 3.7-m (12-ft) travel lanes were provided; these lanes had paved shoulders between 305 and 610 mm (1 and 2 ft) wide for an overall pavement width of 7.9 to 8.5 m (26 to 28 ft). The overlay was to be placed over the entire width of the pavement in two 76-mm (3-in) lifts. This postconstruction cross section is shown in Figure 2 (1).

Preliminary Specifications

The specific job-mix formula originally used in producing the now recycled material consisted of the following gradations (1 mm = 0.039 in):

Sieve Size (mm)	Percentage Passing by Total Weight of Mix
19-6	34.8
6-2	28.7
2-0	30.9

The original 5.6 percent asphalt content was later changed to 6.0 percent because of high voids.

Prior to advertising the project for bidding, highway division engineers estimated the possible range of proportions of crushed asphalt concrete, new aggregate, and new asphalt cement that would be likely to achieve a desirable mixture. Based on experience in past recycling projects, the following proportions and their corresponding tolerances were specified:

Component	Percentage by Total Weight of Mix	Tolerance (%)
Crushed asphalt concrete	78-100	±4
Additional 19×2-mm aggregate	0-20	±4
Additional asphalt cement	0-2	±0.5

In addition, gradation specifications for both the crushed asphalt concrete and the virgin aggregate were developed:

Material	Sieve Size (mm)	Percentage Passing by Weight
Crushed asphalt concrete	51	100
	19	50-90
	2	0-15
Virgin aggregate	25.4	100
	10	95-100
	6	25-50
	2	0-19
	0.074	0-4

The 50-mm (2-in) maximum size indicated for the crushed asphalt concrete was specified to achieve thorough heating of all of the particles. The 19-mm (0.75-in) and 2-mm (No. 10) gradations for the crushed asphalt concrete were specified to minimize the possibility of fracturing the aggregate in the old asphalt concrete and thus minimize the production of new fines. The gradations for the virgin aggregate were specified to ensure that there would be a sufficient percentage of voids in the mix.

Mix Design

The final specifications required the contractor to provide representative samples of crushed material 15 days before producing any mixture for use. The materials section of the Oregon DOT undertook a mix design study on these samples in which the Oregon mix design procedure (modified Hveem method) (2) was used to determine the proper amounts of asphalt and 19×2-mm (0.75 in × No. 10) virgin aggregate that should be added to the crushed material to achieve the highway division's design criteria, which are given below:

Property	Surface	Base	Shoulder
Stability (minimum S-value)			
First compaction	30	30	30
Second compaction	30	-	-
Air voids (%)	≈ 4	≈ 2	≈ 2
Minimum wet strength retained (%)	70	70	70
Film thickness	Sufficient	Sufficient	Sufficient

At times, all criteria could not be met and engineering judgment was used in determining the recommendations. A summary of the recommended asphalt additions and corresponding mix properties for mixes that contained 100, 90, and 80 percent recycled asphalt concrete (concretes 1, 2, and 3) is given in Table 2.

Note that, since the recycled mix was relatively new and ductile, satisfactory results were obtained without the addition of any softening agent.

In addition to the tests to determine mix properties, penetration and viscosity tests were run on the recovered asphalt before and after the addition of different grades and percentages of asphalt cement. Few tests were conducted, however, and the results were inconclusive.

Field Variation of Job-Mix Proportions

Once actual construction began, there were several significant deviations from the recommendations cited above. In Figure 3, the amounts of new asphalt and virgin aggregate recommended by the mix designs for surface and base courses are represented by the solid lines. The broken lines represent extrapolations of the mix design to include a 30 percent addition of virgin aggregate. The large dots shown represent actual mix proportions used during construction operations. All of the proportions include more asphalt than was originally recommended, and the 30 percent addition of aggregate, although not laboratory tested, was used extensively in the field.

The effort to reduce opacity and particulate emissions was mainly responsible for this departure from the recommendations. It was discovered early in the project that pollutant emissions decreased when more virgin aggregate was introduced and also when mixing was done at lower temperatures inside the drum. Higher asphalt contents were necessary at these lower temperatures to maintain good workability.

The possibility that the sample of crushed asphalt concrete used in the mix design was not representative could also account for some of the variation. In the sample obtained for the mix design, the initial asphalt content of the 100 percent recycled mix was 5.6 percent. The average asphalt content of the samples of crushed asphalt concrete obtained during construction was only 4.6 percent. The range of final asphalt contents after the addition of new asphalt cement in the mix design was 5.1-5.6 percent for the base course. Even though more new asphalt was added in mixing operations in the field, the final average asphalt content was 5.4 percent for 23 samples of the top lift and 5.8 percent for 23 samples of the bottom lift. This is very close to that obtained in the mix design after the addition of new asphalt cement.

In addition to the combinations used during construction (Figure 3), a combination of 1.5 percent Shell AR-1000 with 20 percent 19×2-mm (0.75-in × No. 10) aggregate was tried. In addition, 30 percent 6×2-mm (0.25-in × No. 10) aggregate was used with 2.1 percent AR-2000 asphalt. The use of these materials was discontinued because (a) the mix that incorporated the AR-1000 asphalt yielded unacceptable levels of pollutant emissions and (b) the 6×2-mm aggregate did not perform better than the 19×2-mm aggregate and was more costly. Consequently, except for these experiments, AR-2000 asphalt cement and 19×2-mm aggregate were used throughout the project.

CONSTRUCTION PROCEDURES AND EQUIPMENT

In the final construction procedure used in mixing and placing the recycled asphalt concrete, the stockpiled old asphalt concrete was first crushed to the desired aggregate specification by using equipment arranged in the configuration shown in Figure 4. This configuration was adopted after a comprehensive series of experiments in the laboratory, in a commercial crushing plant, and on site before the initiation of paving operations. The material was fed into the crusher by one D-8H crawler tractor equipped with rippers. An additional D-6 crawler tractor was used intermittently during the job, usually for a total of 2 h/day.

The crushed asphalt concrete was then stockpiled. To avoid any problems of "healing together" in the stockpile, the crushing rate was coordinated with the final material production rate to minimize the time that the

Figure 2. Typical roadway section from Woodburn project after rehabilitation with recycled asphalt concrete.

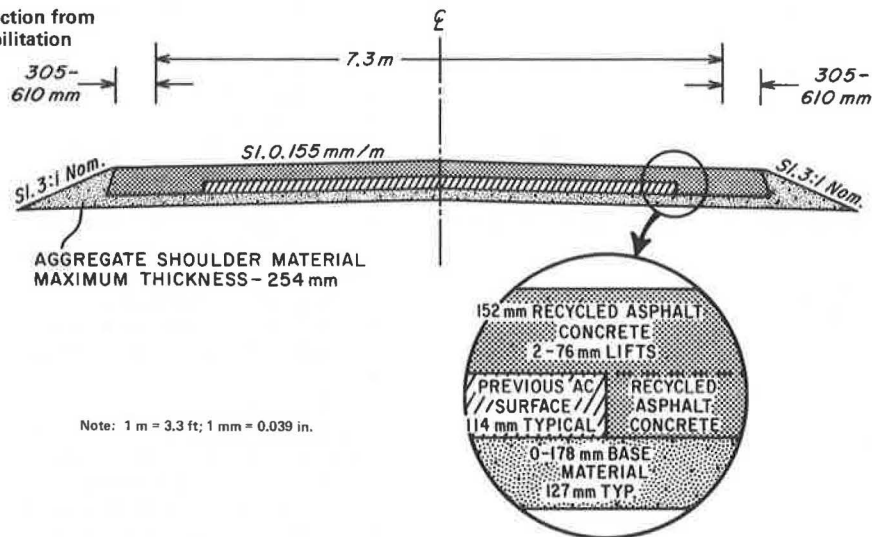
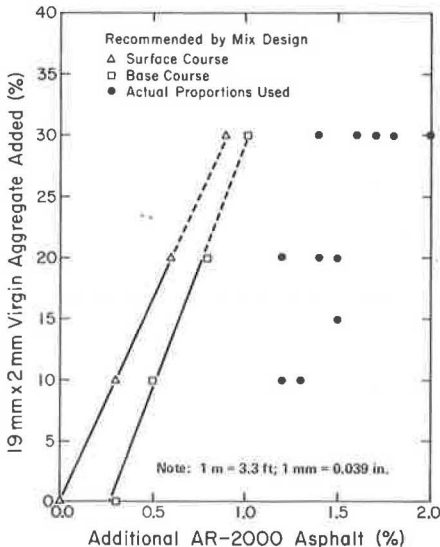


Table 2. Mix properties at recommended additions of new asphalt.

Item	Mix 1 ^a		Mix 2 ^b		Mix 3 ^c	
	Surface	Base	Surface	Base	Surface	Base
Asphalt (%)						
Content in crushed recycled pavement ^d	5.6	5.6	5.0 ^e	5.0 ^e	4.5 ^e	4.5 ^e
Recommended addition	0.0	0.3	0.3	0.5	0.6	0.8
Final content	5.6	5.9	5.3	5.5	5.1	5.3
Mix property						
S-value						
First compaction	30.0	27.0	33.2	32.0	32.6	31.8
Second compaction	36.0	19.8	36.2	27.0	35.6	34.8
Air voids (%)						
First compaction	5.7	4.7	4.3	3.7	4.9	4.3
Second compaction	2.8	1.8	2.6	2.0	2.8	2.0
Bulk specific gravity						
First compaction	2.32	2.33	2.35	2.36	2.35	2.36
Second compaction	2.39	2.40	2.39	2.40	2.41	2.42
Cohesimeter value (C), first compaction	572	648	863	878	485	471

Note: 1 mm = 0.039 in.
^aOne-hundred percent recycled asphalt concrete.
^bNinety percent recycled asphalt concrete and 10 percent 19x2-mm virgin aggregate.
^cEighty percent recycled asphalt concrete and 20 percent 19x2-mm virgin aggregate.
^dPercentage by total weight of mix.
^eAsphalt content in 100 percent recycled asphalt concrete x percentage of recycled asphalt concrete in mix.

Figure 3. Additions of asphalt recommended in mix design and additions of asphalt actually used.

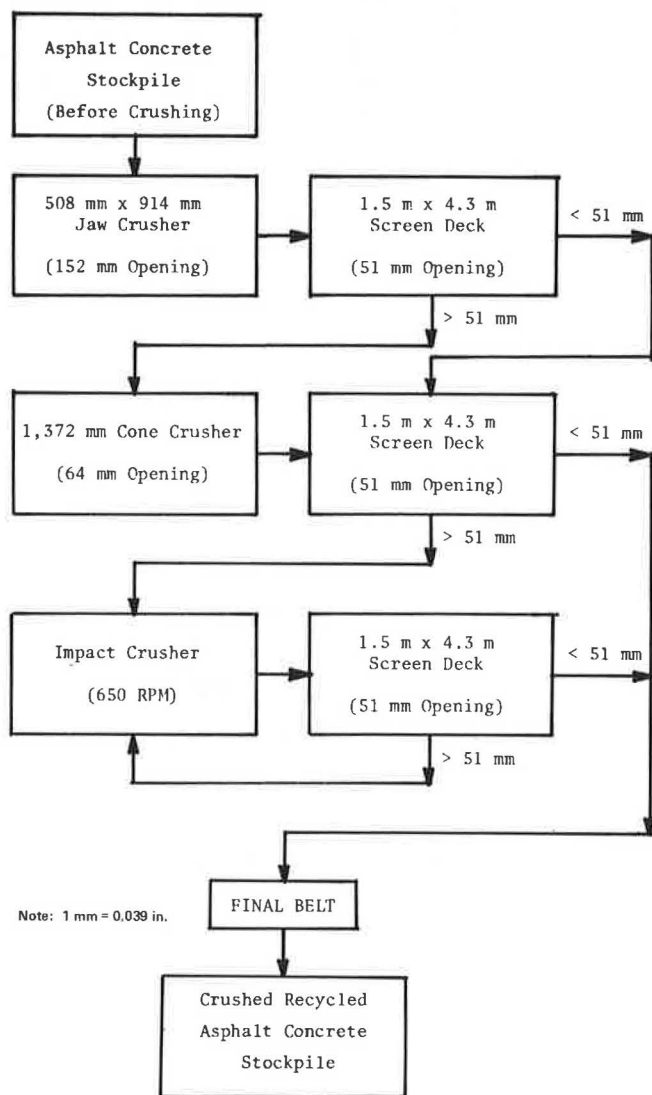


old asphalt concrete remained in the crushed stockpile. The crushed material was picked up with a Cat 980 loader and placed in two of three cold-feed hoppers. The third cold-feed hopper was reserved for virgin aggregate. Proper proportioning of aggregate and old asphalt concrete was accomplished through the use of two Ramsey belt scales, one that weighed new aggregate and one that weighed the blend of crushed asphalt concrete and virgin aggregate.

Water was then added for the purpose of reducing the emission of fine particulates. This was accomplished through the use of a spray bar mounted over the conveyor leading to the drum dryer. This bar was equipped with pressure gauges so that water could be added in known percentages.

A dryer-drum plant manufactured by Boeing Construction Company, with a capacity of 363 Mg/h (400 tons/h), was used to heat and mix the recycled asphalt-aggregate blend with new asphalt. The plant was modified by using the Pyrocone combustion control system developed by Boeing. The burner was set back from the drum, and a stainless steel cylinder was used to conduct the heat to the drum. The Pyrocone, a metal cone perforated with 25-mm (1-in) diameter holes, was placed between the burner and the entrance to the drum

Figure 4. Configuration of final crushing operation.



to allow heat transfer and at the same time provide a barrier between the flame and the recycled material. A high-speed conveyor was also used to feed the cold material into the drum so as to "throw" the material farther from the heat. A steel baffle 4.3 m (14 ft) from the rear of the drum that covered all but 254 mm (10 in) around the perimeter of the drum's inside diameter helped to control dust (3, 4).

The mix was hauled to the paving site by 15.4-m³ (20-yd³) capacity "belly" dump trucks. A windrow of mix was placed a short distance ahead of the Blaw-Knox 220 rubber-tired paver equipped with a slat conveyor pickup machine. Breakdown rolling was accomplished by using an 11-Mg (12-ton) Bomag 220-A vibrator roller. A Buffalo three-leg steel-wheel roller that weighed 12 Mg (13 tons) was used for intermediate rolling; finish rolling was accomplished by use of a 9-Mg (10-ton) Ray-Go vibrator roller, which rolled only static (the vibrating mechanism was not in use, and the roller was being operated as a conventional roller).

SAMPLING AND TESTING OF MATERIALS

As part of the demonstration project, the highway division conducted an ambitious program of sampling

and testing of materials during and after construction. The locations of sampling relative to the various construction processes are shown in Figure 5.

Pavement cores were also obtained and tested after completion of paving operations. The battery of tests performed on each of the sample types is given in Table 3.

DATA COLLECTION

In addition to the program of materials sampling and testing, a major effort was made to document information on weather (including temperature and humidity), levels of emissions, plant production rates, mix temperatures, and fuel consumption and costs.

RESULTS OF MATERIALS TESTS

Gradation

The gradation of the crushed asphalt concrete before removal of the asphalt is shown in Figure 6. The shaded area represents the gradation specifications for this material. No problem was encountered in meeting the specifications except for the material passing the 2-mm (No. 10) screen (the specification was exceeded in 58 percent of the samples tested, but in those samples the amount passing the 2-mm sieve never exceeded 18 percent).

Figure 7 compares the average gradations of the aggregate materials in the recycled asphalt concrete before and after crushing. As the figure shows, the aggregate in the recycled asphalt concrete was finer after crushing, which indicates that both aggregate particles and asphalt-aggregate chunks were fractured. It is uncertain at this point whether this fracturing was caused by the crushing process or the action of the equipment as it worked on the stockpile.

The average gradations of the aggregate material at the final belt and at the street after additions of 20 and 30 percent 19×2-mm (0.75-in × No. 10) virgin aggregate are shown in Figure 8. The figure indicates that there was little difference in the aggregate gradations after the addition of 20 or 30 percent 19×2-mm virgin aggregate. The material with 20 percent additional virgin aggregate is finer in the 6-mm (0.25-in) to 0 sizes.

Both blends are significantly coarser than the aggregate material at the final belt. Again, this would be expected because of the addition of the 19×2-mm (0.75-in × No. 10) aggregate. Note, however, that the percentage passing the 0.075-mm (No. 200) sieve does not differ significantly although it is slightly higher for the material at the final belt than for the blends.

Properties of Recovered Asphalt

Average values for the properties of recovered asphalt in samples taken in the stockpile and at the final crusher belt are given in Table 4. Table 4 also gives the average properties of recovered asphalt for 11 combinations of asphalt and virgin aggregate added to the recycled asphalt concrete. Again, as expected, greater additions of asphalt led to the lower viscosities and higher rates of penetration in the recycled asphalt concrete mixture. Note also that the crushing operation did not seem to affect the properties of the recovered asphalt at all.

Properties of Asphalt Mix

Table 4 also gives the average results of tests to determine asphalt mix properties. These results display

the highest degree of variability, and it is difficult to come to any general conclusions about the effect of the various construction processes on the mix properties.

Statistically, there is a significant difference ($\alpha = 1$ percent) in the means for samples obtained at the stockpile before crushing and at the final belt after crushing for the following tests (5): (a) bulk specific gravity (first and second compaction), (b) Hveem stabilometer (second compaction), and (c) percentage air voids. Since the properties of recovered asphalt were not affected by crushing, it would appear that the mix properties were probably affected by the change in aggregate gradation.

Inspection of the results from box samples obtained at the street shows a significant number of combinations of asphalt and virgin aggregate that do not yield satisfactory mixes from the standpoint of the design criteria for stability and air voids. These problem mixes include the following combinations:

Additional Asphalt (%)	Virgin Aggregate (%)
1.2	10
1.5	15
1.5	20
1.7	20
2.1	30

Figure 5. Location of sampling sites in Woodburn construction operation.

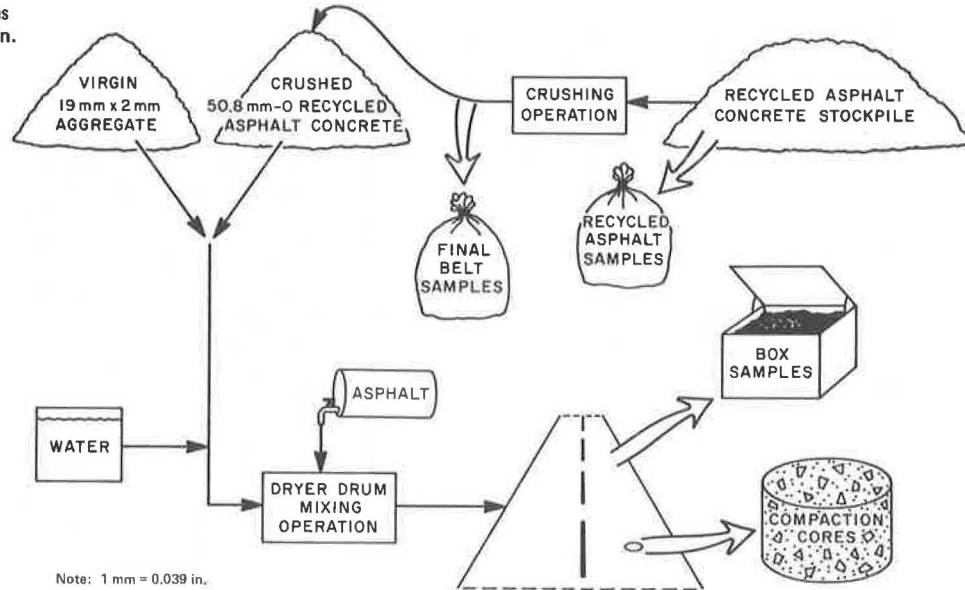


Table 3. Tests performed on sample types during and after construction.

Type of Test	During Construction				Payment Cores (after construction)*
	Recycled Asphalt Concrete		Box Samples	Compaction Cores	
	From Stockpile Before Crushing	From Final Belt After Crushing			
Aggregate properties	Gradations before and after asphalt removal	Gradations before and after asphalt removal	Gradations after asphalt removal	—	Gradations after asphalt removal
Properties of recovered asphalt	Asphalt content Penetration Kinematic viscosity Absolute viscosity	Asphalt content Penetration Kinematic viscosity Absolute viscosity	Asphalt content Penetration Kinematic viscosity Absolute viscosity	—	Asphalt content Penetration Kinematic viscosity Absolute viscosity
Mix properties	Hveem stability (S-value), first and second compaction Hveem cohesiometer (C-value), first compaction only Bulk specific gravity, first and second compaction Percentage air voids, second compaction only Percentage moisture	Hveem stability (S-value), first and second compaction Hveem cohesiometer (C-value), first compaction only Bulk specific gravity, first and second compaction Percentage air voids, second compaction only Percentage moisture	Hveem stability (S-value), first and second compaction Hveem cohesiometer (C-value), first compaction only Bulk specific gravity, first and second compaction Percentage air voids, second compaction only Percentage moisture Index of retained strength	Bulk specific gravity, first and second compaction	Hveem stability (S-value), first and second compaction Bulk specific gravity, first and second compaction Percentage air voids, second compaction only

Note: 1 mm = 0.039 in.
*Top and bottom 77-mm lifts.

At the present time, it is difficult to determine the source of this problem, i. e., whether the basis lies in improper proportioning of materials or in an inherent feature of the recycling process used.

Figure 6. Comparison of materials specifications and average gradation of material at final belt before removal of asphalt or addition of virgin aggregate.

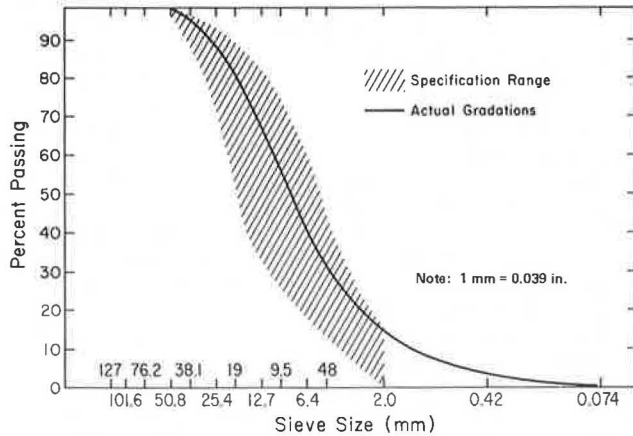
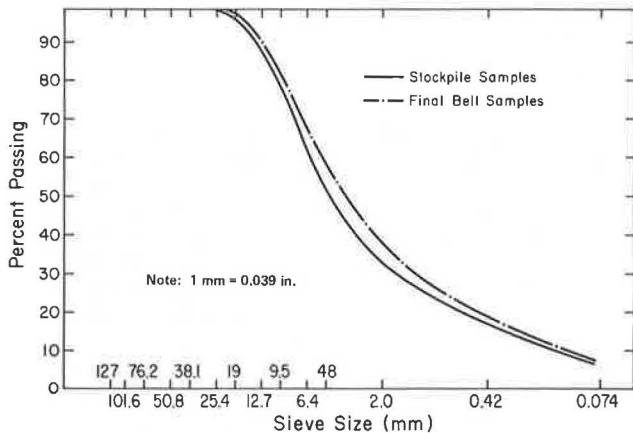


Figure 7. Average gradations of aggregate in stockpile at final belt after removal of asphalt.



Density Tests

Some problems were encountered in meeting compaction requirements, most likely because of low mixing temperatures. The highway division density specification was a minimum of 92 percent of the density achieved for the mix design specimen after second compaction. Figure 9 shows a histogram of the relative compaction achieved on cores obtained from the field based on a comparison of the density of the cores and the density of the mix design specimen at second compaction. Thirty-seven percent of the tests failed to meet the compaction specifications.

MIXING-PLANT EMISSIONS

Because of the experimental nature of this project, the Oregon Department of Environmental Quality granted a variance to allow the contractor to operate outside the present maximum opacity of 20 percent. Since several limitations were included in the variance, considerable effort was made to reduce pollutant emissions.

During the seven weeks of operation, the plant was able to consistently meet a 40 percent average opacity reading without any external control devices. Daily opacity readings followed a downward trend as modifications, experiments, and better plant control were

Figure 8. Average gradation of aggregate material at final belt after crushing and in street with addition of 20 and 30 percent virgin 19x2-mm aggregate.

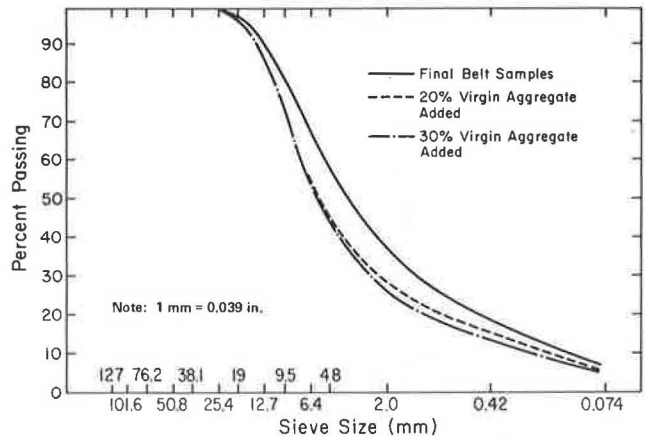


Table 4. Average values for properties of recovered asphalt and asphalt mix data at stockpile, final belt, and street.

Item	Stockpile	Final Belt	Street										
Modifications to crushed recycled asphalt													
Additional AR-2000 asphalt cement (%)	-	-	1.2	1.2	1.3	1.4	1.4	1.5	1.5	1.6	1.7	1.8	2.1
Additional 19x2-mm virgin aggregate (%)	-	-	10	20	20	20	30	15	20	30	20	30	30
Properties of recovered asphalt													
Penetration at 25°C (100 g, 5 s)	46	50	47	48	47	50	53	54	48	55	54	52	57
Viscosity at 60°C (Pa·s)	7712	7048	5921	4538	5854	4667	6075	4530	5060	4125	3954	4021	3680
Viscosity at 135°C (cm ² /s)	828	819	666	536	676	582	613	554	565	549	533	525	499
Asphalt content (%)	4.6	4.6	5.6	5.1	4.8	5.1	4.3	5.4	5.0	5.1	6.0	5.1	5.4
Asphalt mix data													
Bulk specific gravity													
First compaction	2.31	2.29	2.40	2.38	2.35	2.37	2.33	2.40	2.40	2.35	2.40	2.38	2.42
Second compaction	2.38	2.35	2.42	2.46	2.43	2.44	2.40	2.44	2.45	2.42	2.44	2.45	2.46
S-value													
First compaction	38	42	15	33	37	37	38	20	28	38	28	36	26
Second compaction	42	52	5	26	41	32	50	11	15	45	11	37	18
C-value													
First compaction	651	640	626	447	458	521	398	634	612	466	578	554	347
Air voids (%)													
First compaction	4.9	6.2	0.6	4.8	4.1	3.5	6.3	1.4	2.1	4.5	1.2	3.7	1.6
Second compaction	2.0	3.3	0.0	0.2	0.8	0.6	3.4	0.0	0.3	1.9	0.1	0.7	0.0
Moisture (%)													
First compaction	1.66	2.15	0.78	0.74	0.92	0.92	0.92	0.72	0.72	0.84	0.70	0.69	0.81
Index of retained wet strength (%)													
First compaction	-	-	85	92	84	94	73	90	86	83	91	90	87

Note: 1 mm = 0.039 in; 1 Pa·s = 10 poises; 1 cm²/s = 100 centistokes.

initiated. The plant was able to run 6 days with an average of less than 15 percent opacity, which is less than the maximum allowable for conventional operations.

Particulate emissions from stack testing were not to exceed 0.092 g per standard dry cubic meter (0.04 grains/ft³) or a mass rate of 18 kg/h (40 lb/h). The plant was tested on August 23 and found to exceed the specified maximum rate of emissions by a wide margin. Test results showed a grain loading of 0.62 g/m³ (0.269 grains/ft³) and a mass rate of 42 kg/h (92.5 lb/h). It might have been possible to collect the large particulate by using the dust collector and water scrubber that were supplied with the plant. Unfortunately, these devices could not be used because of a shortage of water and lack of space for a settling pond.

Throughout the project, many experiments were tried in an effort to modify emission levels. The most important factors that affected the levels of emissions included mix temperature, asphalt gradation, amount of virgin aggregate and water added, plant production, and weather conditions. Emissions were reduced by

1. Keeping the mix at a cooler temperature, preferably 110°C to 116°C (230°F to 240°F);
2. Using AR-2000 asphalt instead of AR-1000 asphalt;
3. Adding 25 to 30 percent virgin 19×2-mm (0.75-in × No. 10) aggregate;
4. Adjusting the added water to account for weather conditions, especially temperature and humidity; and
5. Limiting plant production to a maximum of 236 Mg/h (260 tons/h).

Figure 9. Histogram of relative compaction achieved in Woodburn project.

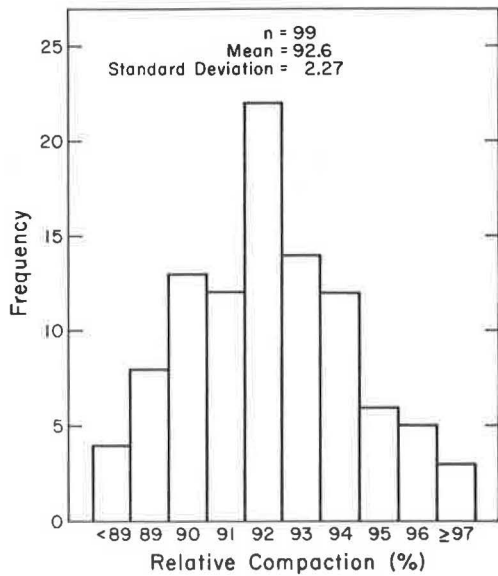


Table 5. Costs and energy use in Woodburn recycling project.

Process	Cost (\$)		Energy Consumption	
	Total	Per Megagram	Total Fuel (L)	Liters per Megagram
Crushing recycled asphalt concrete ^a	67 776.80	1.56	30 056 ^b	0.71
Processing and loading recycled product ^b	314 497.49	5.67	84 937 ^b	1.55
Hauling mix to paving site ^c	86 282.89	1.56	298 555 ^d	5.46
Placing mix ^e	72 222.36	1.26	58 222 ^b	1.06
			9 668 ^b	0.17

Note: 1 Mg = 1.1 tons; 1 L = 0.264 gal; 1 L/Mg = 0.24 gal/ton.

^aApproximately 40 680 Mg.

^bDiesel.

^cApproximately 55 217 Mg of mixture (crushed asphalt concrete, virgin aggregate, new asphalt).

^dBurner.

COST AND ENERGY USE

In the Woodburn recycling project, 55 217 Mg (60 739 tons) of asphalt concrete mix were produced at a total cost of \$540 779.54, or \$9.80/Mg (\$8.90/ton) in place. The recycled asphalt concrete constituted approximately 40 680 Mg (44 750 tons) or 75.7 percent, the virgin aggregate constituted about 13 600 Mg (14 960.2 tons) or 24.6 percent, and the new asphalt cement added about 808 Mg (888.4 tons) or 1.46 percent. The analysis of cost and fuel use is presented for the following areas of operation: feeding and crushing the reclaimed asphalt concrete, processing and loading the recycled product, hauling to the paving site, and performing the paving operation. Table 5 gives a summary of costs and energy consumption for each of these operations.

Major savings in terms of both cost and conservation of natural resources were realized through the use of the recycled asphalt concrete. Asphalt cement was reduced to 1.46 percent by weight of the recycled mix, which resulted in a savings of 2505 Mg (2756 tons) or \$220 472.90 at the \$88/Mg (\$80/ton) bid price on this project. This assumes a 6.0 percent average asphalt content in the conventional mix.

Although no cost or energy information is available in connection with the removal and stockpiling of the old asphalt concrete, it seems reasonable that cost savings were realized over using entirely new aggregate. The unit cost of providing the virgin 19×2-mm (0.75-in × No. 10) aggregate—\$5.53/Mg (\$5.03/ton)—was substantially higher than the crushing costs for the recycled asphalt concrete—\$1.59/Mg (\$1.45/ton). In any event, important natural resources were conserved.

SUMMARY

The technological feasibility of producing recycled asphalt concrete has been demonstrated by this and other paving projects (6, 7). In this project, results of materials tests indicated that the final mixture exhibited properties similar to those of a conventional paving mixture. Early postconstruction evaluation including skid tests and ride measurements have yielded a similar conclusion. Observation, testing, and evaluation of this project will continue; it appears at this point, however, that satisfactory performance has been achieved.

CONCLUSIONS AND RECOMMENDATIONS

As a result of this project, the following conclusions can be drawn:

1. New asphalt concrete material can be successfully recycled.
2. The properties of slightly aged asphalt cement

can be adequately modified through the addition of new "soft" asphalt cements without incorporating recycling additives.

3. Emissions in recycling are a function of many factors, including mix temperature, the grade of new asphalt added, the amount of new aggregate added, the amount of water added, plant production, and weather conditions.

4. Considerable variability in material properties can be expected. The variability in the original mix is compounded by unequal aging of the asphalt cement and further compounded by variability in the additions of new asphalt and rock.

A considerable amount of research work needs to be done in the area of recycled asphalt paving mixtures and in the design of thicknesses based on the use of these materials. At the present time, no long-term information on the in-service performance of these paving materials is available. More work needs to be done to evaluate fundamental material properties and their correlation with (a) types and amounts of softening agents, (b) types and gradations of additional aggregate, and (c) types of mixing techniques. As more of the problems are solved, recycling can become a workable construction alternative to meet changing requirements in the supply of materials.

ACKNOWLEDGMENT

The project described in this paper was constructed under the administrative supervision of John Sheldrake and the direct control of Loren Weber. It required assistance and cooperation from offices and individuals too numerous to mention. Each person's contribution is sincerely appreciated. We extend special thanks, however, to R. G. Hicks of Oregon State University for his efforts in the organization and review of this report.

Financial support for the data collection, sampling, and testing was furnished by the Federal Highway Administration. Support for analysis and evaluation was provided by the Department of Civil Engineering and the Transportation Research Institute, Oregon State University.

The contents of this report reflect our views, and we are responsible for the facts and the accuracy of the data presented. The contents do not necessarily reflect the official views or policies of the Oregon Department of Transportation or the Federal Highway Administration. This report does not constitute a standard, specification, or regulation.

REFERENCES

1. Work Plan for Recycling Asphalt Pavements: FHWA Demonstration Project No. 39. Federal Highway Administration, U.S. Department of Transportation, Negotiated Contract DOT-FH-12-220, Exhibit A, 1976.
2. Laboratory Manual of Test Procedures. Materials and Research Section, Highway Division, Oregon Department of Transportation, Salem.
3. J. Dumler and G. Beecroft; Oregon Department of Transportation. Recycling of Asphalt Concrete: Oregon's First Hot Mix Project. Demonstration Projects Division, Federal Highway Administration, U.S. Department of Transportation, Interim Rept., Nov. 1977.
4. R.W. Smith. A Summer of Recycling: An Update on Asphalt Pavement Recycling. Paving Forum, Winter 1978.
5. W.G. Whitcomb. An Evaluation of Oregon's First Asphalt Recycling Project: Woodburn, Oregon, Summer 1977. Department of Civil Engineering, Oregon State Univ., Corvallis, draft rept., April 1978.
6. P. Bolander and B. Stein; Oregon State University. An Evaluation of the Blewett Pass Recycling Project. Federal Highway Administration, U.S. Department of Transportation, Interim Rept., Feb. 1978.
7. J.A. McGee and A.J. Judd. Recycling of Asphalt Concrete: Arizona's First Project. Arizona Department of Transportation, Phoenix, Jan. 1978.

Publication of this paper sponsored by Committee on Flexible Pavement Construction.

Effect of Portland Cement on Certain Characteristics of Asphalt-Emulsion-Treated Mixtures

Ahmed Atef Gadallah, Cairo University, Cairo, Egypt
Leonard E. Wood and Eldon J. Yoder, School of Civil Engineering, Purdue University,
West Lafayette, Indiana

Findings are reported of a detailed laboratory investigation to evaluate the use of portland cement (1 percent of weight of dry aggregate) as an additive to asphalt-emulsion-treated mixtures (AETMs) and to study the effect of the interaction of portland cement with aggregate gradation and asphalt emulsion content on the design parameters and properties of AETMs by use of Marshall equipment. The evaluation was conducted at different curing stages of the mix. One type of aggregate (sand and gravel) and one type and grade of asphalt emul-

sion were used in the study. A modified Marshall method was used for preparing and testing the specimens. The evaluation of AETM properties produced a number of significant results. The use of portland cement as an additive to the AETM proved to be beneficial in improving its properties. This result must be viewed with caution, however, since it was found that the effect of portland cement on AETM performance was significantly influenced by aggregate gradation, asphalt emulsion content, added moisture content, and curing

stage. The experiments also showed that, because of its importance in the evaluation of AETM properties, the water-sensitivity test should be an integral part of the Marshall design procedure for AETMs.

In spite of the potential advantages of using asphalt-emulsion-treated mixtures (AETMs), they possess some relatively unfavorable characteristics, especially at early curing stages, that limit their use as high-quality paving material. A slow curing rate accompanied by slow development of strength and low resistance to water damage, especially at early curing condition, are the main factors of concern in dealing with the AETM. The use of small percentages of portland cement as an additive improves these characteristics, especially the resistance of an AETM to water damage.

This paper reports the findings of a detailed laboratory investigation of the effect of the interaction of portland cement (1 percent by weight of dry aggregate) with aggregate gradation and asphalt emulsion content on the design parameters and properties of AETMs. One type of aggregate (sand and gravel) and one type and grade of asphalt emulsion were used in the study. The evaluation was conducted at different curing stages of the mix. Autographic Marshall equipment that produces a load-deformation trace was used.

EQUIPMENT AND MATERIALS

The equipment and materials used in this investigation, including the Marshall equipment, stability apparatus, mineral aggregate, and asphalt emulsion, are described elsewhere (1).

TESTING PROCEDURE

The testing procedure used in this study is the same as that described by Gadallah and others (1, 2). Whenever the design called for the use of portland cement (1 percent by weight of dry aggregate) as an additive to the AETM, the portland cement was added to the wet aggregate and mixed immediately before the asphalt emulsion was added.

EXPERIMENTAL DESIGN

The main purpose of this study was to evaluate the use of portland cement as an additive to AETMs and the effect on certain AETM characteristics of the interaction between portland cement and aggregate gradation and asphalt emulsion (AE) content (throughout this paper, asphalt emulsion content refers to the asphalt emulsion residue content in the AETM). The use of additives, aggregate gradation, percentage AE, and curing time were included in the analysis and evaluation. The added moisture content (percentage W) was fixed to one level: 3 percent by weight of the dry aggregate. However, some limited tests conducted at selected mix combinations incorporated the use of 1.5 percent added moisture content (see Figure 1).

With the exception of percentage air voids in the mix, the response (dependent) variables that were used in this study were the same as those used in the previous study by Gadallah and others (1).

ANALYSIS OF RESULTS

Percentage Moisture Retained in the Sample

During mixing and preparation, the mixtures that contained 1 percent portland cement appeared wetter and

had relatively less coating than the mixtures prepared without portland cement additive. However, the cement-treated AETM appeared relatively drier during testing. Generally, this had been the case for all mix combinations.

The test results showed that the percentage moisture retained in the sample (percentage WC_s) was higher for cement-treated AETM samples (AETM that contained 1 percent portland cement) than for the AETM. Figure 2 shows the average percentage of moisture retained for AETM and cement-treated AETM samples. Each data point in the graph represents the average percentage WC_s of the three cells (different percentages of AE) at each curing time and aggregate gradation. The difference in percentage WC_s was about 0.5 percent after one day of curing for all aggregate gradations. This difference decreased as curing progressed.

Dry Unit Weight

The use of 1 percent portland cement in the AETM significantly affected the dry unit weights of the mixtures. In general, the AETM samples had higher dry unit weight (γ_d) than those of the cement-treated AETM. Figure 3 shows γ_d values for both AETM and cement-treated AETM as a function of curing time, aggregate gradation, and percentage asphalt emulsion. It can be seen that the general trend of the effect of portland cement—a decrease in γ_d —does not hold for all mix combinations. In a few cases, the cement-treated AETM provided higher dry unit weights. This is more apparent for mixes that contain FG aggregate after seven days of air-dry curing.

Marshall Stability

The effect of portland cement on values of Marshall stability (P) is influenced by aggregate gradation and percentage AE. The effect on P of the interaction among curing time, aggregate gradation, percentage AE, and portland cement is shown in Figure 4. Among specimens cured for one day, the effect of portland cement is more significant for mixes that contain MG aggregate. In addition, the effect of portland cement is more apparent at low AE contents, and it improves the mix stability for all aggregate gradations. However, when the percentage AE in the mix is increased, aggregate gradation starts influencing the role of portland cement in the mix, reducing its effect. When CG aggregate was used, portland cement did not improve the stability of the mix and in most cases produced a reverse effect. This reduction in stability could be expected because of the relatively poor coating that was obtained when CG aggregate was used with portland cement.

The effect of portland cement was more apparent at the early stages of curing. After relatively long periods of curing, the use of portland cement produced an increase in stability but not in the same degree as that produced at early curing stages (see the results for seven-day curing in Figure 4). The effect of aggregate gradation on the role of portland cement in the mix after seven days of curing was less than its effect for samples cured for one day.

The effect of percentage AE on the stability values of the AETM and cement-treated AETM is more apparent after relatively longer curing periods than at the early stages of curing. In addition, Marshall stability values decreased with increasing percentage AE in the mix (Figure 4).

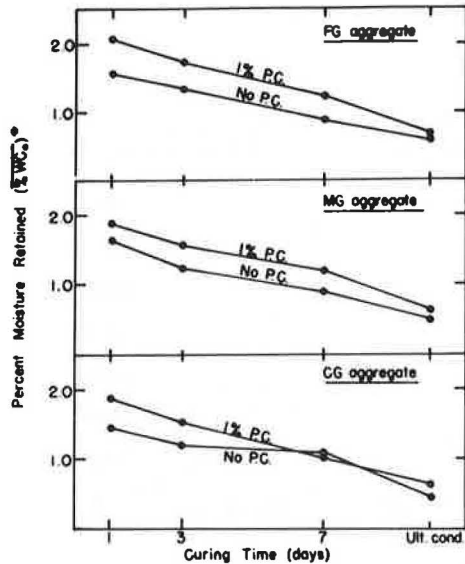
The AETM response parameters depend on the percentage of total liquid (TL) that is available in the mix

Figure 1. Factorial design for study of effect of various factors on AETM properties.

Curing Time (days)	Agg. Gradation (% AE (residue))	% PC	F.G.			M.G.			C.G.			
			2.5	3.25	4.0	2.5	3.25	4.0	2.5	3.25	4.0	
			1.5%	3%	4.5%	1.5%	3%	4.5%	1.5%	3%	4.5%	
(NO P.C.)	1 day	1.5										
		3	x	⊗	x	⊗	⊗	x	⊗	x		
		4.5										
	3	1.5										
		3	x	⊗	x	⊗	⊗	x	⊗	x		
		4.5										
	7	1.5				x	x	x				
		3	x	x	x	x	x	x	x	x	x	
		4.5										
ult.†	1.5				x	x	x					
	3	x	x	x	x	x	x	x	x	x		
	4.5											
(1% P.C.)	1	1.5										
		3	x	⊗	x	⊗	⊗	x	⊗	x		
		4.5										
	3	1.5										
		3	x	⊗	x	⊗	⊗	x	⊗	x		
		4.5										
	7	1.5				x	x	x				
		3	x	x	x	x	x	x	x	x	x	
		4.5										
ult.†	1.5				x	x	x					
	3	x	x	x	x	x	x	x	x	x		
	4.5											

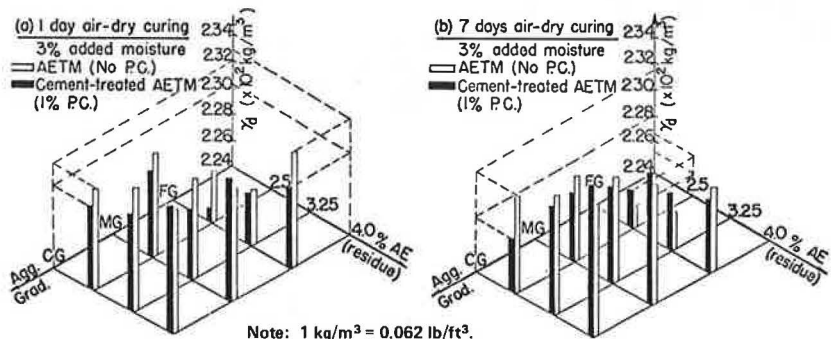
Note:
 x = dry test
 ⊗ = water sensitivity test
 * = percent by weight of the dry aggregate
 † = 3 days curing at 120°F

Figure 2. Effect of portland cement on percentage W_c in the sample.



NOTE:
 1 3% added moisture for all test samples
 2 each data point in the graph represents the average W_c of the 3 mix combinations that contained different % AE

Figure 3. Effect of portland cement on γ_d as a function of aggregate gradation and percentage AE residue.



Note: 1 kg/m³ = 0.062 lb/ft³.

at the time of testing (see Figure 5). Since the cement-treated AETM held more retained moisture than the AETM, percentage TL was more for samples treated with portland cement. In spite of the increase in percentage TL for cement-treated AETM over that for AETM, a gain in stability occurred in most of the cases depending on the aggregate gradation used. The significant effect on stability that is obtained by the use of 1 percent portland cement can be seen in Figure 5, where the stability results for the cement-treated AETM are shown with those for the AETM as a function of percentage TL at the time of testing. The change in percentage TL was obtained through the curing process. For mixes that contain FG and MG aggregates, a substantial increase in stability was obtained by the use of 1 percent portland cement. That is, at a specific percentage TL the cement-treated AETM provided much greater stability than the AETM. However, the use of portland cement with CG-aggregate mixes was not beneficial, especially at a high percentage AE, where a drop in stability occurred.

Marshall Flow

Flow values were not significantly affected by the use of portland cement as an additive to the AETM. The use of portland cement generally reduced flow values for most of the mix combinations, but this difference is not significant because the reduction or, in some cases, the slight increase in flow values that was produced could be expected as a variation in the three replicates of the mix.

Marshall Stiffness and Marshall Index

Asphalt emulsion content, aggregate gradation, and their interaction significantly affected values of Marshall stiffness (S_n) and Marshall index (I_n) (see Figure 6). Generally, when percentage AE is decreased, both S_n and I_n will increase as the mix becomes less plastic, and the slope of the load-deformation curve will be steeper. Marshall index trends are about the same as Marshall stiffness trends but have higher values because of the nature of the parameters themselves. The index values represent the slope of the linear portion of the load-deformation curve, whereas the stiffness values represent the slope of the line that connects the initial or starting loading point with the failure point.

In addition, the use of portland cement in AETM together with the other main factors under study significantly affected the I_n values. However, the S_n values were not significantly affected by the use of portland cement in the AETM. This resulted from the nature of the S_n variable, which is obtained by the direct relation $S_n = P/F$. Flow values F were not significantly affected by portland cement, and they varied randomly

in such a way that they reduced the effect of portland cement on S_m .

Figure 6 shows I_m as a function of aggregate gradation and percentage AE residue for the two curing periods. For specimens cured for one day, the I_m values increased when portland cement was used in the AETM, especially at a low percentage AE. The effect of the portland cement was reduced at a high percentage AE, e.g., 4 percent. In addition, aggregate gradations are shown to

have a significant effect on the behavior of portland cement in the mix. The test data for specimens cured for seven days (Figure 6) show that the cement-treated AETM had higher values than the AETM in almost all mix combinations. The gain in I_m values attributable to the use of portland cement was decreased through the curing process. This leads to the conclusion that, although the effect of portland cement on I_m values at early curing periods varies and depends on aggregate

Figure 4. Effect of portland cement on P as a function of aggregate gradation and percentage AE residue.

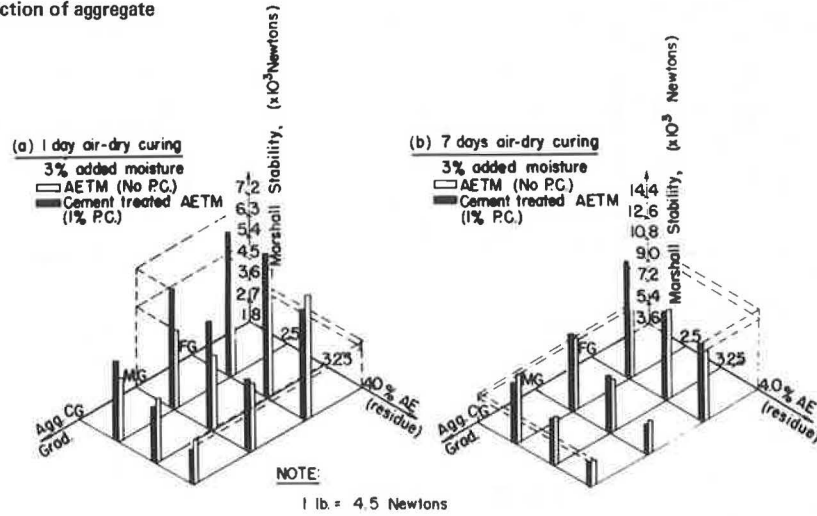


Figure 5. P as a function of percentage TL for AETM and cement-treated AETM.

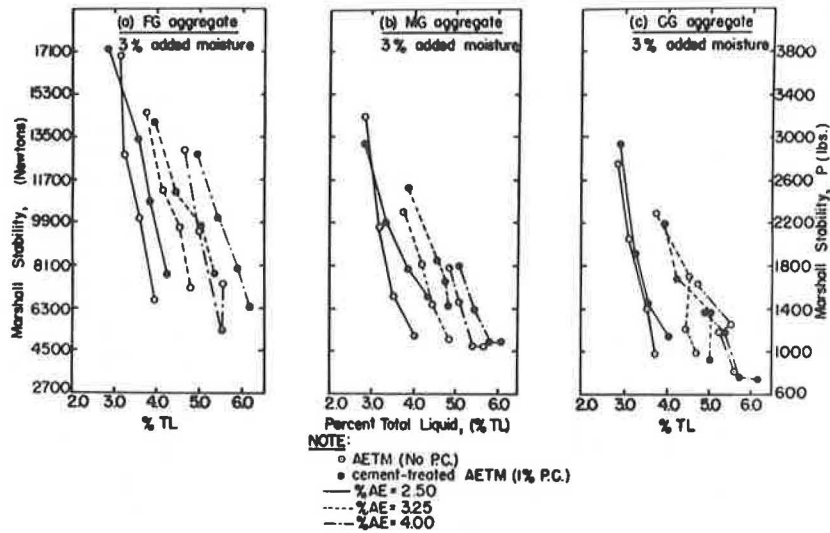


Figure 6. Effect of portland cement on I_m as a function of aggregate gradation and percentage AE residue.

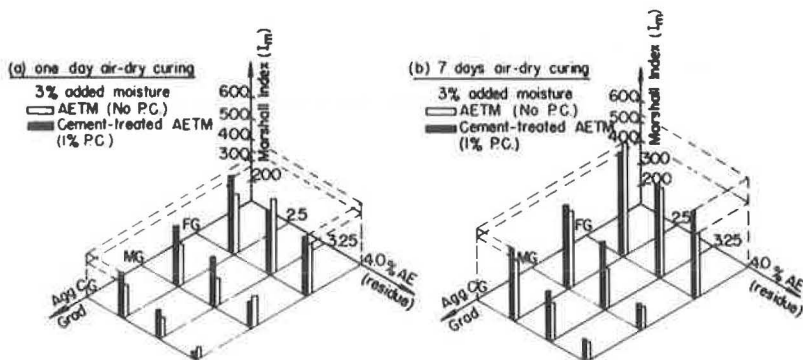


Figure 7. I_m as a function of percentage TL for AETM and cement-treated AETM.

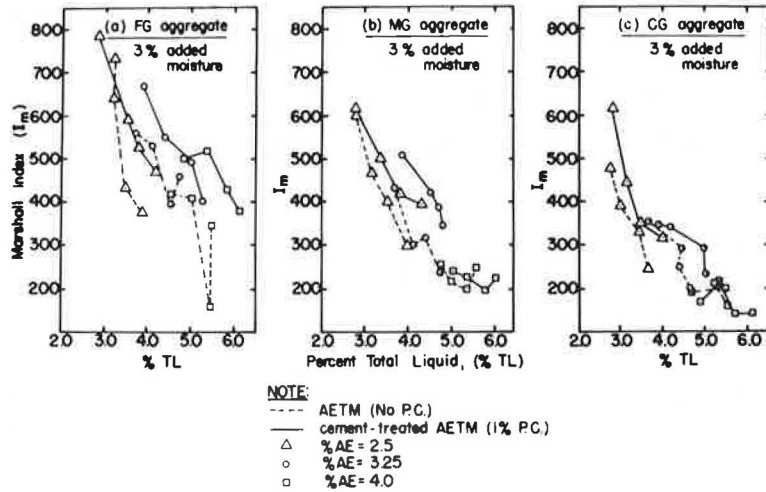


Figure 8. Percentage MA for AETM and cement-treated AETM specimens.

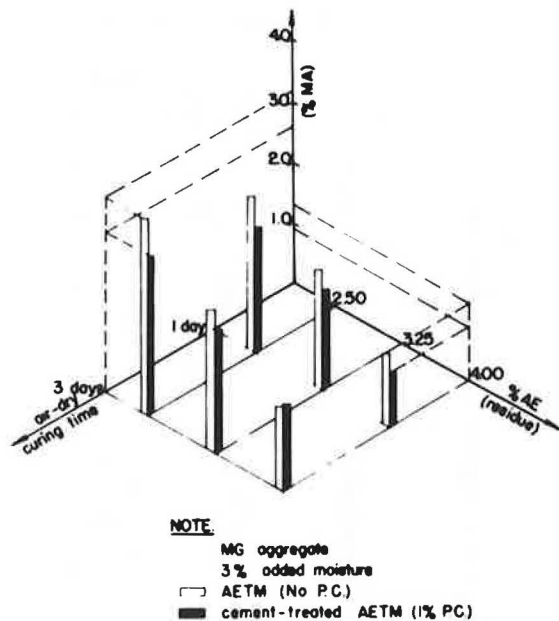
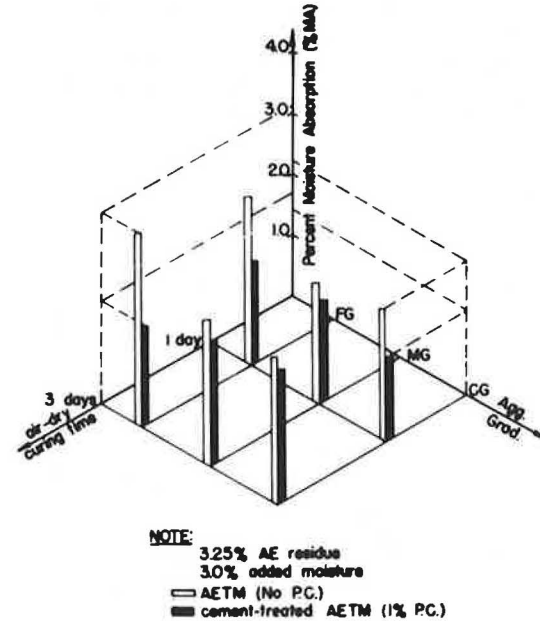


Figure 9. Effect of portland cement on percentage MA for various aggregate gradations.



gradation and percentage AE, its effect after relatively longer periods is beneficial (as far as the increase in I_m is concerned) at almost all levels of aggregate gradation and percentage AE.

S_m followed approximately the same trend as I_m , but the change in S_m values in response to the use of portland cement was less pronounced than the change in I_m values. Again, this is a result of the difference in the nature of the two measures of stiffness. I_m is a measure of the mix characteristics during the duration of loading, whereas S_m is a measure of the mix characteristics at the failure condition and is directly related to the stability and flow values of the mix.

I_m as a function of percentage TL is shown in Figure 7. The trends were obtained by using test results at different curing periods. An increase in the I_m values was obtained by using 1 percent portland cement as an additive to the AETM. At a specific percentage TL available in the specimen, the cement-treated AETM showed a pronounced and significant increase in I_m . The effect of portland cement also depends mainly on aggregate

gradation and percentage AE residue. No gain in I_m or S_m was obtained when CG aggregate was used, especially with a high percentage AE.

RESULTS OF WATER-SENSITIVITY TESTS

Most of the water-sensitivity tests were conducted for mix combinations that contained MG aggregate and for two curing periods—one and three days of air-dry curing. Mix combinations that contained FG and CG aggregate were selected for purposes of comparison (as shown earlier in Figure 1) for mix combinations that contained 3.25 percent AE and 3 percent added moisture.

Percentage Moisture Absorption

As Figure 8 shows, cement-treated AETMs have less moisture absorption (MA) than AETMs without portland cement. The effect of portland cement in reducing percentage MA is more apparent at a low percentage AE

and decreases with an increase in percentage AE. Adding portland cement to the AETM improves the bonding between the components of the mixture and consequently reduces the amount of moisture that is permitted to enter through the system.

Figure 9 shows that portland cement was beneficial in reducing percentage MA in all three aggregate gradations. FG-aggregate mixes showed the largest reduction in percentage MA. Reduction in percentage MA through the use of portland cement resulted in a lower percentage TL being available in the cement-treated AETM than in the AETM, which in turn contributed to the higher parameters of retained strength that were obtained for the cement-treated AETM.

Percentage Retained Stability

The use of 1 percent portland cement significantly improved retained stability in the AETM. The results for dry and soaked stability for AETM and cement-treated AETM at two different curing times are shown in Figure 10. The percentage retained stability for mixes that contained MG aggregate increased to a range of 75 to 81 percent and 79 to 92 percent, respectively, for specimens cured for one and three days; these ranges compare with ranges of 41 to 58 percent and 69 to 81 percent for the AETM without portland cement. The asphalt emulsion content affected the role of portland cement. The effect of portland cement was more

pronounced at a low percentage AE, e.g., 2.5 percent. Percentage retained stability increased with increasing percentage AE for the AETM but decreased with increasing percentage AE for the cement-treated AETM.

In addition, mixes made with FG or CG aggregate are shown to gain resistance to water damage when they are treated with portland cement (see Figure 11). In an earlier discussion that dealt with the effect of portland cement on the dry stability of AETMs, it was shown that the CG-aggregate mixes did not show an appreciable gain in stability when portland cement was used (and, in some mix combinations, showed a slight decrease in stability). It is important, however, to note that using portland cement with CG-aggregate mixes appreciably improved their resistance to water damage. This is another example of the importance of water-sensitivity tests in evaluating the performance of AETMs; using only the results of dry tests is not sufficient for understanding and controlling AETM performance.

Figure 10. Dry and soaked P for AETM and cement-treated AETM (MG aggregate, 3 percent W).

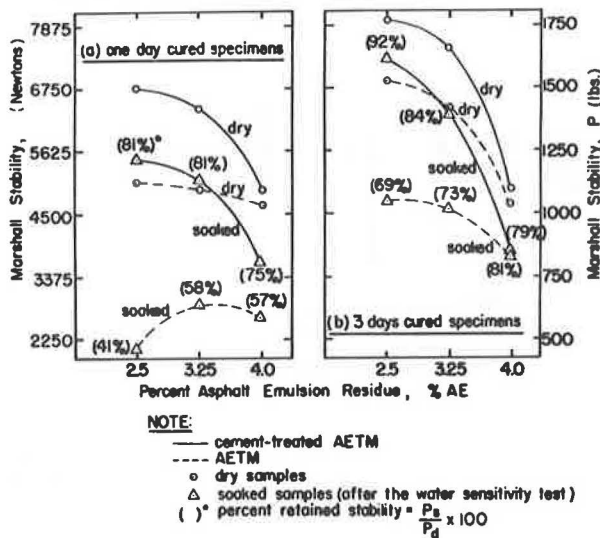


Figure 11. Effect of portland cement on P for various aggregate gradations.

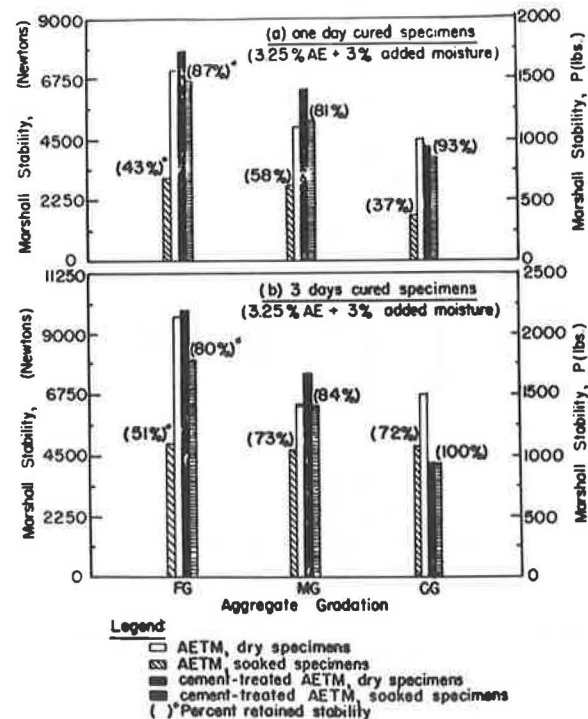


Figure 12. Percentage S_m for AETM and cement-treated AETM (MG aggregate, 3 percent W).

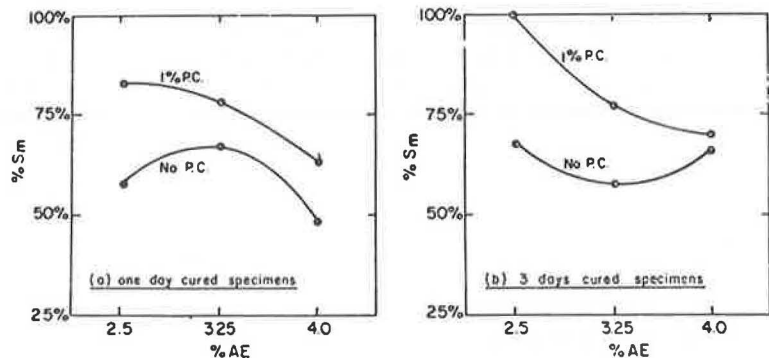
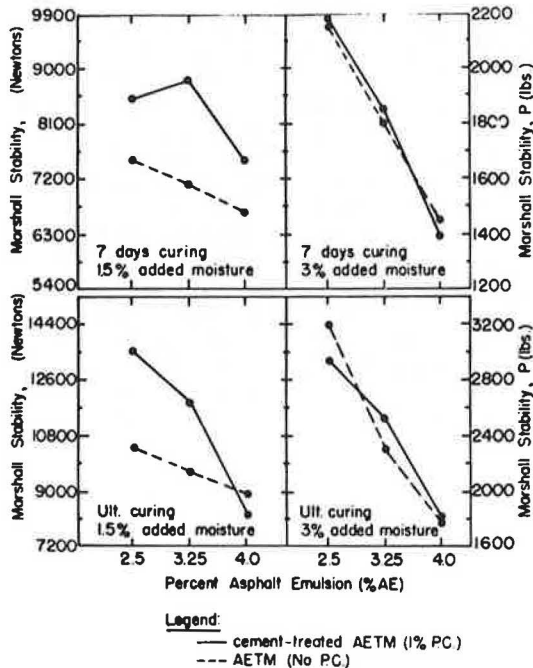


Figure 13. Effect of percentage W on role of portland cement (MG aggregate).



Percentage Retained Marshall Stiffness

The cement-treated AETM showed higher retained S_n values than the AETM when subjected to the action of water. In Figure 12, percentage S_n represents the ratio between S_n after the water-sensitivity test and S_n for the dry samples.

EFFECT OF ADDED MOISTURE CONTENT ON THE ROLE OF PORTLAND CEMENT

To examine the effect of added moisture content (percentage W) on the role of portland cement in the AETM, we examined the results for the limited tests that were run on the cement-treated AETM (MG aggregate and 1.5 percent added moisture) at two curing periods: seven days of air-dry curing and the ultimate curing condition. The effect of portland cement on the AETM properties was more apparent for samples with 1.5 percent W than for samples with 3 percent W.

Figure 13 shows the S_n results for the two levels of added moisture under study (1.5 versus 3 percent). In the figure, the effect of portland cement is more pronounced for samples with less added moisture, which indicates that percentage W affects the action of portland cement in the AETM system.

This parameter is presented here as an example. The other parameters were slightly affected but not to the same degree as P, S_n , and I_n . It should be noted that this portion of the tests was limited and was not intended to provide a detailed evaluation.

SUMMARY OF RESULTS

The use of portland cement as an additive to AETMs has proved to be beneficial in improving the properties of such mixtures. This result must be viewed with caution, however, since it has been found that the effect of portland cement on the performance of AETMs is significantly influenced by aggregate gradation, asphalt

emulsion content, and curing stage. The reported results pertain to AETMs that contained 3 percent added moisture. The significant findings can be stated as follows:

1. AETMs showed less coating when treated with 1 percent portland cement. The cement-treated AETM appeared to be drier than the nontreated AETM during the testing.

2. Cement-treated AETM had a higher percentage W_c than nontreated AETM specimens. However, a portion of this moisture has combined with the portland cement.

3. In general, nontreated AETM specimens possessed higher γ_d than cement-treated specimens, but, since the effects of interaction between portland cement and curing and percentage AE were significant, each case should be studied separately.

4. The effect of portland cement on stability values was influenced by aggregate gradation and percentage AE. At a low percentage AE, the use of portland cement was beneficial in increasing S_n values for all aggregate gradations used. However, when the percentage AE in the mix was increased, the role of portland cement was affected by aggregate gradation. The use of portland cement in CG-aggregate mixes was not beneficial and in some cases resulted in a reduction in stability. This could be attributed to the poor coating that was observed when CG aggregate was treated with portland cement.

5. The effect of portland cement on stability was more apparent at the early curing stage.

6. In spite of the increase in percentage TL that resulted from the use of portland cement, the trends for stability versus percentage TL showed a significant gain in stability when AETMs were treated with portland cement (note that this was also dependent on aggregate gradation).

7. In a limited study, added moisture content affected the role of portland cement in the AETM. The use of 1.5 percent W enhanced the effect of portland cement by increasing the stability values over values for specimens with 3 percent W.

8. F-values were not significantly affected by the use of portland cement. In our opinion, F-values alone are the least significant parameter in explaining AETM performance.

9. Portland cement significantly increased I_n values, but S_n values were not significantly affected because S_n is dependent on P and F. Since F-values were not significantly affected by portland cement and the change in F attributable to the use of portland cement varied, the effect of portland cement on S_n values was reduced.

10. Test results for the unsoaked (dry) specimens showed that S_n increases with decreasing percentage AE in the mix. But mixes with low percentage AE showed the least resistance to water damage. The percentage of retained stability increased through the curing process for all mix combinations.

11. The use of portland cement improved AETM properties and the resistance of AETMs to water damage. The effect of portland cement was more beneficial and apparent for mixes with low percentage AE. The effect of portland cement on resistance to water damage was especially valuable at early curing stages. The use of portland cement improved the resistance to water damage of all three aggregate gradations, especially the CG aggregate.

REFERENCES

1. A. A. Gadallah, L. E. Wood, and E. J. Yoder. Evaluation of Properties of Asphalt-Emulsion-

- Treated Mixtures by Use of Marshall Concepts. TRB, Transportation Research Record 695, 1979, pp. 7-14.
2. A. A. Gadallah, L. E. Wood, and E. J. Yoder. A Suggested Method for the Preparation and Testing of Asphalt Emulsion Treated Mixtures Using Marshall Equipment. Presented at the 1977 Annual Meeting, AAPT, Feb. 1977.
 3. V. L. Anderson and R. A. McLean. Design of Experiments: A Realistic Approach. Marcel Dekker, New York, 1974.
 4. Water Sensitivity Test for Compacted Bituminous Mixtures. Asphalt Institute Laboratory, College Park, MD, June 1975.
 5. Bituminous Emulsions for Highway Pavements. NCHRP, Synthesis of Highway Practice 30, 1975.
 6. A. A. Gadallah. A Study of the Design Parameters for Asphalt Emulsion Treated Mixtures. Joint Highway Research Project, Purdue Univ., West Lafayette, IN, Res. Rept. 30, 1976.
 7. R. H. Gietz and D. R. Lamb. Effects of Filler Composition on Binder Viscosity and Mix Stability. HRB, Highway Research Record 256, 1968, pp. 1-14.
 8. R. W. Head. An Informal Report of Cold Mix Research Using Emulsified Asphalt as a Binder. Proc., AAPT, Vol. 43, 1974.
 9. Autographic Equipment for Marshall Method. Rainhart Co., Austin, TX, Catalog 760.
 10. R. J. Schmidt and P. E. Grof. The Effect of Water on the Resilient Modulus of Asphalt-Treated Mixes. Proc., AAPT, Vol. 41, 1972.
 11. R. J. Schmidt and others. Performance Characteristics of Cement-Modified Asphalt Emulsion Mixes. Proc., AAPT, Vol. 42, 1973.
 12. Symposium on Design and Construction of Pavements with Emulsions. Proc., AAPT, Vol. 44, 1975, pp. 281-365.
 13. R. L. Terrel and C. K. Wang. Early Curing Behavior of Cement Modified Asphalt Emulsion Mixtures. Proc., AAPT, Vol. 40, 1971.
 14. P. J. Van de Loo. Creep Testing: A Simple Tool to Judge Asphalt Mix Stability. Proc., AAPT, Vol. 43, 1974.

Publication of this paper sponsored by Committee on Characteristics of Nonbituminous Components of Bituminous Paving Mixtures.

Fatigue Performance of a Bituminous Road Mix Under Realistic Test Conditions

L. Francken, Centre de Recherches Routières, Brussels

A study whose purpose was the verification of Miner's rule for estimating the cumulative damage resulting from the phenomenon of fatigue is reported. A repeated-bending apparatus driven by a minicomputer, which was devised to generate and control stress or strain waves of variable amplitudes, is described. The fatigue behavior of a bituminous mix subjected to nine different loading patterns (simple, random, and block) was determined. The influence of rest periods of different lengths was studied for these cases. It is concluded that (a) to the extent that the spectrum of load amplitudes is known, a prediction method derived from Miner's law is applicable with an acceptable accuracy for random sequences that include no rest periods and (b) rest periods markedly increased fatigue life for the three loading patterns considered. These initial conclusions were used to derive a generalized form of Miner's law for loading conditions in which both stress amplitudes and the duration of rest periods are variable. This generalized law was verified by simulating actual conditions of traffic loading in fatigue tests.

Intensive worldwide laboratory research on the mechanical properties of bituminous mixes has led to the establishment of methods of estimating fatigue performance (or number of loading cycles at failure). One of the major criticisms of these methods concerns the simplicity of applied loading. It is a fact that the continuous cycles of loading of constant stress or strain amplitude generally applied in laboratory tests are not realistic enough to simulate the compound-loading conditions to which a road material is subjected under actual traffic loads.

To take account of compound loading in structural design methods, Miner's law is used. Miner's law assumes a linear cumulative effect of damage irrespec-

tive of the true history of the applied loads. Several authors who have made experimental investigations to estimate the degree of accuracy of this law (1-6) have come to different conclusions depending on the type of loading history used.

In fact, the experimental approach to realistic conditions may be manifold: Even when it ignores variations in temperature, the realistic test history must include a succession of loading cycles followed by rest periods that are distributed randomly in both duration and size according to statistical distributions that reflect traffic characteristics. Fundamental understanding of such a process can only be attained through a stepwise progression in the degree of complexity of test conditions.

Enough is now known about the fatigue process under simple loading to allow a better understanding of more complicated loading patterns. For this reason, the Centre de Recherches Routières has undertaken an experimental research project to study realistic fatigue testing.

EXPERIMENTAL PROCEDURE

The mechanical part of the apparatus used in this research is identical to that used in earlier investigations (7): Trapezoidally shaped specimens 9×3 cm at the base, 35 cm in height, and 3 cm thick are fixed at their larger bases and submitted to a bending force that acts tangentially to their smaller bases by means of an electromagnetic exciter. Transducers fitted to the tops of the

specimens and connected to the input of an analog-to-digital converter allow the continuous measurement of force and displacement.

A periodic command signal computed by a 16K data processor is fed to the power amplifier of the exciter by a digital-to-analog converter. This signal is servocontrolled and fitted to the preset reference level according to the mean measured amplitudes of either force or displacement (calculated over 16 consecutive cycles). The mode of loading of the test may thus be controlled stress or controlled strain. The control level depends on the values introduced by the user before the start of the test.

At each cycle, the computed control can be performed at a different level of stress or strain, proportionally, to a sequence of up to 8000 integer numbers between 0 and 15 (called here "level indices") introduced in memory registers by the user and continuously scanned by the computer program, one number being assigned to each cycle. By looping on this numerical sequence, the processor is able to generate any distribution of stress or strain amplitudes in any order of succession to be decided by the user.

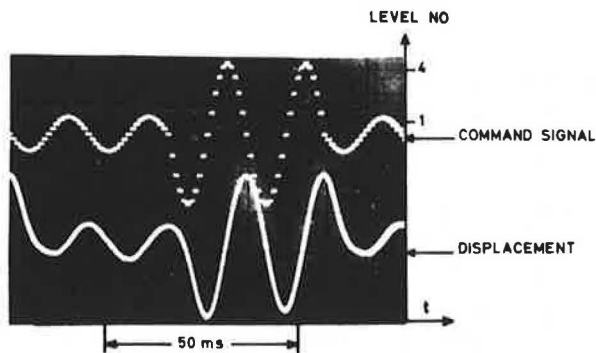
Typical test conditions, such as cycle blocks with different lengths, pseudorandom sequences, or stationary sine waves, can easily be generated and controlled merely by introducing the appropriate sequence of level indices in memory before the start of the test. Rest periods can be obtained by introducing zero values at the desired places in the sequence.

Figure 1 shows the sinusoidal signal generated at a frequency of 50 Hz by using a sequence of four numbers (1, 1, 4, 4) as well as the corresponding displacement signal. Other loading patterns are also visible in the photographs shown in Figure 2.

A fatigue test can be run on one sample once the initial strain or stress at level index 1 has been assigned by the user during the starting procedure. The fatigue curve of the mix is obtained from several fatigue tests run at different initial stress or strain values at level index 1. Histograms of the level indices as well as of the amplitudes of force and displacement are continuously implemented while the test is in progress. Values of the resilient modulus and relevant numbers of cycles are recorded every time the uncontrolled signal (displacement or force) has varied by a fixed fraction of its initial value.

Seven control tests are executed at each loading cycle to detect the rupture of the specimen or any failure of the system. Histograms and recorded values that describe the mechanical evolution of the sample are listed at the end of the test, just before the shutdown of the power supply of the whole system.

Figure 1. Variable-amplitude command signal and corresponding displacement of viscoelastic specimen.



The equipment works fully automatically and complies with German specification DIN 51228.

MIX COMPOSITION

One of the major problems in the fatigue testing of composite materials is the broad scatter of observed life-times. Because of this, in any investigation of the influence of factors that affect fatigue behavior, many experiments must be performed to get a statistically significant result.

The mix used in this investigation was selected for its low variability in test results (low standard deviation about mean life). It contains 35 percent stones, 52.8 percent sand (particles <2 mm), and 12.2 percent 0.075-mm limestone filler bound with 8 percent bitumen of 40-50 penetration grade. This type of mix, similar to British hot-rolled asphalt, is used in Belgian road construction as a wearing course to be covered with precoated chippings.

EFFECT OF LOADING HISTORY AND REST PERIODS

The tests conducted on the selected mix in the first part of the experimental program consisted of the nine loading patterns shown in Figure 2. These experiments were carried out under controlled stress and at constant temperature (15°C) and frequency (55.6 Hz, period = 18 ms).

The results of the normal fatigue test C_0 were used as reference for the other conditions; the mean cumulative fatigue life obtained under these conditions was close to one.

The statistical distribution of amplitude levels (number of cycles per level) shown in Figure 3 was used in all the tests carried out at eight levels. This nearly Gaussian distribution centered on the fourth level (mean = 4 and standard deviation $\sigma = 1.12$) has a shape that is similar to the spectrum of contact pressures induced by commercial vehicles on Belgian roads (8).

Rest periods were introduced after each loading cycle on tests C_1 , C_2 , B_1 , B_2 , R_1 , and R_2 . In the B block tests, the number of cycles repeated in each block was fitted to obtain the loading spectrum in Figure 3. The different blocks were arranged in increasing or decreasing order to avoid abrupt level changes. Rest periods in tests B_1 and B_2 were gathered in one block and placed between the blocks of level 1 beginning or ending the pattern of repeated loading. The fatigue life of the mix was determined for each type of test on at least eight specimens tested at different stresses.

The set of test conditions considered here allows the investigation of the influence of (a) the arrangement of the different amplitudes of stresses, (b) the effect of rest periods and their length on fatigue life, and (c) the combination of these two factors.

Fatigue Life Under Simple Loading

First, fatigue tests were carried out on the mix in accordance with the usual procedure, i.e., constant amplitude of stress without rest periods. The fatigue law can be expressed as

$$\epsilon_1 = KN_1^{-a} = \epsilon_{N=10^6} (N_1/10^6)^{-a} \quad (1)$$

where

- ϵ_1 = initial strain,
- K = factor dependent on mix properties,
- N = cycles to failure, and
- $-a$ = an empirical factor.

Figure 2. Compound test conditions.

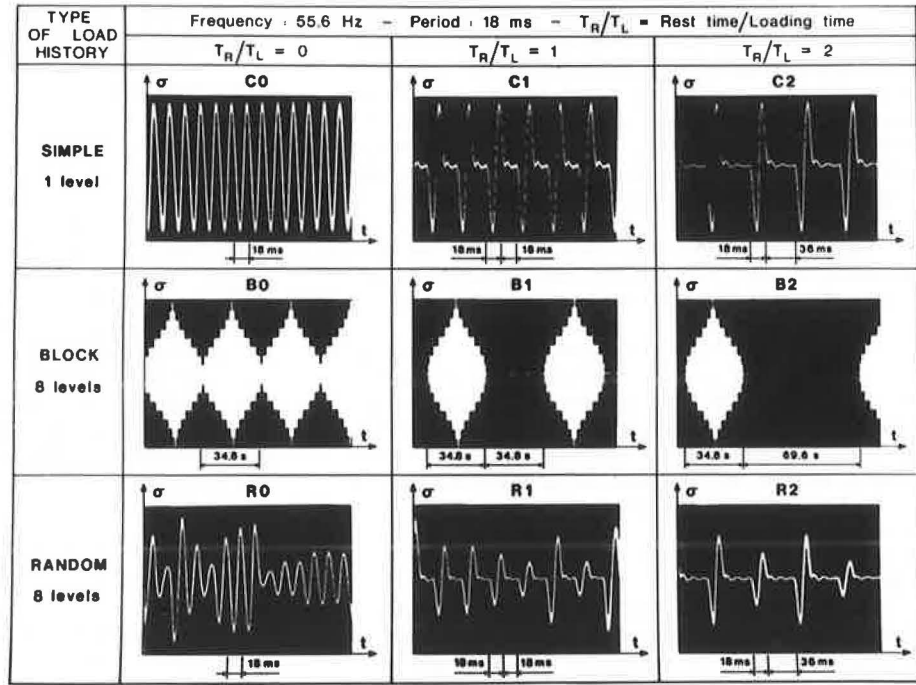
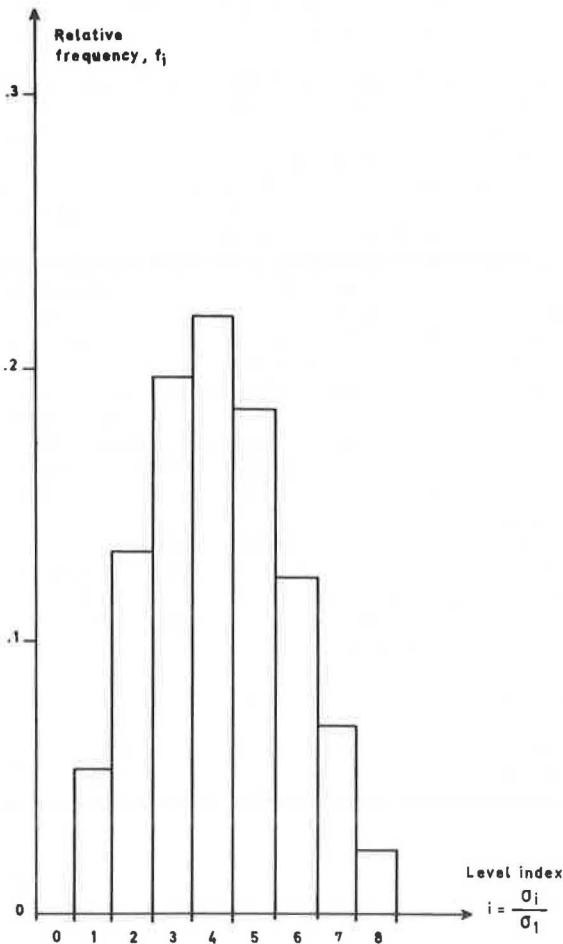


Figure 3. Spectrum of load amplitude for compound tests.



The parameters of the fatigue law were obtained by least-squares adjustment through the experimental points shown on the double log scale in Figure 4. Notice that these points are located along a curve that is not exactly straight. The fracture lives corresponding to the lowest and highest levels of applied stress are systematically higher than those than can be predicted by Equation 1.

This particular shape, which is visible thanks to the low scatter in the experimental results, reveals that the general form of the fatigue law (Equation 1), although close to the observed points, may lead to underestimated values of fatigue life, especially in the case of very small stresses where the slope of the fatigue curve is lower.

A relation of the following type gives a better fit of the experimental results and can be used to calculate interpolated fatigue lives:

$$\log \epsilon = C(\log N)^D \tag{2}$$

Results and Interpretation of Compound Tests

The usual way of interpreting results of compound fatigue tests is to calculate for each specimen the cumulative cycle ratio M :

$$M = \sum_{i=1}^q (n_i/N_i) \tag{3}$$

where

- q = total number of applied loading levels,
- n_i = number of applied loading cycles at level i , and
- N_i = fatigue (or service) life of the mix under simple fatigue test at level i .

The deviation from unity of the mean M -value obtained from different fatigue tests for a given loading pattern indicates the degree of discrepancy from Miner's hypothesis.

It is possible to establish a generalization of the fatigue law for the case of tests carried out at q stress

Figure 4. Fatigue diagram for simple mode of loading (C_0 = controlled stress at constant amplitude).

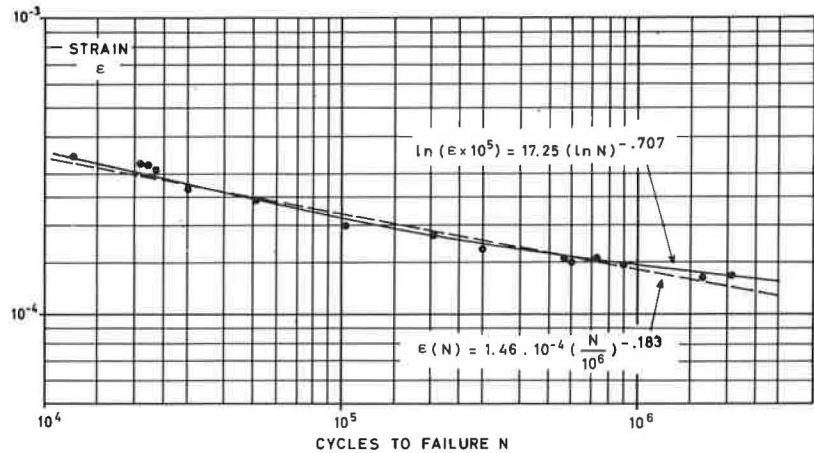


Table 1. Results of compound tests.

Type of Test	Number of Tests	Based on Fatigue Law $\epsilon = K(FN)^{-a}$					Based on Equation 2			
		$\epsilon_{N=10^6}$ (0.10^4)	a	Correlation Coefficient	Standard Deviation of Log Life	$M = \sum_{i=1}^q n_i/N$	Standard Deviation on M	M	Standard Deviation on M	$\sum n_i/N_T$ at $N = 10^6$
C_0	14	1.46	0.183	-0.99	0.041	1.07	0.414	1.04	0.313	1.03
C_1	8	1.79	0.192	-0.99	0.058	3.39	1.262	3.04	1.333	3.73
C_2	12	1.96	0.167	-0.98	0.068	4.83	1.884	4.78	2.849	5.58
C_3	15	2.17	0.177	-0.94	0.098	9.27	4.376	6.104	4.132	7.65
C_{10}	8	2.42	0.208	-0.99	0.061	19.62	7.467	7.91	6.48	9.72
C_{20}	8	2.76	0.150	-0.91	0.122	32.84	20.53	11.78	17.66	11.11
B_0	15	1.64	0.168	-0.99	0.041	1.676	0.447	1.686	0.588	2.15
B_1	7	1.70	0.191	-0.99	0.028	2.47	0.628	2.174	0.606	2.71
B_2	8	1.93	0.173	-0.997	0.033	4.260	0.732	3.288	1.734	4.24
R_0	14	1.60	0.152	-0.99	0.043	1.337	0.501	1.414	0.568	1.79
R_1	16	1.89	0.199	-0.97	0.072	4.881	1.820	3.336	1.766	4.34
R_2	14	2.06	0.182	-0.98	0.054	6.672	1.671	4.478	2.198	5.82

levels by using the following assumptions:

1. The fatigue law at constant level is given by Equation 1 with the same exponent a for all levels.

2. The spectrum of the q stresses σ_i is known, which means that frequencies $f_i = n_i/N_T$, where N_T is the total number of loading cycles applied up to failure, are known for the q -level indices $i = \sigma_i/\sigma_1$.

If these assumptions are verified, M can be expressed as a function of the parameters of the fatigue law, the strain ϵ_1 at level 1, and the stress spectrum, as follows:

$$M = N_T (\epsilon_1/K)^{1/a} \sum_{i=1}^q (f_i i^{1/a}) \quad (4)$$

In the case in which Miner's law is valid ($M = 1$), the following relation arises between N_T and ϵ_1 :

$$(\epsilon_1/i) \left(\sum_{i=1}^q f_i i^{1/a} \right)^a = K N_T^a \quad (5)$$

This expression is identical to the prediction technique proposed by Deacon and Monismith (6) for both random and repeated block loading.

Equation 4 shows that the relation between initial strain at level 1 ($\epsilon_1 = \epsilon_i/i$) and total service life N_T is identical to the simple fatigue law given in Equation 1 if the initial strain at the lowest level is multiplied by a correcting factor

$$F = \left(\sum_{i=1}^q f_i i^{1/a} \right)^a \quad (6)$$

that depends only on the loading spectrum and on the exponent a of the fatigue law. The value of this factor for the loading spectrum in Figure 3 is 5.26.

Equation 5 allows the graphical interpretation of the results of tests (carried out at different levels and obeying the same distribution function) on the same basis as the simple fatigue test by plotting the corrected strains $\epsilon_i F$ versus N_T . Hence, Miner's law can be verified by determining the parameters K (or $\epsilon_{N=10^6}$) and a of this modified fatigue diagram and by comparing the resulting values with the relevant values at the simple fatigue test C_0 . The numerical results obtained in this way for the nine loading patterns considered are given in Table 1. Strain corresponding to a life of 10^6 cycles was calculated by use of Equation 5 for each case.

Notice that, although the slope a of the fatigue law varies between 0.15 and 0.20 from one test series to another, this variation is not systematically related to the type of test. On the other hand, important variations in the strain $\epsilon_{N=10^6}$ in connection with the loading history are to be seen:

1. When the loading pattern contains no rest periods, the variation is only 12 percent.

2. When rest periods are present, the variation may increase by more than 30 percent.

The same trend is observable when one considers the cumulative cycle ratios:

1. Without rest periods, longer service lives are obtained for compound-loading patterns, and the random case appears to be intermediate between the simple fatigue test and the block test. Because of the low value of the power factor a of the fatigue law, the 25 percent

increase in service life observed for the random case may be considered relatively unimportant.

2. When rest periods are incorporated in the tests, the increase in service life becomes more important and Miner's law completely fails even for the simple case C2, where the service life is practically multiplied by a factor of 5. This lengthening of life is of the same order of magnitude if rest periods are combined with the random type of loading.

Another important feature of these test results is the fact that, irrespective of loading history, the M obtained are always increasing with N_T . This means that the lengthening of the fatigue life is greater for the lower initial strains. This effect, which was observed in each of the six compound test series that included rest periods, may be attributed to the fact that (a) more experimental points were located in the almost horizontal part of the fatigue curve and (b) the presence of very low stresses might play a role similar to that played by rest periods. Because of that effect and in order to base our judgment on comparable test conditions, a value of M corresponding to a total fatigue life of 10^6 cycles was calculated by interpolation (see the final column in Table 1).

Up to rest periods of 2, the average M and $M(10^6)$ are very close. The difference becomes more important when longer rest periods are inserted between the loading cycles. To investigate this factor, test series C, at constant amplitude, was run with rest periods up to 20 (tests C6, C10, and C20). In the last case, a difference of a factor of 3 could be observed between \bar{M} and $M(10^6)$.

The evolution of $M(10^6)$ as a function of the length of rest periods is shown in Figure 5. An empirical relation of the following form can be used to describe the lengthening effect caused by rest periods:

$$M(T_R/T_L) = 1 + 2.8(T_R/T_L)^{0.44} \tag{7}$$

It should be noted that this relation is only valid for the mix used in this investigation.

GENERALIZED FORM OF MINER'S LAW

The main conclusions of this experimental program are that

1. Miner's law can be considered a good approximation of the total lifetime of a mix when no rest periods are inserted between the loading cycles.

2. When rest periods are present, the life of the mix is extended by a factor M depending on the length of the rest periods.

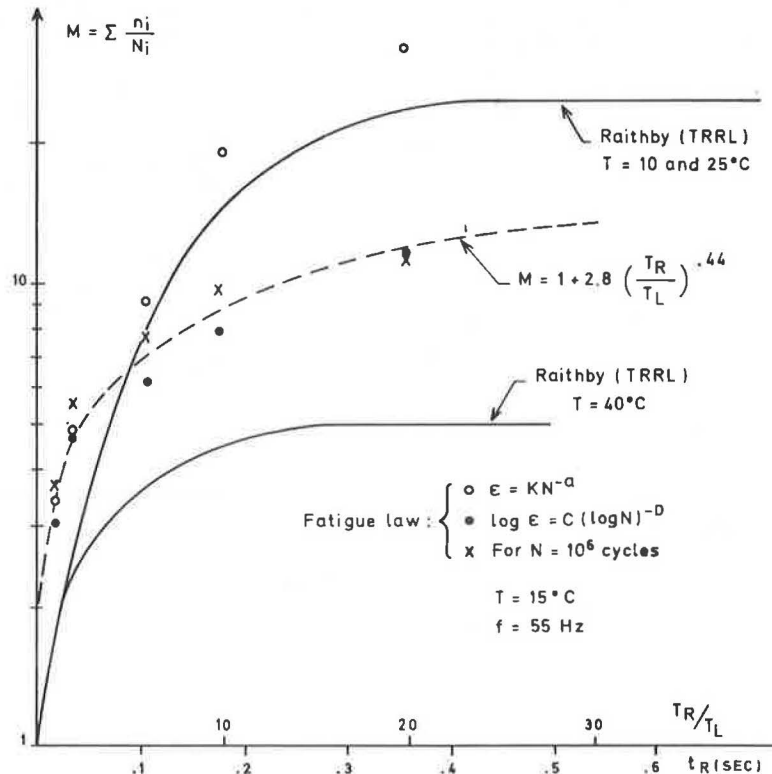
It is possible, on these bases, to establish a generalized form of Miner's law for the case in which the frequency is constant and both the applied stress amplitudes and the lengths of the consecutive rest periods vary randomly during a fatigue test.

To derive an expression equivalent to Miner's law, first we consider a loading cycle as consisting of two parts: a sinusoidal stress cycle of amplitude σ_i applied during time T_L followed by a rest period of duration T_R . The different stress levels σ_i are distributed in I discrete classes, and the rest periods T_R are distributed in J classes so that $\sigma_i = i\sigma_1$ (with $i = 1, 2, \dots, I$) and $T_R = jT_L$ (with $j = 1, 2, \dots, J$). Each loading cycle is thus defined by two indices (i, j) statistically distributed according to a two-dimensional distribution function $f(i, j)$.

If N_T is the total life at a given initial strain ϵ_1 , the fractional life of any type of loading cycle is $n_{i,j}/N_{i,j} = f(i, j) N_T / N_i M(j)$. The summation over indices i, j provides a new expression for the cumulative cycle ratio M' :

$$M' = N_T \sum_{i=1}^I \sum_{j=1}^J f(i, j) / N_i M(j) \tag{8}$$

Figure 5. Effect of rest periods on fatigue life.



By applying Miner's hypothesis ($M' = 1$) and replacing N_1 deduced from Equation 1 in this formula, the relation between initial strain ϵ_1 at level 1 and the total life N_T becomes

$$(\epsilon_1/i) \left\{ \sum_{i=1}^i \sum_{j=1}^j [f(i, j)i^{1/a}/M(j)] \right\}^a = KN_T^a \quad (9)$$

which again is similar to the normal fatigue law (Equation 1) provided ϵ_1 is multiplied by a correction factor that depends on a , the distribution function $f(i, j)$, and $M(j)$.

EXPERIMENTAL VERIFICATION BY TRAFFIC SIMULATION

Procedure

Experimental verification of the generalized Miner's law was performed on the tested mix so that Equations 1 and 7 can be used to calculate N_1 and $M(j)$. As a further step toward an actual field situation, the distribution functions $f(i, j)$ and the configuration of the rest periods were adjusted so that they reflected as closely as possible the loading conditions induced by commercial traffic observed on major roads in Belgium (8). Thus, the simulation performed in the test program described here deals with heavy, strongly canalized traffic.

The statistical study of this traffic has shown that 95 percent of the commercial vehicles belong to the five types of vehicles shown in Figure 6. Approximately a third of these vehicles were unloaded; in this study, therefore, a total of 10 categories of vehicles (5 loaded and 5 unloaded) were taken into consideration. Characteristics of these vehicles are also shown in Figure 6.











For the experimental simulation, each vehicle is represented by two, three, or four axles. Each axle is represented by a sinusoidal pulse of amplitude $\sigma_i = i\sigma_1$ ($1 \leq i \leq 7$) followed by a rest period $T_R = jT_L$ ($7 \leq j \leq 30$) to simulate the time gap between successive axles or between a rear axle and the next vehicle ($j = 30$). This

limitation at 30 of the time between successive vehicles was imposed to maintain a reasonable duration for the tests. As shown in Figure 5 and demonstrated by Raithby and Sterling (2,3), there is a limiting value of M above $j = 20$; thus, the limitation at 30 should not seriously affect the realism of the test results.

The magnitude of the pulses (indices i) attributed to the different axles was chosen in order to approach as closely as possible a normal distribution $P(i)$ (mean $\bar{i} = 4.5$ and standard deviation $\sigma = 1.39$) similar to that of the contact pressures observed on the road. The resulting two-dimensional distribution $f(i, j)$ and the corresponding one-dimensional distribution $f(i) = \sum_{j=1}^j f(i, j)$ [adjusted to $P(i)$] are given below:

i	j	$f(i, j)$ (%)	$f(i)$ (%)	$P(i)$ (%)
1	17	1.1	1.1	1.22
2	17	1.9	5.8	5.72
	21	0.4		
	23	0.8		
	25	2.7		
3	22	8.9	17.8	16.0
	30	8.9		
4	7	2.3	27.3	26.8
	20	0.8		
	21	0.8		
	22	17.7		
	29	1.1		
	30	4.6		
5	17	6.1	26	26.8
	29	2.2		
	30	17.7		
6	7	3.9	15.6	16
	29	5.6		
	30	6.1		
7	7	0.8	6.7	5.72
	20	1.7		
	23	1.7		
	30	2.5		

Figure 6. Characteristics of simulated traffic.

STATE	Vehicle type	Relative frequency (%)	Code N°	Number of axles	Level index i of axle number				Rest period j of axle number			
					1	2	3	4	1	2	3	4
LOADED		45.03	1	2	4	5	-	-	22	30	-	-
		2.10	2	3	4	7	7	-	21	7	30	-
		5.59	3	3	5	5	6	-	17	29	30	-
		9.86	4	4	5	6	6	6	17	25	7	30
		4.23	5	4	6	7	7	7	25	23	20	30
UNLOADED		22.40	11	2	3	3	-	-	22	30	-	-
		1.01	12	3	2	4	4	-	21	7	30	-
		2.76	13	3	1	4	4	-	17	29	30	-
		4.89	14	4	2	2	4	4	17	25	7	30
		2.11	15	4	2	2	4	4	25	23	20	30

Each type of loading sequence that defines a particular vehicle type was put in the computer memory. During the tests, the generation of the loading sequence simulating the passage of an individual vehicle was initiated by the computer each time the code number of that vehicle was met in a pseudorandom sequence of 8000 integer numbers distributed according to relative vehicle frequencies (Figure 6). Figure 7 shows an oscillogram for the passage of three vehicles during such a simulated-traffic fatigue test.

The number $n_{i,j}$ of loading cycles that belongs to each vehicle type is continually counted while a fatigue test is in progress so that the individual distribution function $f(i, j)$ is accurately known for each fatigue test. It should be noted that the distributions obtained in practice were always identical to the input distribution function as given in the table above.

Results

Fatigue tests were carried out on 16 specimens subjected to different values of initial strain at level 1 ($0.5 \times 10^{-4} < \epsilon_1 < 0.9 \times 10^{-4}$). This variation of initial strain amounts to observing the strain waves generated by actual traffic at different depths of the road pavement. The conditions applied as well as the results obtained in each case are given in Table 2.

Figure 7. Traffic simulation obtained by combining variable-amplitude sine waves and rest periods of different lengths.

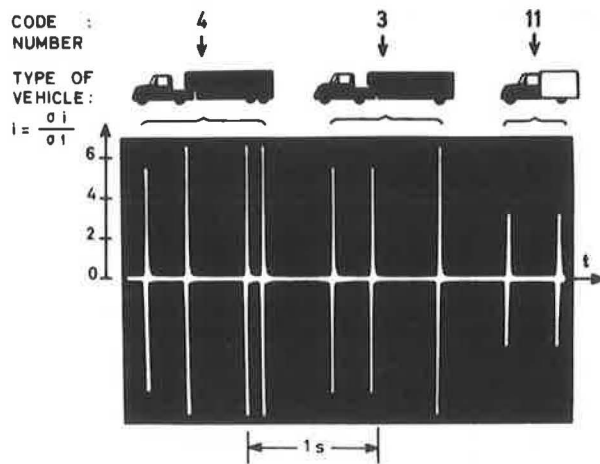


Table 2. Results of fatigue tests for simulated traffic.

Initial Strain $\epsilon_1 \times 10^4$	Number of Cycles N_T	Number of Vehicles	Cumulative Cycle Ratio at Failure			
			From Equation 1		From Equation 2	
			M	M'	M	M'
0.57	182 077	66 342	7.94	0.922	6.42	0.72
0.57	370 649	140 562	16.29	1.90	13.17	1.47
0.61	257 089	96 902	17.06	1.98	12.2	1.36
0.62	188 756	70 937	13.36	1.51	9.26	1.02
0.66	109 168	40 887	10.21	1.18	6.52	0.72
0.67	110 152	41 069	11.48	1.09	7.09	0.69
0.69	117 135	43 920	14.39	1.68	8.42	0.93
0.70	52 427	19 576	6.92	0.81	3.95	0.44
0.76	46 678	17 587	9.69	1.13	4.69	0.52
0.78	37 013	13 738	9.01	1.05	4.06	0.45
0.81	23 705	8 701	6.68	0.78	2.82	0.31
0.82	30 300	11 158	9.29	1.09	3.81	0.42
0.83	21 150	7 682	6.92	0.81	2.75	0.30
0.87	17 411	6 287	6.93	0.81	2.52	0.28
0.89	16 082	5 833	7.48	0.88	2.55	0.28
Mean			10.24	1.18	6.01	0.66
Standard deviation			3.51	0.40	3.46	0.38

The M cumulative fatigue lives deduced from the usual procedure (Equation 4) can be compared with that obtained from the generalized law (Equation 8) in which the fatigue lives N_i and the function $M(j)$ are respectively given by Equations 1 and 7. The improvement of the prediction technique is clearly visible in the individual values as well as in the mean values. A fatigue curve that obeys Equation 9 can be drawn by plotting $\epsilon_1 = \epsilon_i/i$ versus N_T in a log-log scale.

CONCLUSIONS

1. The results obtained in this research clearly show that it is possible to predict the fatigue life of a bituminous mix submitted to a stress history in which both the stress amplitude and the length of the consecutive rest periods vary randomly.

2. Use of this prediction method necessitates precise knowledge of (a) the fatigue law under continuous sinusoidal cycling, (b) the distribution function of applied amplitudes and rest periods, and (c) an empirical function that relates the cumulative cycle ratio M to the length of the rest periods.

3. There is experimental evidence that this method can be applied to actual traffic conditions.

4. The experimental procedure described in this paper allows the simulation of a broad variety of loading patterns and an unlimited choice of statistical distributions of loads and rest periods. It can thus be easily applied in many cases where heavier and less flexible machines are used.

5. Future research in this field should be concentrated on factors that were not considered in this study, such as mix composition and temperature variations.

6. Further research is also needed on the influence of this modified cumulative law on structural pavement design methods directed toward the limitation of fatigue failure.

ACKNOWLEDGMENT

The research program described in this paper was accomplished at the Centre de Recherches Routières under the direction of J. Reichert and was financially supported by l'Institut pour l'Encouragement de la Recherche dans l'Industrie et l'Agriculture. I am grateful to J. Verstraeten, V. Veverka, and J. Romain for their help and interest and to W. Sandra, who carried out the laboratory tests with care and precision, M. Crusnaire, who contributed to the design of the equipment, and J. Demolder, J. Pin, and P. Coignoul, who prepared the mixes.

REFERENCES

1. R. Guericke. Intervention Contribution. Proc., 2nd RILEM International Symposium on Tests on Bitumens and Bituminous Materials (Budapest, 1976), Vol. 2, pp. 85-94.
2. K. D. Raithby and A. B. Sterling. The Effect of Rest Periods on the Fatigue Performance of a Hot-Rolled Asphalt Under Reversed Axial Loading. Proc., AAPT, Vol. 39, 1970, pp. 134-147.
3. A. B. Sterling. Discussion. Proc., 3rd International Conference on the Structural Design of Asphalt Pavements (London, 1972), Vol. 2, pp. 84-86.
4. J. McElvaney. Discussion. Proc., 3rd International Conference on the Structural Design of Asphalt Pavements (London, 1972), Vol. 2, pp. 268-272.
5. J. McElvaney and P. S. Pell. Fatigue Damage of Asphalt Under Compound Loading. Transportation

- Engineering Journal, ASCE, Vol. 100, No. TE3, 1974, pp. 701-718.
6. J. A. Deacon and C. L. Monismith. Laboratory Flexural Fatigue Testing of Asphalt Concrete with Emphasis on Compound Loading Tests. HRB, Highway Research Record 158, 1967, pp. 1-32.
 7. J. Verstraeten. Moduli and Critical Strains in Repeated Bending of Bituminous Mixes. Proc., 3rd International Conference on the Structural Design of Asphalt Pavements (London, 1972), Vol. 1, pp. 729-738.
 8. A. de Henau. Véhicules et Circulation dans le Cadre du Dimensionnement des Chaussées. La Technique Routière, Brussels, Vol. 12, No. 1, 1967, pp. 1-19.

Publication of this paper sponsored by Committee on Characteristics of Bituminous Paving Mixtures to Meet Structural Requirements.

Effect of Laboratory Curing and Compaction Methods on the Stress-Strain Behavior of Open-Graded Emulsion Mixes

R. G. Hicks, Department of Civil Engineering, Oregon State University, Corvallis

Ronald Williamson, Region 6, U.S. Forest Service, Portland, Oregon

L. E. Santucci, Chevron Research Company, Richmond, California

Research into the curing of open-graded asphalt emulsion mixtures is described. Relations that characterize the development of the resilient modulus at different curing temperatures are developed, and comparisons are made between air curing and vacuum curing. The Marshall hammer and the vibratory air hammer are compared to determine the effects of compaction methods on resilient modulus. The results of testing at various levels of density are also reported. It was found that open-graded emulsion mixes develop final values of resilient modulus that vary with curing temperature and tend to be higher for increased curing temperatures. Vacuum curing was found to produce the highest values of resilient modulus. A comparison of methods of compaction showed that samples compacted by the vibratory hammer develop lower modulus values than samples compacted by the Marshall hammer. A comparison of test results obtained at different levels of density indicated that as density increased there was a substantial increase in modulus.

Open-graded emulsion mixes are mixtures of open-graded aggregates and emulsified asphalt, usually CMS-2. An open-graded mixture is characterized by high void contents of about 20-30 percent and less than 10 percent of the material passing the 2-mm (no. 10) screen (1). Common U.S. Forest Service specifications for aggregate gradations are given below (1 mm = 0.039 in):

Sieve Size (mm)	Percentage Passing
25	100
12.5	45-70
9.5	
4.75	0-20
2	0-6
0.075	0-2

The success of early projects led to increased use of open-graded emulsion mixes; it became evident, however, that the performance of these mixes varied. Simple modifications of methods of thickness design for hot mix were not always successful. Early failures of some projects have recently resulted in a reduction in the use

of open-graded emulsion mixes by one of its largest users, Region 6 of the U.S. Forest Service (2). Although the causes of these failures have usually not been precisely determined, the emulsion mix has often been blamed whether it contributed or not. The common solution to failure is to increase the pavement thickness by adding an overlay and thus burying the problems.

As a result of this varied performance of open-graded-mix pavements, Region 6 of the U.S. Forest Service contracted with Oregon State University to develop a procedure for designing pavements with these materials. The overall objective of the project is to develop a procedure for determining layer coefficients for use in the Region 6 version of the AASHTO design guides (3). Specifically, the program includes development of

1. Test equipment and procedures to characterize stress-strain behavior of open-graded emulsion mixes,
2. A procedure for assigning layer coefficients for open-graded emulsion mixes by using the test data generated together with layered theory, and
3. A plan for extensive verification in the field of the proposed procedure to establish layer coefficients.

This paper describes work done to determine the effects of curing and compaction methods on the stress-strain behavior of open-graded emulsion mixes as a part of the first of these objectives. For hot-mix asphalt concrete, factors that are known to have a considerable effect on pavement performance include quality and gradation of aggregate, grade of asphalt, quality control of construction, and amount of traffic. These factors also affect the performance of open-graded emulsion mixes. Curing conditions also appear to have an important effect on the behavior of emulsion mixes (4).

This study examines chiefly the effects of time and temperature on curing. The effects of methods of com-

pecting laboratory samples are also described in a comparison of a vibratory air hammer and the Marshall hammer. Finally, in an illustration of the effects of density, results from this study are compared with those obtained by the Chevron Research Company (5) in tests on identical materials.

MATERIALS

The materials used in this research are considered to be typical of materials used by Region 6 of the U.S. Forest Service in Portland, Oregon.

Aggregate

The aggregate used in all tests was provided by the materials laboratory of Region 6 of the U.S. Forest Service. This aggregate was a crushed basaltic material from Rivergate Rock Products near Portland. All material was sieved and then recombined to the gradation specifications given below (1 mm = 0.039 in):

Sieve Size (mm)	Percentage Passing
25	100
12.5	57.5
9.5	35
4.75	10
2	3
0.075	1

Common aggregate tests were performed by the Region 6 laboratory to determine aggregate properties. The results of these tests are given below (1 g/cm³ = 62 lb/ft³):

Property	Test Method or Specification	Amount
Rodded unit weight (g/cm ³)	AASHTO T 19-74	1.67
Durability index	California test method 229	
Coarse		58.0
Fine		44.4
Specific gravity (%)	AASHTO T-85	
Bulk		2.57
Saturated surface dry		2.66
Apparent		2.81
Absorption		3.24
Los Angeles abrasion loss (%)	AASHTO T-96	18.1
Sand equivalent	California test method 217	
Air dry		63.9
Prewet		60.6

Asphalt Emulsion

The asphalt emulsion used in this work was a CMS-2

Table 1. Properties and specifications of CMS-2 asphalt emulsion.

Property	ASTM Method	Specification	Actual
Viscosity at 50°C (s)	D 88	50-450	188
One-day settlement (%)	D 244	<5	-
Storage stability test, one day	D 244	<1	-
Particle charge	D 244	Positive	-
Sieve test (%)	D 244	<10	nil
Oil distillate by volume of emulsion (%)	D 244	<12	8
Residue (%)	D 244	>65	67
Penetration at 25°C	D 5	100-250	168
Ductility at 25°C, 5 cm/min (cm)	D 113	>40	-
Solubility in trichloroethylene (%)	D 2042	>97.5	-
Viscosity of residue			
At 135°C (cm ² /s)	D 2170		3.12
At 60°C (Pa·s)	D 2171		97.9

Note: t°C = (t°F - 32)/1.8; 1 cm = 0.39 in; 1 cm²/s = 100 centistokes; 1 Pa·s = 10 poises.

emulsion provided by Chevron USA, Inc. This is the type and source of asphalt used to date in the majority of projects constructed in the Pacific Northwest (4). The specifications and measured properties for this asphalt emulsion are given in Table 1. The emulsion content used for all experiments was equal to 6 percent of the dry aggregate weight.

SAMPLE PREPARATION

Several factors were considered important in sample preparation. The most important are described below:

1. Coating—The amount of coating varies with the fines content of a sample because of the increased surface area. An increase in fines may break the emulsion before it has a chance to coat completely. Coating after breaking is difficult if not impossible without more cutter stock to lower the viscosity of the residual asphalt. Because of possible variation in coating, three samples were prepared for each test condition.

2. Compaction—All samples used for the curing study were compacted in a cylindrical mold by using a Marshall hammer, four lifts, and 50 blows for each lift [9.75 blows/cm (25 blows/in)]. The sample was 10 cm (4 in) in diameter and 20 cm (8 in) in height. The resulting density was between 1.77 and 1.85 g/cm³ (110 and 115 lb/ft³). This density was initially chosen as being representative of open-graded emulsion mixes. A subsequent survey of existing projects has shown that the average density of open-graded emulsion mixes is 1.95 g/cm³ (121 lb/ft³) (4).

3. Handling—Freezing of the samples was required to remove the samples from the molds, and rubber membranes were applied to facilitate handling and to help prevent the samples from slipping.

Since the Marshall hammer was observed to cause some degradation of the aggregate, an evaluation of the use of a vibratory hammer in laboratory compaction was also included as part of this study. The vibratory air hammer that was used was equipped with a 10-cm (3.9-in) diameter rigid metal foot, and compaction was accomplished by using the vibratory effects of the hammer rather than impact forces typical of the Marshall hammer.

CURING

A number of curing methods have been proposed for the testing of emulsion mixes. The methods evaluated include the following:

1. Vacuum curing—Vacuum-cured samples were encased in a thin rubber membrane and two end plates through which a vacuum was applied. Vacuum curing was done at 24°C ± 2°C (75°F ± 4°F), and resilient modulus was measured at frequent intervals.

2. Air curing—Air-cured samples were cured at 24°C ± 2°C (75°F ± 4°F). To prevent the samples from slumping, they were confined in a rubber membrane in which the ends were left open.

3. Oven curing—Oven curing of emulsion mix samples is difficult because of the tendency for the mix to slump. The confining pressure of a rubber membrane applied to these samples was sufficient to allow curing at 38°C ± 2°C (100°F ± 4°F) without slumping problems. The oven used to cure all samples allowed air to flow through it, but no forced air was used.

4. Curing at 5°C (40°F)—Samples cured at 5°C were cured in a 5°C ± 1°C (40°F ± 2°F) refrigerator. None of the samples exhibited slumping tendencies.

For each variable studied, samples were prepared in triplicate to minimize the chances of variability in testing. Initial (uncured) properties of the samples prepared and tested for this study are given in Table 2. These properties were obtained one day after sample preparation.

TEST EQUIPMENT

Two tests that can be used to measure the stress-strain characteristics of open-graded emulsion mixes are the diametral test (5) and the repeated-load triaxial test (6). The diametral test has several advantages in that it is relatively inexpensive, the small samples are easier to fabricate and handle, and the equipment is relatively easy to use. Its main limitation is that it is limited to a maximum confining pressure of 101 kPa (1 atm). This confining pressure does not replicate the high confining pressures typical of the heavy loading found on Forest Service roads (7).

The device used in the repeated-load triaxial test can be used to apply high confining pressures and to evaluate both plastic and elastic response. But the device requires a highly skilled operator, and the larger test samples are difficult to prepare, cure, and handle. Because of the ability of this device to apply high confining pressures, it was used for all tests conducted in this study. The triaxial cell used was similar to a conventional cell but larger so as to accommodate a 10×20-cm (4×8-in) specimen and the deformation-measuring devices.

The repeated stresses were applied by using a pneumatic system similar to that developed by Seed and Fead (8). The repeated deviator stresses are applied at a frequency of 20 load cycles/min and at a pulse duration of 0.1 s. The 20-cycles/min frequency allowed the sample sufficient time to recover from the previous load so that plastic deformation of the sample was not a problem.

The response of the sample to applied stresses was measured by using two linear variable differential transformers (LVDTs). To accurately record the real deformation of the sample, the LVDTs were placed inside the triaxial cell and attached to the specimen with a pair of clamps placed at the quarter points.

Table 2. Initial properties of samples of open-graded emulsified asphalt.

Sample Number	Description	Liquid Content (%)	Aggregate Moisture (%)	Density (g/cm ³)	Air Voids ^a (%)
0	Uncured	6.0	0	1.81	29.3
1	Cured at 15°C	6.0	0	1.82	29.0
2				1.82	29.0
3				1.80	29.8
4	Cured at 24°C	6.0	0	1.83	28.5
5				1.80	29.7
6				1.84	28.4
7	Cured at 38°C	6.0	0	1.84	28.2
8				1.81	29.6
9				1.83	28.6
10	Vacuum cured	6.0	0	1.85	27.9
11				1.88	26.7
12				1.86	27.6
13	Compaction study	6.0	0	1.79	30.2
14				1.79	30.1
15	AR-4000	3.9	0	1.74	34.5
16				1.81	31.8
17				1.82	31.4

Note: 1 g/cm³ = 62 lb/ft³; t°C = (t°F - 32)/1.8.

^aSpecific gravity of aggregate = 2.81.

TEST PROGRAM

The basic procedure for testing elastic behavior by use of the repeated-load triaxial cell was developed in earlier tests (6,7). To avoid effects of plastic deformation, samples were subjected to 1000 repetitions of a preconditioning stress. After preconditioning, the sample was subjected to a standard test sequence that consisted of 100 repetitions of each stress condition. Standard tests at low confining pressures (i.e., $\sigma_3 = 0$) were not conducted for uncured and partially cured samples because of slumping problems. Most tests were conducted at 24°C ± 1°C (75°F ± 2°F). All samples were allowed sufficient time to reach the test temperature before testing.

RESULTS

Uncured Specimens

Three samples were used to establish the stiffness properties of the uncured emulsion mixes as a function of confining pressure σ_3 and the sum of principal stresses θ (for the triaxial test, $\theta = \sigma_d + 3\sigma_3$ where σ_d = repeated vertical stress).

Partially Cured Specimens

The average gain in stiffness for two stress conditions for partially cured specimens is shown in Figures 1, 2, and 3. Note that in all instances there is an increase in modulus with time of curing. The rate of increase in stiffness is, however, a function of the curing temperature. It should be mentioned that, although the average results show the expected trends, some of the individual results are quite erratic. This is discussed further in a later section of this paper.

Open-Graded Hot Mix

To estimate maximum stiffness, three samples of open-graded hot mix were prepared to the same density as the emulsion mixes and tested at two temperatures [23°C and

Figure 1. Resilient modulus versus curing time for cure condition of 5°C and test temperature of 24°C.

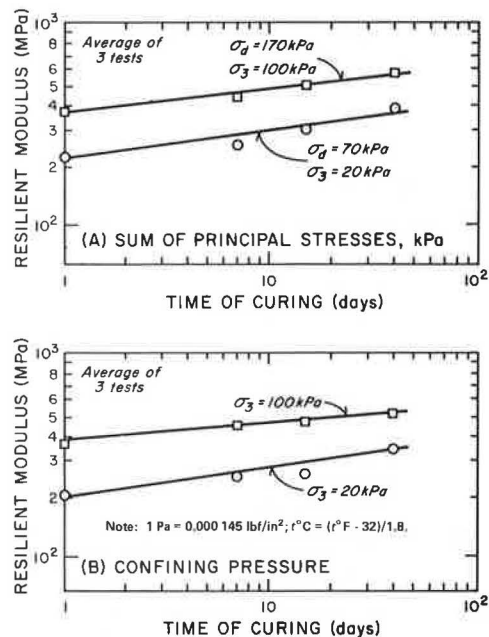


Figure 2. Resilient modulus versus curing time for cure condition of 24°C and test temperature of 24°C.

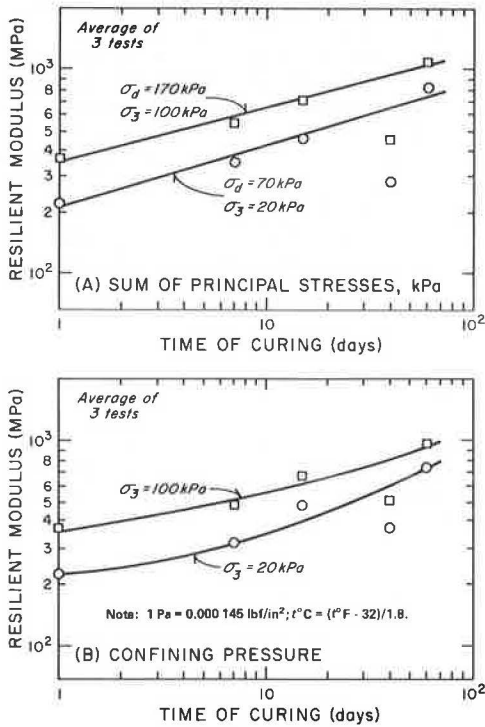
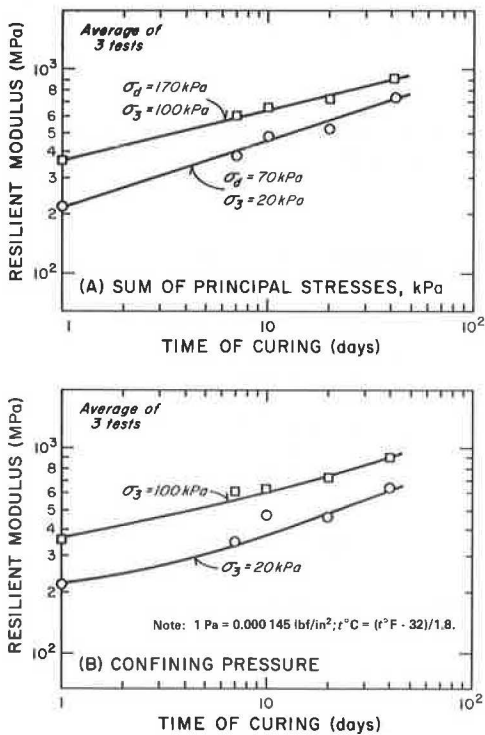


Figure 3. Resilient modulus versus curing time for cure condition of 38°C and test temperature of 24°C.



27°C (73°F and 81°F)]. All samples were tested in accordance with the standard sequence. In all instances, the modulus was affected by confining pressure σ_3 . As σ_3 increased, the modulus increased. In addition to the observed stress dependency, the modulus is also affected by temperature. Figure 4 shows the effect of tempera-

ture on the modulus for two confining pressures. At 32°C (90°F), it can be expected that the modulus of open-graded hot mix will be about 483 MPa (70 000 lbf/in²). At 24°C (75°F), the modulus varies from 1069 to 1862 MPa (155 000 to 270 000 lbf/in²), depending on the confining pressure. These values, as expected, are greater than the corresponding modulus values obtained on partially cured, open-graded cold mix. These values are considered estimates only because the viscosity of the emulsion mixes and the asphalt cements did not agree closely [~ 100 versus ~ 383 Pa·s (1000 versus 3830 poises)].

Vacuum-Cured Specimens

The results of tests on the three vacuum-cured samples are summarized in Figure 5. Of particular interest is the gain in stiffness as a function of time of curing and sum of principal stresses (θ). The corresponding value of stiffness for the open-graded hot mix is also shown in Figure 5.

Figure 6 shows the development of stiffness for two stress conditions. Note that, if the curing curves are extended to the ultimate (AR-4000), approximately 300 h (or 12 days) of vacuum curing would be required to reach this value.

Compaction Study

The results of the test on samples prepared to the same density by using the Marshall and vibratory hammers are summarized in Figure 7, which shows the actual modulus values for each compaction method and their development over time. Figure 8 shows the development of modulus with time for one stress condition [$\sigma_d = 69$ kPa (10 lbf/in²), $\sigma_3 = 21$ kPa (3 lbf/in²), and $\theta = 131$ kPa (19 lbf/in²)]. As indicated, the samples compacted by the vibratory compactor are less stiff at the early stages of curing. Although the results are limited, they do show that different compaction methods may yield different results. If vibratory compaction is used, one can expect a greater tendency to tender mixes. As the samples are cured, the effect of compaction is lessened.

Samples compacted by the Marshall hammer may show more stiffness at early stages of curing because of some crushing of the aggregates, which results in increased grain interlock. As the samples are cured, however, the stiffness of the mix results more and more from the presence of asphalt, and the resulting stiffness values are similar to one another.

Figure 4. Average modulus for open-graded hot mix versus temperature (from regression equations).

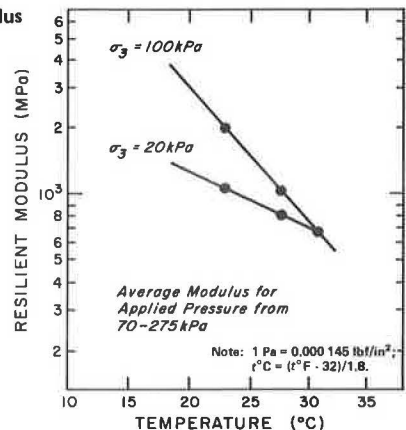


Figure 5. Resilient modulus versus sum of principal stresses.

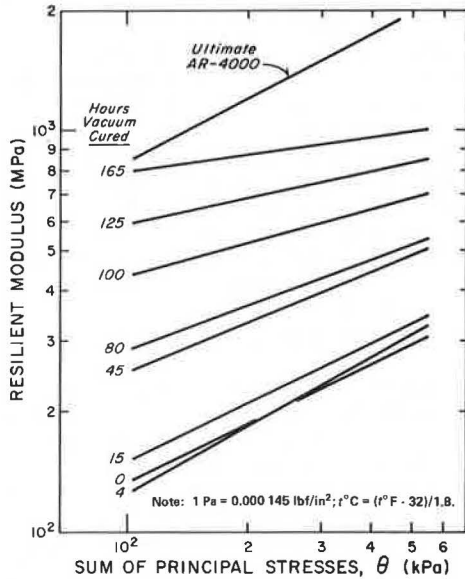
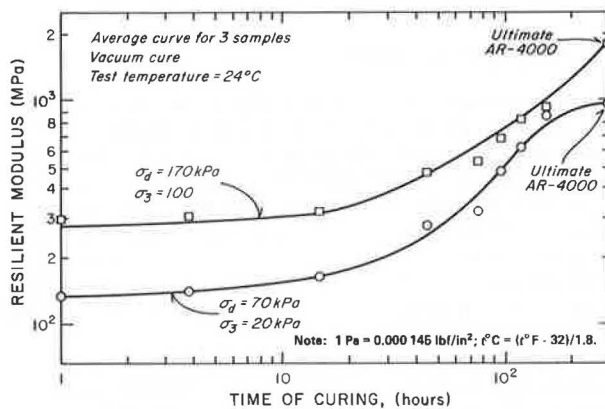


Figure 6. Resilient modulus of open-graded emulsion mixes versus curing time.



DISCUSSION OF RESULTS

Variability

It was expected that the stiffness of all of the open-graded mixes would always increase with time. However, comparison of test results for several individual samples at different durations of curing showed that gains in stiffness do not always occur in the expected manner. It was also reasonable to assume that samples that were prepared, cured, and tested in a similar manner would produce similar results. But there was considerable variation in regression coefficients for samples tested at the same stage of curing and prepared in the same way. These variations appear to be beyond any normal experimental error. Furthermore, they were considerably greater than the variations found by Chevron Research Company in tests of similar materials in which the diametral test apparatus was used.

It is suspected that much of the variation found in the samples tested at Oregon State University was caused by the following factors:

1. Sample size—The 10×20-cm (4×8-in) sample size used in the repeated-load triaxial test apparently does

Figure 7. Variation in resilient modulus with curing time, type of compaction, and sum of principal stresses.

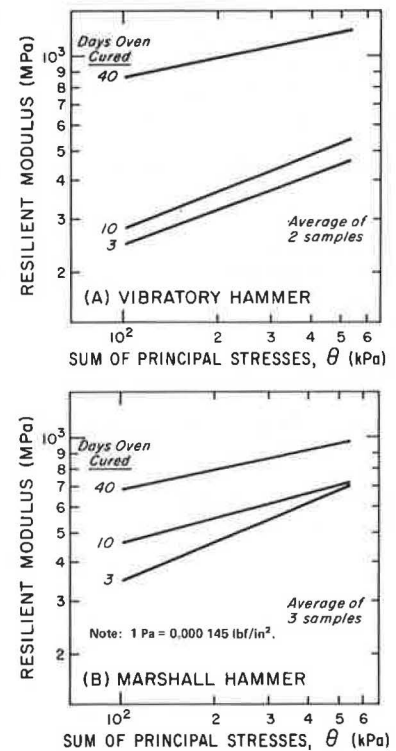
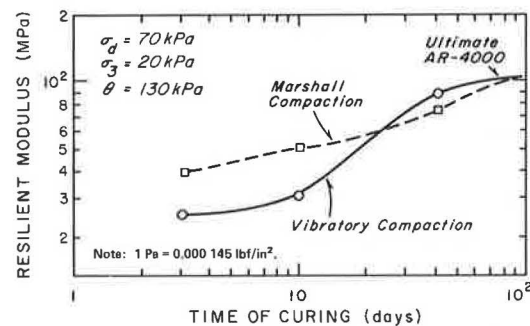


Figure 8. Resilient modulus versus curing time for specimens prepared by using Marshall and vibratory compaction procedures.



not cure in a uniform fashion. The smaller 6×10-cm (2.5×4-in) sample size used in the diametral procedures would probably cure more uniformly. Since all samples were cured in a membrane, curing could only take place at the exposed ends; this apparently led to the uneven curing.

2. LVDT clamps—In all tests conducted at Oregon State University, the load clamps were fastened to the sample of open-graded mix at the quarter points. It was sometimes difficult to position the LVDTs without causing some binding between the LVDT core and the LVDT itself. Part of this problem can probably be eliminated by using more rigid clamps.

Although there were variations of stiffness development for a given sample and also variations in modulus between samples for a given condition and duration of cure, the results of average sample results show the expected trend—a gradual increase in stiffness with time.

Effect of Type of Curing

The type of curing had an effect on the rate of stiffness

development in the open-graded emulsion mix. Samples cured at 24°C and 38°C (75°F and 100°F) exhibited a more rapid gain in stiffness than those cured at 5°C (40°F) regardless of stress conditions. This effect, which is shown in Figure 9, indicates that projects placed during late fall or in areas where the temperature may remain around 5°C would not be expected to gain in stiffness at a very rapid rate. In fact, the stiffness at the end of 90 days of curing at 5°C is less than 50 percent that of the ultimate modulus. But this does not necessarily mean more damage or a need for thicker layers because, as we will show, the modulus would be higher if measured at 5°C.

Effect of Density

Test results presented earlier were performed on sam-

Figure 9. Effect of type of curing on rate of stiffness development.

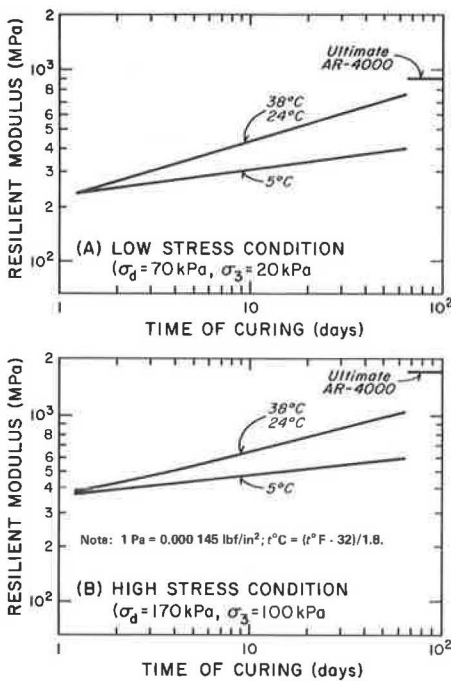
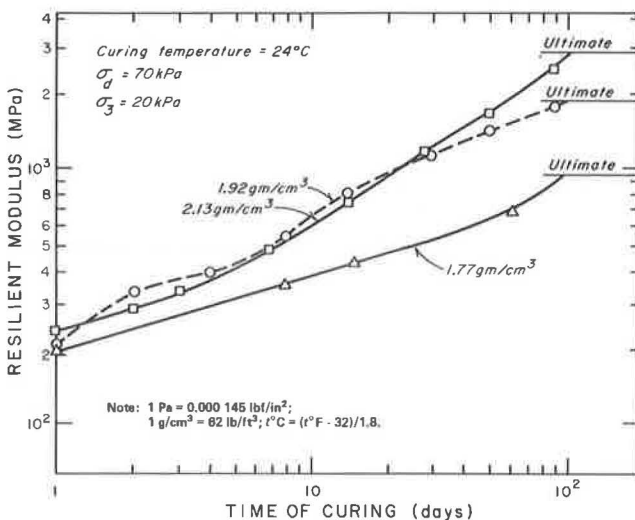


Figure 10. Resilient modulus of open-graded emulsion mixes versus curing time.



ples prepared to a density of approximately 1.77 g/cm³ (110 lb/ft³). Results from the survey of field performance indicated that an average density for open-graded emulsion mixes is about 1.93 g/cm³ (120 lb/ft³).

Tests were run by Chevron Research Company on mixes similar to those tested at Oregon State University but at densities considerably higher than 1.77 g/cm³ (110 lb/ft³). Densities used in the Chevron study were approximately 1.92 and 2.13 g/cm³ (119 and 132 lb/ft³). The average moduli for samples tested at approximately 69-kPa (10-lbf/in²) repeated stress (σ_d) and 21-kPa (3-lbf/in²) confining pressure (σ_3) are shown in Figure 10 together with the Oregon State University data for samples compacted to 1.77 g/cm³. In all instances, the modulus increased with time of curing and with level of density. The rate of development, however, varied slightly.

The results shown in Figure 10 were also used to develop a family of curves to show the variation in resilient modulus of open-graded emulsion mixes with density (Figure 11). This family of curves shows the dramatic effect of time of curing and density on stiffness. At 1.77 g/cm³ (110 lb/ft³), the modulus would range from approximately 483 to 966 MPa (70 000 to 140 000 lbf/in²), whereas at high levels of density [2.3 g/cm³ (132 lb/ft³)], the modulus would range from 1725 to 2760 MPa (250 000 to 400 000 lbf/in²). This emphasizes the importance of achieving a good density in this type of mix, particularly if stiffness is any indicator of good performance.

Effect of Type of Compaction

The limited number of tests performed on samples prepared to the same density by means of different compaction techniques indicated that there is a substantial effect on stiffness at the early stages of curing. Figure 8 shows that at early stages of curing samples prepared by using an impact hammer yield a higher stiffness than those compacted by a vibratory hammer. After approximately 20 days of curing, the stiffness values are similar, and both approach the ultimate value of the AR-4000 open-graded hot mix.

This indicates the importance of the type of compaction in the development of stiffness in emulsion mixes. Exclusive use of vibratory compactors may lead to tender mixes at early stages of curing. Beyond 20 days, however, there appears to be no significant difference

Figure 11. Resilient modulus of open-graded emulsion mixes versus density.

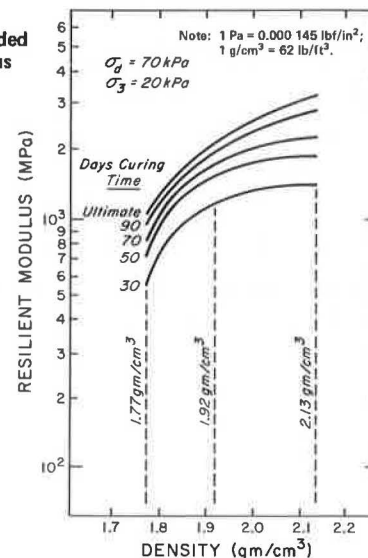
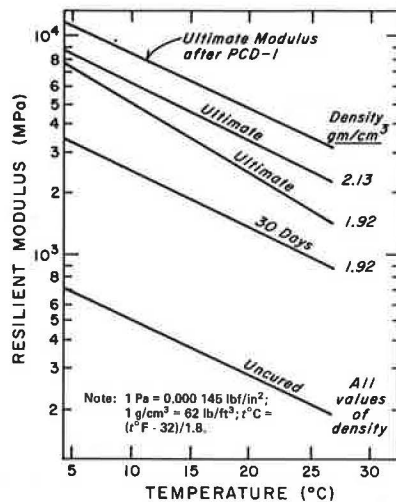


Figure 12. Resilient modulus versus test temperature.



between the stiffness values obtained for the different types of compaction. Further study in this area is certainly warranted.

Effect of Temperature

Limited tests were also performed to establish the effect of temperature on the modulus of open-graded emulsion mixes. Chevron Research Company performed tests on mixes at 23°C and 5°C (73°F and 40°F). Results of these tests are summarized in Figure 12. Note that the average ultimate modulus at 23°C and at a density of 2.13 g/cm³ (132 lb/ft³) is approximately 2827 MPa (410 000 lbf/in²). Samples prepared at a density of 1.92 g/cm³ (119 lb/ft³) had an average modulus of approximately 1965 MPa (285 000 lbf/in²). The modulus of samples tested at 5°C ranges from 6895 to 9239 MPa (1 000 000 to 1 340 000 lbf/in²), depending on density. The results obtained for open-graded emulsion mixes at a high level of density compare very favorably with the variation in modulus with temperature of dense-graded asphalt mixes reported by the Asphalt Institute (9). As density is lowered to 1.92 g/cm³, the slope of the temperature-stiffness relation for open-graded emulsion mixes is not very different from that for conventional mixes. By assuming relatively constant slopes for different stages of curing, stiffness-temperature relations were also developed for 0 and 30 days of curing. This relation still needs verification.

Comparison of Laboratory and Field Modulus Values

The average density of all cores was 1.95 g/cm³ (121 lb/ft³); the average modulus was 1806 MPa (262 000 lbf/in²) at a confining pressure of 21 kPa (3 lbf/in²). From Figure 11, the laboratory-determined modulus at $\sigma_3 = 21$ kPa would vary from 1806 to 2275 MPa (180 000 to 330 000 lbf/in²), depending on the duration of curing. It therefore appears from this limited test program that results for laboratory-prepared samples are very similar to those for field cores.

CONCLUSIONS

Open-graded emulsion mixes exhibit different rates of

development of resilient modulus for different curing conditions. The final resilient modulus varies with curing conditions and is higher at higher curing temperatures. The highest resilient modulus is obtained by using a vacuum-cure procedure. This value for modulus also appears to compare well with the average modulus determined on cores taken from 14 projects. Further testing should be undertaken before this conclusion is assumed to be valid.

The variation in the development of modulus with temperature demonstrates the need to consider environmental conditions when designing and working with emulsion mixes. This work is not of adequate scope to be used to predict environmental effects on curing and modulus development. More work, including considerations of mix density, cure temperature, and humidity, would be necessary to predict environmental effects adequately.

ACKNOWLEDGMENT

We wish to express our gratitude to Region 6 of the U.S. Forest Service, whose financial assistance made this research possible. We would also like to express appreciation for the assistance received from the Federal Highway Administration, Chevron USA, Inc., and Chevron Research Company and for the cooperation of the various agencies that furnished the needed materials and information.

REFERENCES

1. E. S. Richardson and W. A. Liddle. Experience in the Pacific Northwest with Open Graded Emulsified Asphalt Pavements. Federal Highway Administration, U.S. Department of Transportation, Implementation Package 74-3, July 1974.
2. R. K. Williamson. Status Report on Emulsified Asphalt Pavements in Region 6, the U.S. Forest Service. U.S. Forest Service, Portland, OR, Feb. 1976.
3. Transportation Engineering Handbook: Chapter 50—Pavements. U.S. Forest Service, Jan. 1974.
4. D. R. Hatch and R. G. Hicks. Performance of Open Graded Emulsion Mixes. Department of Civil Engineering, Oregon State Univ., Corvallis, Jan. 1977.
5. R. J. Schmidt. A Practical Method for Measuring the Resilient Modulus of Asphalt-Treated Mixes. HRB, Highway Research Record 404, 1972, pp. 22-32.
6. I. V. Kalcheff and R. G. Hicks. A Test Procedure for Determining the Resilient Properties of Granular Materials. Journal of Testing and Evaluation, Vol. 1, No. 6, Nov. 1973, pp. 474-475.
7. R. G. Hicks, J. Walter, L. Bodyfelt, and C. Cutting. A Test Procedure to Characterize the Elastic Behavior of Open Graded Emulsion Mixes. Oregon State Univ., Dec. 1976.
8. H. B. Seed and J. W. N. Fead. Apparatus for Repeated Loading Tests on Soils. ASTM, Special Tech. Publ. 254, 1959.
9. Interim Guide to Full Depth Asphalt Paving Using Various Asphalt Mixes. Pacific Coast Division, Asphalt Institute, Sacramento, CA, 1976.

Effects of Textures and the Aggregates That Produce Them on the Performance of Bituminous Surfaces

J. J. Henry, Pennsylvania State University, University Park
S. H. Dahir, Pennsylvania State University, Middletown

Results of a Pennsylvania State University study of the characteristics of pavement surface textures and the aggregates that produce them are reported. The primary requirements of bituminous surfaces are durability and safety. Surface microtexture induces high levels of friction at low vehicle speeds, and surface macrotexture facilitates the drainage of water from the tire-pavement interface and reduces glare and splash and spray. Aggregate gradation largely determines the design of pavement surfaces. It is concluded that, to retain microtexture, the aggregate must contain a high proportion of hard mineral content embedded in a softer matrix or be composed predominantly of sharp, hard crystals well cemented in a porous configuration. To provide and retain adequate macrotexture, aggregate particles must be hard and tough and 3 to 19 mm (0.12 to 0.75 in) in size. Angular, bulky particles perform better than rounded, flaky particles. Textures that improve skid resistance on wet surfaces were found to reduce glare and splash and spray, thereby increasing the safety of the surface.

Criteria for pavement surfaces vary according to different driver situations and environmental requirements, particularly in some critical urban sections. Obviously, in all situations it is desirable to construct the most economical surface, one that will last the life span expected of it with the least need for maintenance and provide the safest and most comfortable built-in performance—i. e., a surface that will be durable and, when wet, will present minimal or no hazard in the sense of skidding or hydroplaning potential under normal use. It is also desirable that the same surfaces meet other criteria: least noise, least tire wear, minimal energy consumption through minimal rolling resistance, minimal splash and spray, and no glare or other detrimental color-related effects.

Satisfactory fulfillment of some of these criteria, such as those associated with glare and splash and spray, may be compatible with the attainment of the primary requirements of wear resistance and skid resistance and may present little or no problem. Other requirements may not be attainable to a satisfactory degree unless the primary considerations of wear resistance and skid resistance are compromised or unless other measures, such as restrictions on speed and truck traffic, are taken. The use of studded tires is another factor that complicates problems of noise, rolling resistance, and wear and the hydroplaning potential associated with worn wheel tracks. Obviously, such factors require special consideration.

In this paper, the characteristics of surface textures and aggregates that will provide and retain skid resistance and wear resistance are discussed. Compatible factors such as light reflection, glare, and splash and spray, which are alleviated by the same aggregate and surface characteristics, are also briefly discussed.

SURFACE TEXTURE

To provide safe vehicle travel by providing built-in

safeguards against skidding and hydroplaning and to alleviate other surface-related problems such as glare and splash and spray, a pavement surface must possess and maintain an adequate surface texture throughout its useful life.

Relation Between Skid Resistance and Pavement Texture

When water is present on the road surface, it forms a lubricating film between the tire and the pavement and thus reduces the direct contact between them. Therefore, wet-pavement friction is less than dry-pavement friction.

As vehicle speed increases, it becomes more difficult for water to escape from under the tire. This water acts as a lubricant, and skid resistance decreases. The rate of decrease of skid resistance with speed varies for different surfaces. Some pavements may have high skid resistance at low vehicle speeds but relatively low skid resistance at high vehicle speeds. On the other hand, some pavements have intermediate skid resistance at low speeds but maintain adequate resistance as speed increases.

The measure of skid resistance is the skid number (SN), which is defined as 100 times the coefficient of friction measured in accordance with ASTM E 274. The variation of skid number with speed is specified by the skid number gradient (SNG) or the percentage normalized gradient (PNG). SNG is defined as the rate of decrease in skid number with increasing speed, and PNG is defined as the percentage of the rate of decrease in skid number with increasing speed.

Skid number is a function of surface texture. Pavement texture is subdivided into macrotexture and microtexture. Macrotexture, which is a function of aggregate gradation, provides passages for water to escape from the tire-pavement interface. Microtexture, which is a function of the asperities and surface roughness of individual aggregate particles, penetrates the water film to provide direct contact with the tire. A surface that has good microtexture ensures a high skid number at low speeds. Macrotexture becomes more important as speed increases. The combined effects of macrotexture and microtexture interact to provide adequate skid resistance at high speeds. These effects were reported by Kummer and Meyer (1), who concluded that at low speeds skid number is determined by microtexture and at high speeds by both microtexture and macrotexture.

Model for Skid Number-Speed Relation

To establish the relation between pavement texture and skid number at any speed, it is necessary first to

establish a model for skid-number behavior with speed. In a study at Pennsylvania State University, three models were considered; the following was chosen on the basis of its suitability for subsequent correlation with texture data:

$$SN = ac^{-bV} \quad (1)$$

where a and b are constants and V is the test speed.

To test the ability of this model to fit actual data over a wide range of test speeds, SN data collected during the 1976 test season on six pavements at test speeds from 16 to 80 km/h (10 to 50 mph) were used. Least-squares regression analyses produced the results shown in Figure 1. It can be seen that the model fits the data extremely well within the precision of the test procedure. For this model, the parameter b is proportional to PNG and therefore should be a function of macrotexture parameters only. PNG is independent of speed and is defined as

$$PNG = (-100/SN) [d(SN)/dv] \quad (2)$$

Rearranging and integrating from $V = 0$ to V ,

$$\int_{SN_0}^{SN_V} [d(SN)/SN] = - (PNG/100) \int_0^V dv \quad (3)$$

Figure 1. Skid number versus vehicle speed.

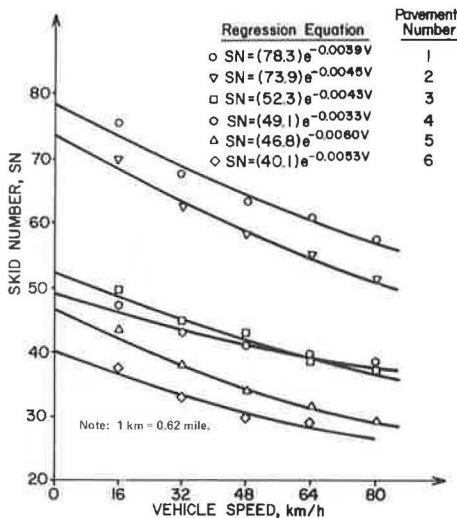


Table 1. Microtexture values.

Cutoff Frequency (cycles/m)	RMSH (μm)					
	Site 1	Site 2	Site 3	Site 4	Site 5	Site 6
400	30.5	29.7	32.1	16.9	24.2	27.7
500	28.0	27.5	28.4	15.2	21.7	22.4
630	23.8	23.8	24.5	14.2	19.8	20.2
800	20.8	19.8	21.5	13.1	17.7	17.4
1 000	18.4	17.7	17.6	12.0	15.5	15.2
1 250	16.0	17.0	15.6	11.3	13.4	12.4
1 630	13.9	14.8	13.4	10.6	11.2	10.6
2 000	11.7	12.6	11.4	10.2	9.5	8.9
2 500	9.6	11.1	9.3	9.1	8.0	7.5
3 150	7.8	8.8	7.5	8.1	6.6	5.7
4 000	6.4	7.3	5.9	7.4	5.3	4.6
5 000	5.1	5.7	4.8	6.9	4.2	3.66
6 300	4.1	4.5	3.9	6.1	3.38	2.95
8 000	3.25	3.66	3.07	5.5	2.72	2.36
10 000	2.49	3.10	2.46	5.0	2.13	1.88
12 500	1.93	2.62	2.03	4.4	1.68	1.52
16 300	1.50	2.16	1.68	3.94	1.30	1.24

Note: $1 \mu\text{m} = 0.039 \times 10^{-3}$ in.

This produces the proposed Pennsylvania State University model for skid resistance-speed behavior:

$$SN = SN_0 e^{-(PNG/100)V} \quad (4)$$

where SN_0 = the zero-speed intercept, a function of microtexture, and PNG = the percentage normalized gradient, a function of macrotexture. The significance of this finding is that it will separate the effects of microtexture and macrotexture if it is possible to obtain microtexture parameters that predict SN_0 and macrotexture parameters that predict PNG.

Measurement and Correlation of Texture Parameters and Skid Number

It has been customary to subdivide pavement texture into microtexture and macrotexture. The division between the two, however, has not yet been determined rationally. Power spectrum analysis (2) can produce 20 or more third-octave subdivisions of pavement texture, each of which provides a texture parameter. To aid in the evaluation of aggregates for paving systems, techniques that can be applied to small samples can provide information for selecting the geometrical configuration of aggregates. Profiling techniques and the British portable tester can be used on laboratory samples before and after polishing or abrasive wear.

To predict pavement performance, two texture parameters were selected for further evaluation by using the data of the 1976 test season at Pennsylvania State University. The two parameters were the root-mean-square texture heights (RMSH) of the microtexture and the macrotexture. In addition, the British pendulum number was considered as an alternative microtexture parameter. The value of RMSH for the microtexture depends on the lowest space frequency (f_c) considered in the microtexture. Table 1 gives the RMSH for cutoff frequencies from 400 to 16 300 cycles/m (10 to 410 cycles/in). These were computed from the power-spectrum-level data for the six surfaces by using the following relation:

$$RMSH(f_c) = \sqrt{\int_{f_c}^{\infty} S(f) df} = \sqrt{\sum_{i=c}^{\infty} S(f_i) \Delta f_i} \quad (5)$$

where

$S(f)$ = mean square spectral density;
 f_i = center frequency, i th third-octave band; and
 Δf_i = frequency interval of i th third-octave band.

A linear regression of RMSH at each cutoff frequency with the values of SN_0 from Figure 1 was performed. The correlation coefficients determined for each cutoff frequency are shown in Figure 2. The cutoff frequency with the highest correlation coefficient is 1630 cycles/m (41 cycles/in) [0.41-mm (0.016-in) wavelength] with 2000 cycles/m (50.5 cycles/in) [0.5-mm (0.02-in) wavelength] providing only slightly lower correlation. On the basis of this evidence, microtexture should be defined for skid-resistance purposes as consisting of asperities that are less than 0.5 mm wide. This is consistent with earlier observations in which the 0.5-mm width was suggested (3).

A least-squares regression analysis produced the following relation:

$$SN_0 = 9450(RMSH)_{2000} - 44.4 \quad (6)$$

Figure 2. Correlation coefficient between zero-intercept SN and RMSH at different cutoff frequencies.

Cutoff Frequency x 100	4	5	6.3	8	10	12.5	16.3	20	25	31.5	40	50	63	80	100	125	163
Correlation Coefficient	0.44	0.60	0.55	0.53	0.66	0.79	0.87	0.82	0.73	0.62	0.34	0.22	0.11	0.05	0.00	0.00	0.03

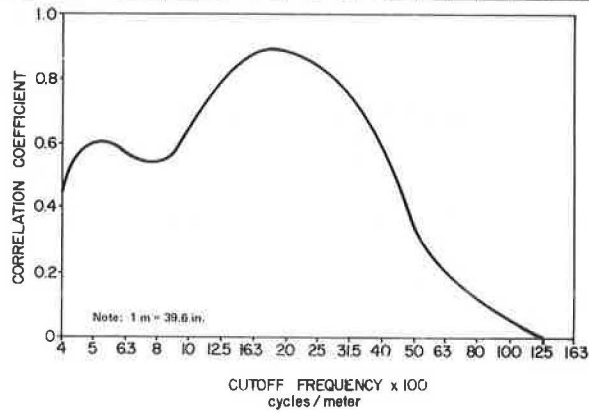
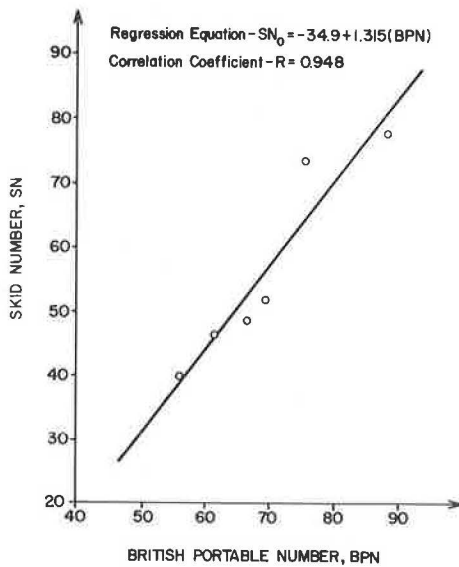


Figure 3. Zero-intercept SN versus BPN.



where $(RMSH)_{2000}$ is the root-mean-square height of the microtexture (in millimeters) with a cutoff frequency of 2000 cycles/m (50.5 cycles/in).

Correlation of SN_0 with British Portable Number

The British portable numbers (BPNs) of the test sites are given below:

Test Site	BPN
1	88.2
2	75.7
3	69.4
4	66.6
5	61.8
6	56.3

A very good correlation was observed between BPN and SN_0 , as shown in Figure 3. The correlation equation is

$$SN_0 = 1.315(BPN) - 34.9 \tag{7}$$

An analysis of 20 sites in West Virginia (4) provided a similar result:

$$SN_0 = 1.38BPN - 31 \tag{8}$$

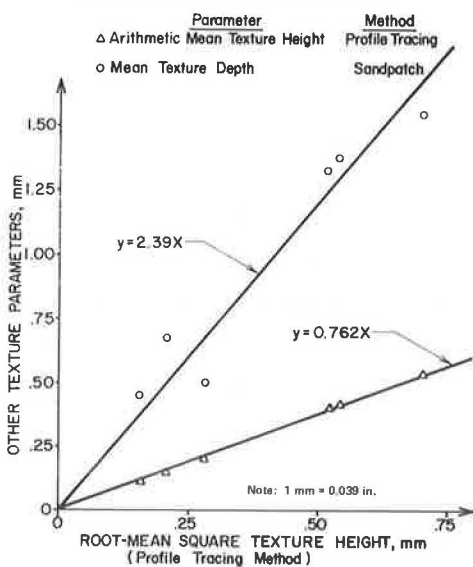
The good correlation of BPN with SN_0 indicates that BPN is sensitive only to the microtexture of the top surfaces of the aggregate. However, the profiling technique provides quantitative information on the size of the microtexture, which is useful in the selection of aggregates.

Correlations of PNG and RMSH Macrottexture

Macrottexture data from the six test sites in the study were obtained. RMSH and arithmetic mean height (AMH) were obtained by direct processing of the profile data. Sand-patch data for mean texture depth (MD) were also obtained. The strong correlation among these three parameters (see Figure 4) suggests that any one of them could be used as a macrottexture parameter with similar results. A correlation between RMSH and PNG was investigated by using a relation of the form $y = d_0x^{d_1}$. When data from a study on 20 pavements in West Virginia (4) are used, the following result is obtained:

$$PNG = 41RMSH^{0.52} \tag{9}$$

Figure 4. Relations of macrottexture values.



where RMSH is the root-mean-square height of the macrotexture in millimeters and the PNG units are given in hours per kilometer.

Prediction of Skid Resistance from Texture Parameters

By combining Equations 4, 6, and 9, SNs can be predicted from the RMSH of the microtexture ($RMSH_{2000}$) and the RMSH of the macrotexture.

Results from the larger data sample obtained in West Virginia (4) provide the following relation between skid resistance and texture parameters:

$$SN = (1.38BPN - 31)e^{-0.41VRMSH^{-0.52}} \quad (10)$$

Measured and predicted skid numbers are shown in Figure 5. When only sand-patch data (MD in millimeters) are available for macrotexture measurements, the correlation shown in Figure 4 can be combined with Equa-

Figure 5. Predicted SN versus measured SN.

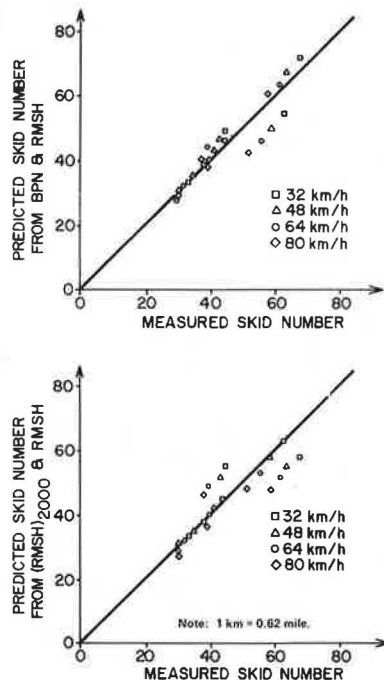
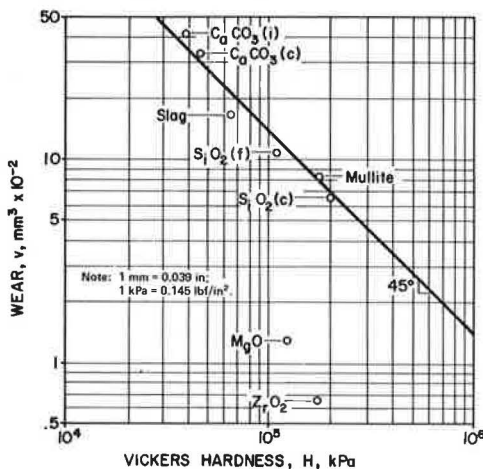


Figure 6. Log wear versus log hardness for minerals softer than SiO_2 abrasive.



tion 10 to estimate skid resistance according to the following equation:

$$SN = (1.38BPN - 31)e^{-0.65VMD^{-0.52}} \quad (11)$$

V in all equations is in kilometers per hour.

It should be pointed out that these relations (Equations 10 and 11) do not take into account the influence of seasonal variations. However, they do establish the influence of texture on skid resistance and provide insight into the requirements of texture for adequate skid resistance.

Thus, laboratory methods can be used to estimate skid numbers at any speed from representative samples of pavement systems. In designing aggregates for good skid resistance at low vehicle speeds, it is important to provide a high degree of microtexture in asperity scales below 0.5 mm (0.02 in). For high speeds, it is also important to provide large values of RMSH or MD. For aggregates that polish to a given BPN or to a known minimum $RMSH_{2000}$ (microtexture), the required macrotexture can be computed for a desired level of skid resistance at the design speed.

AGGREGATE CHARACTERISTICS

To meet the requirements of long-lasting, safe surfaces, the aggregates used in the surface must be able to retain high levels of surface texture by resisting undue wear and polishing under prevailing traffic and environmental conditions. Other considerations are often superimposed on these primary requirements. This discussion is concerned mainly with the primary requirements, but aggregate characteristics are also related to other factors that are compatible with the primary requirements and are improved when desirable surface aggregates are used.

Aggregate Properties That Resist Wear and Polishing

In a research effort at Pennsylvania State University, Stiffler (5) found mineral hardness to be the most important property in wear resistance (Figure 6). To resist wear, an aggregate must be composed of hard, strongly bonded, interlocking mineral grains such as, for example, most quartzites and diabases (6). To resist polishing under heavy traffic, an aggregate must be composed of a high proportion (50 to 70 percent) of hard mineral crystals (Mohs hardness > 5) embedded in a matrix of softer minerals such as sandstone, arkose, and other gritty aggregates (see Figure 7) (7). However, the mineral grains must be strongly bonded so that nondetrimental, slow differential wear will occur. Alternatively, the aggregate must be composed of all, or almost all, hard crystals well bonded in a porous configuration. The pores replace the softer matrix and allow irregular fracture and slow wear to occur. This process results in the maintenance of high friction without unduly rapid wear. Examples of aggregates in this group include calcined bauxite and some expanded slags, shales, and slates (8).

Other Aggregate Characteristics Required to Retain Surface Texture

Other characteristics that result in initial desirable surface textures and assist in maintaining them over the expected life of the surface include particle shape, size, and gradation (9). Bulky, angular particles will

Figure 7. BPN friction values (ASTM E 303 versus hard mineral content.

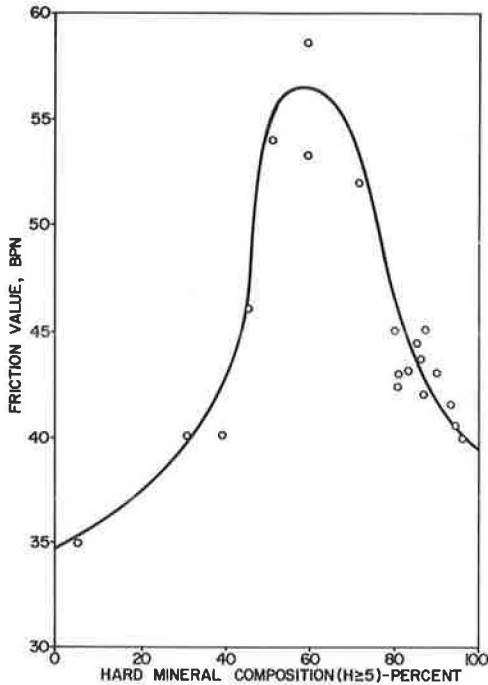
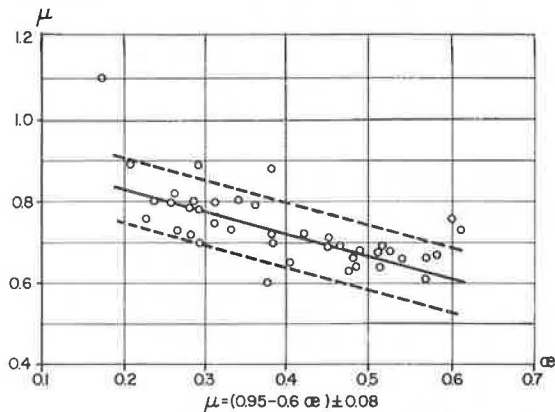


Figure 8. Correlation between skid resistance μ and reflective quality α .



obviously provide macrotextures that are superior to those that result from the use of flaky, rounded particles. The microtexture is largely a function of aggregate mineralogy. Aggregate gradation has a profound effect on the process of designing the macrotexture into the pavement surface. On high-speed highways, it has been found desirable to provide a high level of surface macrotexture to facilitate fast water drainage in the tire-contact area (10). A design for open-graded friction courses developed by personnel at the Federal Highway Administration and modified by others (11) has been widely accepted. To be highly effective, an open-graded surface must combine the desired macrotexture with a high level of microtexture. This is done by using crushed, polish-resistant, wear-resistant aggregates such as tough sandstone, graywacke, or hard expanded shale or slate.

A question often arises as to what size of particles and what size of grains within each particle will result in optimum surface designs. There appears to be a consensus among paving engineers and investigators

that, where coarse aggregate is used, particle size should be in the range passing the 19-mm (0.75-in) sieve and retained on the 2.36-mm (no. 8) sieve. It has been shown that, in this range, halving the nominal maximum size raises the skid number by about eight units (12, 13).

An important part of the process of finding adequate solutions for pavement surface designs is to ensure that performance will be maintained over the design life of the surface. Often, aggregate property requirements for providing skid resistance and wear resistance are not compatible. For example, some wear must occur continuously so that skid resistance is maintained at adequate levels. To reach and maintain high levels of skid resistance and wear resistance, however, aggregates must be sought that have properties that will largely satisfy both requirements. The table below (14) gives target values for such aggregate properties (1 $\mu\text{m} = 0.039 \times 10^{-3}$ in; 1 mm = 0.039 in):

Property	Range
Mohs hardness	
Hard fraction	8-9
Soft fraction	6-7
Minimal differential hardness	2-3
Percentage of hard fraction	
Natural aggregate	50-70
Artificial aggregate	20-40
Hard grains or crystals	
Size (μm)	150-300, avg 200
Shape	Angular tips ($<90^\circ$)
Percentage porosity (vesicularity)	25-35
Optimum pore size (μm)	125
Aggregate particles	
Size (mm)	3-13
Shape	Conical, angular ($<90^\circ$)
Los Angeles abrasion (%)	<20
Aggregate abrasion value (%)	<8
Aggregate impact value (%)	<20
Polished stone value (BPN)	>75

OTHER EFFECTS OF TEXTURE AND AGGREGATE ON SURFACE PERFORMANCE

In designing a surface to be primarily wear- and skid-resistant, the designer can include other highly desirable performance considerations in the design without compromising the primary objectives. Two such considerations that pertain to driving safety are (a) light reflection and glare and (b) splash and spray.

Light Reflection and Glare

Generally, daytime driving poses no serious problems of light reflection or glare except when a wet pavement reflects dazzling sun rays. Problems of light reflection and glare are principally related to night visibility, particularly on wet pavement surfaces. Work has been done by Fredsted in Denmark on the problem of nighttime light reflection on pavements (an informative 1965 report by Fredsted, the source of which is not known, is titled Road Surfaces' Influence on Road Safety). Fredsted states that light reflections may be diffuse, preferential, or retroreflective and that the latter category is not applicable to road surfacings. He states further that preferential reflections may cause dazzling and uneven distribution of luminance, which produces a mirror-like effect on water film. This can be avoided only by using a coarse-textured surface that permits surface asperities to penetrate the water film. Fortunately, coarse-textured surfaces are also required to improve skid resistance.

Figure 8, taken from Fredsted's work, indicates

Table 2. Effect of surfaces on spray.

Site	Surface	Avg Quantities of Spray Collected (g)	
		Experiment 1	Experiment 2
1	Fine cold asphalt to British Standard 1690 using blast-furnace slag aggregate, impervious	87	93
2	Hot-rolled asphalt to British Standard 594 with 12-mm chippings rolled into surface, impervious	111	133
3	Bridport surface dressing made with 10-mm rounded gravel, impervious	76	71
4	Meldon surface dressing made with 10-mm chippings, impervious	66	75
5	Mixed aggregate, bitumen-macadam to British Standard 1621 with 10-mm rounded gravel and crushed quartzite, slightly pervious	-	107
6	Quartzite, bitumen-macadam to British Standard 1621 with 10-mm crushed quartzite, pervious	0	-

Note: 1 mm = 0.039 in.

that surfaces that exhibit the least preferential reflection offer the highest skid resistance. Fredsted also found that the diffuse reflective qualities of light decrease substantially when the road surface becomes wet. Using light-colored aggregates in bituminous surfaces was found to alleviate this problem. A blend that contained 30 percent light-colored coarse aggregate (e.g., Synopal) in a darker mass was found to be effective in producing color contrast to assist the driver in perceiving the roadway for a safe distance [50 to 100 m (160 to 320 ft)], particularly if the light-colored aggregate protrudes 0.6 mm (0.024 in) or more above the darker aggregate. Furthermore, it was found that this color-contrast effect applies to white stripes as well.

As a result of studies on surface-reflection characteristics in the United Kingdom, Sabey (15) concluded that all evidence points toward the need for macroscopically rougher textures to improve both skid resistance and visibility. Sabey added that other requirements include harshness of aggregates for skid resistance, harshness and angularity of projections for night visibility, and porosity of surface for general visibility. Marek and others (16) stated that reflective aggregates are desirable for contrasting the road surface and its surroundings provided the aggregate particles do not create a glare condition as, for example, do glassy particles.

In summary, it can be concluded that wet-road visibility can be improved and glare reduced by incorporating light-colored, nonshiny (nonglassy) aggregates in a coarse-textured, porous pavement surface.

Splash and Spray

Drivers will agree that splash and spray constitute an important problem that impairs visibility, especially at night. Accordingly, any improvement that contributes to the lessening of splash and spray contributes to driving safety.

Maycock (17) defined splash as large droplets of water that are associated with deep water or low speeds and are squeezed from the tire-contact area and thrown off the tire. He defined spray as an envelope of very fine droplets that are carried in the turbulent air stream around the vehicle and are associated with shallow water or high speed.

Several investigators in the United States, the United Kingdom, and other countries have studied various types and configurations of mudflaps to alleviate the problem of vehicle splash and spray on wet surfaces, but only a few have attempted to vary the surface texture. In fact, the only significant published works on this aspect of the problem that we could discover are those by Maycock (17) and Brown (18).

Performing tests on a "standard fine, cold asphalt" surface, Maycock found that, at a distance of 9 m (30

ft) behind a commercial vehicle, the amount of spray was very small at speeds lower than 48 km/h (30 mph) but increased substantially with increasing speed. In the range of 72-120 km/h (45-75 mph), the density of spray varied with speed according to the following equation (17, p. 6): Spray density = constant X (speed)^{2.6}.

Maycock made tests on six bituminous surfaces; four were impervious, one slightly pervious, and one very pervious (porous). The conclusion of the study was that the surface dressings performed slightly better than the smoother asphaltic surfaces. However, the very porous macadam surface was outstanding in reducing spray: Almost all of the water that fell onto the surface drained into it very quickly. Results of the experiments made on the six surfaces at 96 km/h (60 mph) are given in Table 2 (17, p. 8).

Brown (18) describes six experimental open-textured bituminous-macadam pervious surfacings, of which four had 19-mm (0.75-in) and two had 10-mm (0.4-in) nominal top-size coarse aggregate. All the surfaces were constructed with the same coarse and fine grit-stone aggregate. Brown's principal conclusion is that all six experimental pervious surfacings retained their spray-reducing properties after being subject to heavy traffic for almost two years even though there was a 20 to 50 percent reduction in permeability and about a 33 percent reduction in air voids. Brown points out that the sections had proper cross slope to prevent water puddles (which cause splash), and that air voids after traffic compaction were on the order of 20 percent.

The work of Maycock and Brown and observations by others (10) point up the significance of open-graded bituminous pavement surface texture in reducing splash and spray, glare, skidding risk, and the hydroplaning potential of wet surfaces at high speeds.

CONCLUSIONS

The following conclusions are supported by the findings reported in this paper:

1. To provide a skid-resistant bituminous surface, the surface must have and retain an adequate microtexture and, for high-speed travel, must also possess an adequate macrotexture.

2. For skid-resistance purposes, it was found that texture components with a wavelength of less than 0.5 mm (0.02 in) can be considered microtexture and those with a wavelength of 0.5 mm or greater can be considered macrotexture.

3. To provide and retain the microtexture, surface aggregate must be polish resistant, i.e., have a high proportion of hard mineral crystals embedded in a softer matrix, as in sandstone, or have hard crystals well cemented in a porous configuration, as in calcined bauxite and expanded slag. To provide and retain the

macrotecture, aggregate particles must be hard, tough, bulky, preferably angular, and 3 to 19 mm (0.12 to 0.75 in) in size. Aggregate gradation determines the design of surface texture.

4. There are various methods for measuring texture. Those found most useful at Pennsylvania State University include profile tracers for both microtexture and macrotecture, the British pendulum tester for microtexture, and the sand-patch method for macrotecture.

5. By using regression equations developed at Pennsylvania State University, skid number at zero speed can be estimated from BPN microtexture measurement (Equation 8). Skid number at any speed can be estimated from BPN and a macrotecture measurement (Equation 12).

6. Textures that provide skid-resistant wet surfaces also reduce glare, splash and spray, and the potential of hydroplaning.

7. High levels of skid and wear resistance can be achieved and can be maintained over the design life of a bituminous pavement surface if the target values for aggregate properties (14) can be achieved.

ACKNOWLEDGMENT

This paper is based on research sponsored by the Federal Highway Administration, U.S. Department of Transportation. The work was conducted at the Pennsylvania Transportation Institute, Pennsylvania State University. Several faculty members and students aided in the research. Many valuable suggestions during the conduct of the research were contributed by J. M. Rice of the Office of Research, Federal Highway Administration.

The contents of this paper reflect our views and we are responsible for the facts and accuracy of the data presented. The contents do not necessarily reflect the official views or policies of the Federal Highway Administration. This paper does not constitute a standard, specification, or regulation.

REFERENCES

1. H. W. Kummer and W. E. Meyer. Tentative Skid Resistance Requirements for Main Rural Highways. NCHRP, Rept. 37, 1967.
2. J. M. Lawther and J. J. Henry. Characterization of Pavement Macrotecture by Profile Spectral Analysis. National Bureau of Standards, U.S. Department of Commerce, Final Rept., 1974.
3. J. M. Rice. Seasonal Variations in Pavement Skid Resistance. Public Roads, Vol. 40, No. 49, March 1977.
4. M. C. Leu and J. J. Henry. Prediction of Skid Resistance as a Function of Speed from Pavement Texture Measurements. TRB, Transportation Research Record 666, 1978, pp. 7-11.
5. A. K. Stiffler. Relations Between Wear and Physical Properties of Roadstones. In Control of Pavement Slipperiness—Asphalt Pavement Cracking, HRB, Special Rept. 101, 1969, pp. 56-68.
6. S. H. Dahir and W. E. Meyer. The Polishing Characteristics of Common Rock Types Used as Aggregate in Bituminous Pavement Surfaces. Journal of Testing and Evaluation, ASTM, Vol. 6, No. 1, Jan. 1978, pp. 52-59.
7. S. H. Dahir and W. G. Mullen. Factors Influencing Skid Resistance Properties. HRB, Highway Research Record 376, 1971, pp. 136-148.
8. J. R. Hosking. Aggregates for Skid Resistant Roads. Transport and Road Research Laboratory, Crowthorne, Berkshire, England, Rept. LR693, 1976.
9. F. J. Benson. Effects of Aggregate Size, Shape, and Surface Texture on the Properties of Bituminous Mixtures—A Literature Survey. In Effects of Aggregate Size, Shape, and Surface Texture on Properties of Bituminous Mixtures, HRB, Special Rept. 109, 1970, pp. 12-22.
10. Guidelines for Skid Resistant Pavement Design. AASHTO, Washington, DC, 1976.
11. Open-Graded Friction Courses for Highways. NCHRP, Synthesis of Highway Practice 49, 1978.
12. J. R. Hosking. The Effect of Aggregate on the Skidding Resistance of Bituminous Surfacing: Factors Other than Resistance to Polishing. Transport and Road Research Laboratory, Crowthorne, Berkshire, England, Rept. 553, 1973.
13. W. G. Mullen, S. H. Dahir, and N. F. El-Madani. Laboratory Evaluation of Aggregates, Aggregate Blends, and Bituminous Mixes for Polish Resistance. TRB, Transportation Research Record 523, 1974, pp. 56-64.
14. S. H. Dahir. Petrographic Insights into the Susceptibility of Aggregates to Wear and Polishing. TRB, Transportation Research Record 695, 1979, pp. 20-27.
15. B. E. Sabey. Accidents: Their Cost and Relation to Surface Characteristics. Presented at a Symposium of the Cement and Concrete Assn., Birmingham, England, Nov. 1973.
16. C. R. Marek and others. Promising Replacements for Conventional Aggregates for Highway Use. NCHRP, Rept. 135, 1972.
17. G. Maycock. The Problem of Water Thrown Up by Vehicles on Wet Roads. British Road Research Laboratory, Crowthorne, Berkshire, England, Rept. 4, 1966.
18. J. R. Brown. Pervious Bitumen-Macadam Surfacing Laid to Reduce Splash and Spray at Stonebridge, Warwickshire. Transportation and Road Research Laboratory, Crowthorne, Berkshire, England, Rept. LR536, 1973.

Publication of this paper sponsored by Committee on Characteristics of Bituminous-Aggregate Combinations to Meet Structural Requirements.

Skid Resistance of Bituminous-Pavement Test Sections: Toronto By-Pass Project

J. Ryell, J. T. Corkill, and G. R. Musgrove, Ontario Ministry of Transportation and Communications, Downsview

As part of a program to determine the most suitable method of improving the driving qualities of Canada's Highway 401 Toronto By-Pass, 18 bituminous test sections were constructed in 1974 on the existing concrete pavement. The test sections include dense-graded and open-graded bituminous mixes that contain a variety of aggregate types including traprock, steel slag, and blast-furnace slag. A comprehensive test program in which the skid characteristics of various test sections were monitored by brake-force and side-force skid trailers and texture was analyzed by use of photo-interpretation techniques is described. Skid resistance was measured in weather conditions that varied from drizzle to slush from heavy snow by using a continuously recording side-force-friction trailer. Not all of the mixes have provided the required level of skid resistance, particularly in the driving lane and the center lane where large numbers of trucks travel. The most striking results of the project are (a) the excellent performance of bituminous mixes that contain crushed traprock or slag screenings as the fine aggregate and (b) the low skid resistance of many mixes in which the fine aggregate consists of natural sand blended with limestone screenings. All mixes were characterized by a general decline in skid resistance during the first four years as texture depths were reduced by compaction under traffic. The first phase of pavement improvement on the Toronto By-Pass, in which bituminous overlays were used with an open-graded surface-course mix, is described. Data on mix composition, skid resistance, and noise characteristics are also presented.

In its present form, the pavement of the Highway 401 Toronto By-Pass is the result of an extensive reconstruction program carried out between 1963 and 1973 when the original 4-lane pavement was widened to a 12-lane system of collector and express lanes. Exposed concrete pavement was chosen for this highway because it showed the best potential for providing a long service life under anticipated heavy traffic conditions. Traffic on the freeway has increased dramatically in recent years: Traffic on the central section between Dufferin Street and Keele Street increased from 111 000 vehicles/day in 1967 to 199 000 vehicles/day in 1976.

The original surface texture of the concrete pavement on the freeway provided satisfactory skid resistance in its early life. Unfortunately, the use of tungsten carbide studs on tires between 1966 and 1971 rapidly wore away the original surface texture, exposing the limestone aggregates in the concrete. Heavy traffic has since polished the surface and produced a pavement with a texture depth that is only about one-tenth of that desired.

In the summer of 1974, 18 bituminous-overlay test sections were constructed on a 2.4-km (1.5-mile) section of the westbound express lanes immediately west of the Allen Expressway. The project evaluated traditional dense-graded and open-graded mixes with varied stone contents. Coarse aggregates were selected on the basis of their anticipated high resistance to polishing; they consisted of traprock (a very hard, fine-grained basaltic quarried material), blast-furnace slag, and steel slag. Natural sand, limestone screenings, traprock screenings, and slag materials were used as the fine aggregates, and in some mixes blends of two materials were used. Other test mixes included sand asphalts that contained small fractions of coarse aggregate and a mastic type of bituminous mix. An asbestos filler was added to some mixes.

The objective of the project was to determine the most suitable bituminous surface-course mix for future short- and long-term programs to improve the driving quality, and especially the skid resistance, of the pavement. This paper describes the mix design and materials and the performance and properties of the test sections during the first four years of service. In the first phase of pavement improvement on the Toronto By-Pass in 1976, 1977, and 1978, an open-graded bituminous surface-course mix was used that contained traprock aggregates. The skid-resistance measurements and noise characteristics of this mix are reported.

BITUMINOUS TEST SECTIONS

Materials and mix proportions for the bituminous test sections were selected on the basis of the experience of the Ontario Ministry of Transportation and Communications with the skid resistance of freeway surface-course layers, a review of mixes used by other agencies, and an earlier, small pilot project to determine the practicality of using several special mixes. Seventeen mixes were evaluated in single-course thicknesses of 25 or 38 mm (1 or 1.5 in). Test section 1-19 was a repeat of section 1 but was placed over a 38-mm-thick bituminous base-course layer. Each test section was 137 m (448 ft) long and 16 m (52 ft) wide [11-m (36-ft) pavement plus 5-m (16-ft) shoulders]. A previous paper (1) has described the construction and skid-resistance performance of the test sections during the first year.

The composition and characteristics of the test mixes are given in Tables 1 and 2, and the aggregate gradations used in several sections are shown in Figures 1-3. The type of surface-course mix specified for main highways in Ontario—known as HL1—is a dense-graded mix in which crushed traprock, a very hard, fine-grained basaltic quarried material, is used as the coarse aggregate.

Test sections 1 to 6 consist of HL1 mixes in which the coarse-aggregate content is progressively increased to obtain a greater density of stone particles at the surface. The mix used in test section 1 is typical of many HL1 mixes used on main highways in Ontario. The type of fine aggregate used in these six sections was varied since the composition and percentage of such material are known to have a marked effect on the initial texture and stability of the mix. The mixes that contain traprock screenings as the fine aggregate used a lower content of asphalt cement than mixes that contain a natural sand. Short-fiber asbestos filler was added to mixes 5 and 6 to increase the flexibility of the bituminous overlay and to provide better resistance to reflective cracking from the concrete pavement base.

Test sections 7 to 10 are termed modified HL1 mixes since slag coarse aggregates were used in place of the normal traprock stone. Slag aggregates have been used with success in surface-course bituminous mixes in Europe and North America, and Fromm and Corkill (2) have reported on their performance on small test sections in Ontario. The materials used in these sections

came from the steel industry in Hamilton, Ontario.

Steel-making slag is the term used to describe material that results from the production of steel from iron in open-hearth, basic-oxygen, and electric-arc furnaces. The crushed particles are hard and coarse textured and have a higher unit weight than do natural aggregates. Test section 7 used steel-slag screenings as the fine aggregate in conjunction with the slag coarse aggregate. In section 8, a blend of natural sand and limestone screenings was mixed with the slag coarse aggregate.

Blast-furnace slag describes material that results from the manufacture of iron from iron ore, limestone, and coke in blast furnaces. The product is air cooled before crushing and screening, and the surface of the particles has a rough, vesicular appearance. Test section 9 used blast-furnace slag screenings as the fine aggregate in conjunction with slag coarse aggregate, and in section 10 the fine aggregate consisted of a blend of natural sand and limestone screenings. Because of its higher absorption characteristic, blast-furnace slag requires more asphalt cement than other aggregates.

Bituminous mixes in test sections 11 and 12 can be described as sand-asphalt mixes that use traprock screenings as the fine aggregate. Both mixes contained

small percentages of coarse aggregate in the form of 6-mm (0.25-in) traprock chips and asbestos-fiber filler.

Test sections 13 to 16 consist of open-graded mixes designed for high permeability to facilitate rapid drainage of surface water into, and laterally through, the surface-course layer. Open-graded mixes have been used in North America since the 1950s (3). These mixes use a combined aggregate grading with a large fraction of single-sized coarse aggregate and a relatively small amount of material passing the 2.36-mm (no. 8) sieve. The smaller-sized material plus the asphalt cement fills only a portion of the voids created by the single-sized coarse aggregate, and this results in a mix with a large volume of voids. The traprock aggregates used in the four mixes were processed to meet the special requirements of open-graded bituminous mixes (Figure 3). Traprock screenings were washed to reduce the fraction of material passing the fine sieves, and the material in the coarse aggregate retained on the 10-mm (0.375-in) sieve was screened off. Mixes 13 and 14, which contain 67 percent coarse aggregate and had 12.2 percent pavement voids after three months in service, meet the requirements for open-graded mixes established for the project.

Table 1. Composition of test mixes.

Test Section	Type of Mix	Coarse Aggregate Retained on 4.75-mm Sieve		Fine Aggregate Passing 4.75-mm Sieve		Filler Material		Percent Retained on 4.75-mm Sieve ^a	Asphalt (percent by weight of mix)	
		Type	Percent	Type	Percent	Type	Percent			
1	HL1									
	L	TR	45	41	41			43.8	5.4	
	F			LS	14				5.4	
2	HL1									
	L	TR	45	NS	41			48.2	5.4	
	F			TRS	14				5.3	
3	HL1									
	L	TR	45	TRS	55			47.5	4.1	
	F								4.0	
4	HL1									
	L	TR	55	NS	34			54.1	4.8	
	F			LS	11				4.8	
5	HL1									
	L	TR	60	NS	28	ASB	2	58.1	5.6	
	F			LS	10				5.7	
6	HL1									
	L	TR	60	TRS	38	ASB	2	62.3	5.3	
	F								5.4	
7	Modified HL1									
	L	SL	45	SLS	55			46.8	5.3	
	F								5.2	
8	Modified HL1									
	L	SL	50	NS	38			47.1	5.7	
	F			LS	12				5.7	
9	Modified HL1									
	L	BF	45	BFS	55			43.2	8.0	
	F								7.8	
10	Modified HL1									
	L	BF	40	NS	45			40.5	6.8	
	F			LS	15				6.5	
11	Sand									
	L	TR	14	TRS	84	ASB	2	5.4	7.1	
	F								7.0	
12	Sand									
	L	TR	9	TRS	89	ASB	2	6.9	7.0	
	F								7.2	
13	Open-graded, F	TR	67	TRS	33			60.5	5.9	
	14	Open-graded, F	TR	67	TRS	31	ASB	2	71.7	5.8
		15	Open-graded, F	TR	30	TRS	70			29.3
16			Open-graded, F	TR	30	TRS	68	ASB	2	31.4
	17		Mastic, F	TR	70	TRS	19	MF	9	75.2
		1-19 ^b	HL1							
L			TR	45	NS	41	ASB	2	47.4	5.4
F				LS	14				5.4	

Notes: 1 mm = 0.039 in.

L = laboratory mix designs, F = field-laboratory tests, TR = traprock, LS = limestone screenings, NS = natural sand (glacial deposit), TRS = traprock screenings, ASB = short-fiber asbestos, SL = steel slag, SLS = steel-slag screenings, BF = blast-furnace slag, BFS = blast-furnace-slag screenings, and MF = mineral filler (finely crushed limestone).

^aBased on field-laboratory extraction tests.

^bSame as section 1 but constructed over a 38-mm-thick bituminous base course.

Mixes 15 and 16, which contain 30 percent coarse aggregate, cannot be categorized as open-graded mixes since the pavement void contents—6.7 and 7.2 percent, respectively—are much lower than those generally specified for such mixes.

Test section 17 consists of a mastic type of mix based on the German Gussasphalt technology (4) and modified so that the material could be mixed and placed by conventional hot-mix plant and paving equipment. Machine-laid Gussasphalt has been widely used on the German Autobahn system since 1954. The demonstrated long life and durability of Gussasphalt is the most important reason for its widespread use in Germany. The mastic mix used in test section 17 was based on work carried out by the Michigan Department of State Highways and Transportation (5).

The asphalt cement used in the test sections was 85-100 penetration grade except for the mastic mix in section 17, which used a harder 60-70 grade.

TRAFFIC

A permanent counting station is situated immediately east of the project. Average daily traffic volumes for

twenty-eight 24-h periods in 1975 are given below:

Lane	Vehicles per Day	
	Total	Commercial
Driving	12 900	3740
Center	17 300	1900
Passing	14 600	150

Volumes of commercial vehicles were manually recorded during a 24-h period in midsummer.

SKID-RESISTANCE STANDARDS

Skidding is a major factor in a large proportion of high-

Table 2. Characteristics of test mixes.

Test Section	Type of Mix	Marshall Stability (kN)	Marshall Flow (mm)	Voids in Mineral Aggregate (percent by volume)	Voids (percent by volume)
1	HL1				
	L	7.22	2.64	16.9	2.8
	F	11.62	2.97	17.5	3.7
2	HL1				
	L	7.22	2.64	17.2	3.0
	F	12.75	3.43	15.0	0.8
3	HL1				
	L	14.15	4.23	12.9	1.2
	F	15.14	3.92	13.5	2.0
4	HL1				
	L	7.69	2.61	16.0	2.7
	F	13.45	3.15	14.2	1.2
5	HL1				
	L	8	3.84	14.2	1.0
	F	8.46	5.77	16.0	0.9
6	HL1				
	L	9.73	5.82	15.2	1.0
	F	11.42	4.79	18.6	3.4
7	Modified HL1				
	L	15.64	4.10	18.5	2.7
	F	16.18	3.38	18.7	3.3
8	Modified HL1				
	L	9.6	3.31	17.3	2.3
	F	13.29	3.51	17.7	1.9
9	Modified HL1				
	L	12.58	3.28	24.0	6.9
	F	14.78	3.82	23.1	6.1
10	Modified HL1				
	L	8.78	2.66	17.9	2.9
	F	14.02	2.50	17.0	2.2
11	Sand				
	L	9.26	6.97	17.7	0
	F	9.66	10.30	19.5	0.2
12	Sand				
	L	11.78	4.92	16.8	0
	F	8.38	11.56	20.7	1.1
13	Open-graded,				
	F	6.48	3.25	20.6	4.7
14	Open-graded,				
	F	7.51	3.05	19.6	4.0
15	Open-graded,				
	F	11.9	4.92	16.3	0.7
16	Open-graded,				
	F	9.4	7.82	18.6	0.2
17	Mastic, F	8.38	14.54	21.0	1.0
	HL1				
	L	7.22	2.64	16.9	2.8
1-19*	F	12.55	3.72	14.6	0.4

Notes: 1 kN = 225 lbf; 1 mm = 0.039 in.
 L = laboratory mix designs; F = field-laboratory tests.
 *Same as section 1 but constructed over a 38-mm-thick bituminous base course.

Figure 1. Aggregate gradations for test section 1.

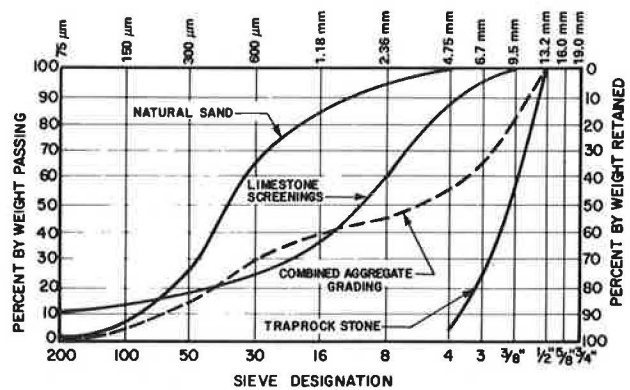


Figure 2. Aggregate gradations for test section 7.

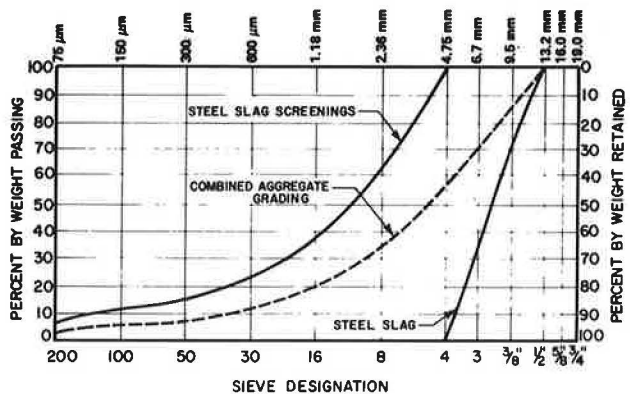
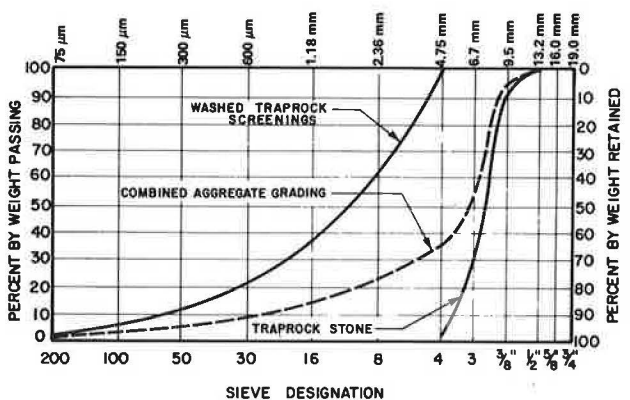


Figure 3. Aggregate gradations for test section 13.



way accidents, especially at high traffic speeds and volumes and in wet conditions. The goal for highway engineers must be to construct and maintain roadway surfaces at an optimal level of skid resistance so that skidding accidents are kept at the minimal practicable level.

National Cooperative Highway Research Program (NCHRP) Report 37 (6) discusses minimum skid-resistance values and recommends tentative requirements for main highways based on an analysis of skid values and accident data. Based on that report and in view of the absence of intersections, sharp bends, and steep gradients on Highway 401, a skid number of 31 measured by the ASTM brake-force trailer at 100 km/h (60 mph) is taken as the desired or target level for purposes of comparison between the pavement surfaces evaluated.

TEST METHODS

Pavement skid resistance and the physical parameters of the surface texture were measured by using four methods: the American Society of Testing and Materials (ASTM) brake-force trailer, the Mu-meter trailer, the British sideways-force-coefficient routine investigation machine (SCRIM) (10), and photo-interpretation.

Brake-Force Trailer

In North America, the most commonly accepted technique for measuring the skid resistance of pavements is based on the use of a skid trailer that conforms to ASTM Standard E274. The test unit consists of a towing vehicle and a brake-force trailer. The test measures the steady friction force generated when the standard tire of the locked left test wheel slides over wet pavement at a constant traveling speed. During the test, a specified quantity of water from the supply system in the tow truck is discharged through a nozzle in front of the test tire to produce a water-film thickness of 0.5 mm (0.02 in). The tread of the standard tire on the brake-force trailer has seven plain ribs. The measured friction force is described as the skid number (SN).

Each test section on the project was tested 10 times during the first four years of service. Initial measurements were completed immediately after construction and subsequently in the spring and fall of each year. Tests were carried out in the wheel paths of each lane at speeds of 50 and 100 km/h (30 and 60 mph). Results

of the tests are summarized in Table 3 and Figure 4.

Mu-Meter

The Mu-meter is a continuously recording friction-measuring trailer that measures the side-force friction generated between the test surface and two pneumatic tires. The tires are mounted on free-running wheels set at a fixed toe-out angle of 7.5° to the line of drag. Vehicle test speed was 64 km/h (40 mph). In February and March 1975, when the test sections were approximately 18 months old, tests were performed to determine skid resistance on the driving lanes in a variety of weather conditions that ranged from drizzle to slush from heavy snow. Test results for four selected bituminous test sections and the adjacent smooth, polished concrete are shown in Figure 5. The skid values shown represent the average number of continuous passes over the pavement sections. Because of the variations in precipitation and pavement conditions that can sometimes occur in a short period of time, the weather and pavement conditions indicated may vary slightly between different pavement sections. The significance of the test data lies in the indicated change in pavement friction that occurs as pavement conditions become more adverse (as conditions change from drizzle to heavy rain to slush).

SCRIM

The SCRIM device (10) is a continuous testing instrument that measures the coefficient of sideway force of the pavement surface (similar to the Mu-meter). The test wheel is inclined at 20° to the line of travel and rolls free over pavement that has been wet by a watering truck. The smooth test tire is inflated to a pressure of 345 kPa (50 lbf/in²). Since SCRIM has its own deadweight and suspension system, there is a known static reaction between tire and pavement. A signal from an electric load cell provides the sideway-force input into the recording system. The recorded data are then processed by computer, and a printout is produced that summarizes coefficients of side-force friction for each test section.

The SCRIM testing was carried out in August 1978 in conjunction with brake-force-trailer tests. Both vehicles traveled at 60 km/h (37 mph) and tested each section five times so that a comparison could be made between the friction values measured by the two devices.

SCRIM is the standard skid-measuring trailer used in Great Britain. The Transport and Road Research

Table 3. Skid numbers measured by ASTM brake-force trailer.

Test Section	Driving Lane				Center Lane				Passing Lane			
	50 km/h		100 km/h		50 km/h		100 km/h		50 km/h		100 km/h	
	Initial	Four Years	Initial	Four Years	Initial	Four Years	Initial	Four Years	Initial	Four Years	Initial	Four Years
1	51	29	32	21	49	31	36	22	49	34	36	26
2	50	31	34	21	50	33	35	24	51	35	36	28
3	60	34	45	27	62	34	47	28	63	40	47	33
4	54	31	37	25	55	32	39	25	57	36	40	30
5	48	33	31	24	47	32	31	24	50	35	40	29
6	48	34	37	29	48	33	38	28	50	37	37	31
7	62	41	48	33	61	40	46	31	63	44	49	35
8	61	34	38	27	57	33	33	27	60	35	36	23
9	50	40	37	33	52	40	38	34	57	42	40	35
10	48	33	37	25	48	33	38	27	50	38	37	31
11	50	36	38	28	50	37	41	29	54	41	40	31
12	45	35	29	27	49	38	38	28	51	41	30	30
13	43	33	42	29	45	33	43	29	51	37	41	32
14	41	33	37	30	44	33	40	29	45	36	36	31
15	51	34	40	26	44	34	43	27	58	40	44	31
16	47	35	37	27	50	36	41	28	54	41	41	29
17	41	31	28	27	40	32	30	26	37	34	28	25
18	43	29	33	20	41	30	33	21	46	33	30	25

Note: 1 km = 0.62 mile.

Figure 4. Skid resistance versus time for selected test sections.

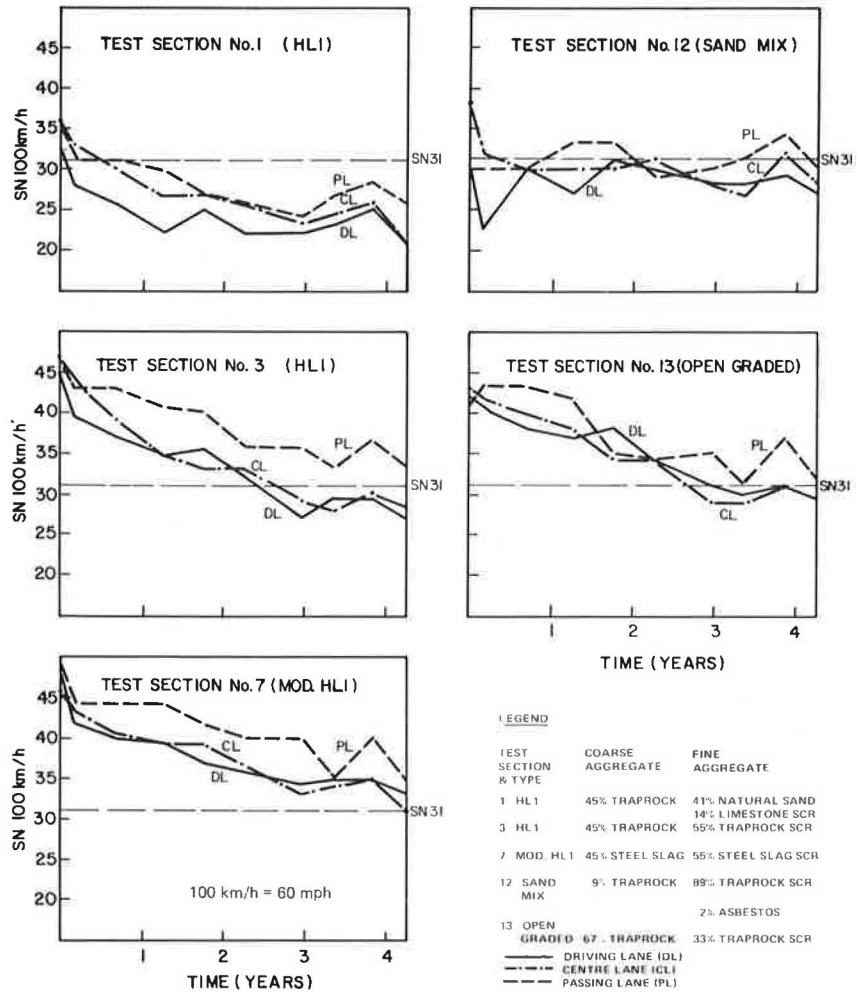
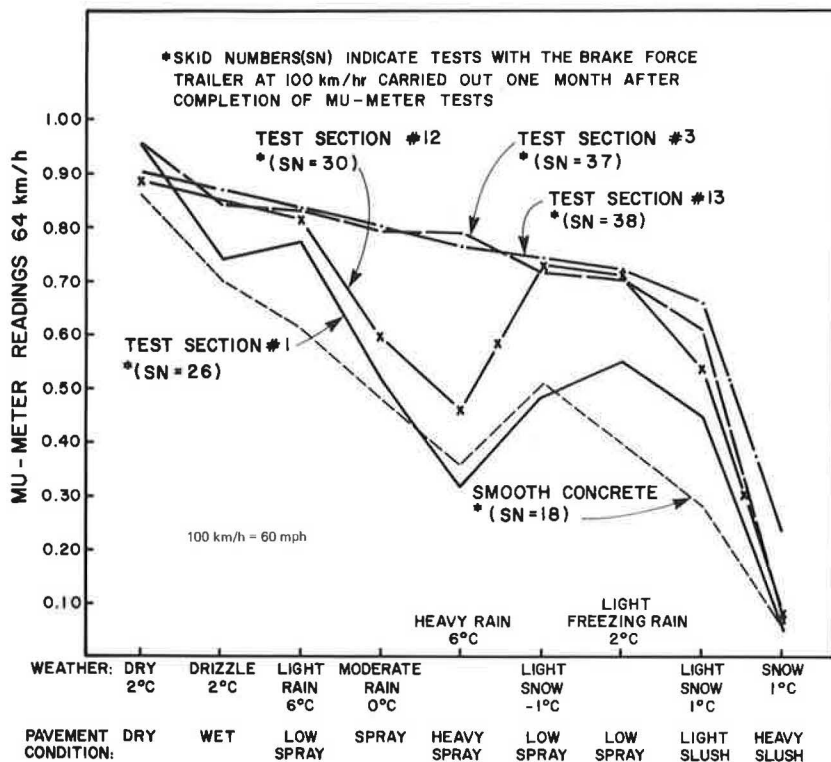


Figure 5. Mu-meter measurements of skid resistance in the driving lane in various weather conditions.



Laboratory has developed proposals for minimum standards of skid resistance that take into account the degree of difficulty at a site and include a risk rating to be determined by the accident potential of the site (11). These minimum coefficient values of side-force friction, measured at 50 km/h (30 mph), range from 0.30 for easy sites to 0.75 for very difficult sites. For alignment and traffic volumes similar to those of the Toronto By-Pass, values between 0.45 and 0.55 are specified.

Photo-Interpretation

The photo-interpretation method (7) is based on the interpretation of stereo pairs of color photographs of the pavement texture taken by using a specially designed camera box and light source. The color slides are examined by a skilled photo-interpreter to determine various texture parameters such as height and width of macroprojections, angularity of stone particles, and harshness of microtexture (see Figure 6). The textures are then classified in accordance with ASTM Standard E 559—Tentative Recommended Practice for Classifying Pavement Surface Textures Suitable for Skid-Resistance Photo-Interpretation.

In this research, photographs were taken in the wheel paths of each test section immediately after construction and subsequently twice each year. The photo-interpretation test was used to study the parameters of the pavement textures achieved immediately after construction and as changes occurred under traffic. A summary of the initial and 21-month macrotexture parameters

for the driving, center, and passing lanes on the project is given in Table 4. These parameters indicate the significant changes in pavement texture that have occurred in some test sections during the early life of the pavement.

SKID-RESISTANCE CHARACTERISTICS

A bituminous surface-course mix must first provide an adequate level of skid resistance and then ensure that the required skid-resistance properties are retained for the design life of the pavement.

The initial skid resistance of all test sections in the Toronto By-Pass project was high (Table 2) and in general met or exceeded the target value of 31 at 100 km/h (60 mph). Most sections exhibited a significant decline in skid resistance during the first four years of service, particularly in the driving and center lanes where the heavy truck volumes are concentrated. This decline in skid resistance is attributed to compaction of the bituminous mixes under traffic, which resulted in impressment of the coarse-aggregate particles into the matrix of the mix. Macrotexture depths (parameter A in Figure 6 and Table 3) declined rapidly in many test sections and in some cases were virtually nonexistent after less than two years of service.

The rate of compaction depends on volume and type of traffic and the mix composition of the pavement layer. Once maximum compaction has been achieved, the density of the macroprojections on the surface will change little. Changes in pavement skid resistance after this

Figure 6. Texture parameters.

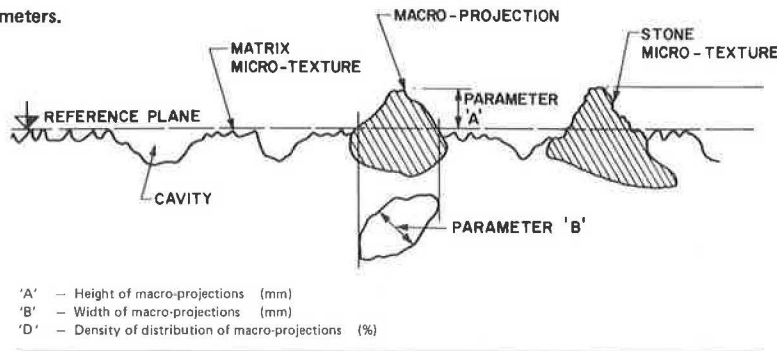


Table 4. Initial and 21-month surface macrotexture parameters.

Test Section	Driving Lane								Passing Lane							
	Initial				21 Months				Initial				21 Months			
	SN ₁₀₀	A (mm)	B (mm)	D (%)	SN ₁₀₀	A (mm)	B (mm)	D (%)	SN ₁₀₀	A (mm)	B (mm)	D (%)	SN ₁₀₀	A (mm)	B (mm)	D (%)
1	32	0.43	3.0	20	25	0	0	0	36	0.38	4.0	32	27	0.43	3.8	23
2	34	0.38	4.8	30	27	0	0	0	36	0.45	4.0	28	32	0.45	4.0	30
3	45	1.00	4.4	72	36	0.80	3.8	37	47	1.00	4.4	78	40	0.80	4.0	75
4	37	0.65	4.8	32	25	0.70	3.8	22	40	0.75	4.4	50	32	0.50	3.8	30
5	31	0.65	6.0	25	25	0.40	4.0	15	40	0.60	6.8	35	30	0.60	7.2	27
6	37	1.00	4.8	42	35	0.75	4.0	32	37	0.95	4.8	50	37	0.70	5.6	57
7	48	0.95	3.8	52	37	0.60	4.0	24	49	0.95	3.4	58	42	0.75	3.2	45
8	38	0.80	4.0	27	28	0.45	3.6	15	36	0.55	4.0	30	30	0.45	4.0	23
9	37	0.60	4.0	42	37	0.43	4.8	25	40	0.70	3.8	45	40	0.48	3.2	45
10	37	0.65	4.8	27	25	0	0	0	37	0.65	4.8	30	34	0.48	4.0	30
11	38	0.60	2.8	24	28	0	0	0	40	0.45	3.6	35	32	0	0	0
12	29	0	0	0	31	0	0	0	30	0	0	0	33	0	0	0
13	42	N/A	N/A	N/A	38	0.90	6.0	45	41	1.30	6.0	45	35	1.00	5.6	45
14	37	0.80	2.8	40	35	0.65	3.8	35	36	0.75	3.6	45	37	0.75	3.6	45
15	40	0	0	0	29	0	0	0	44	0	0	0	36	0	0	0
16	37	0.48	3.0	25	32	0.45	3.2	15	41	0	0	0	38	0	0	0
17	28	0.90	5.2	70	30	1.00	5.2	65	28	0.70	6.0	75	26	0.65	6.0	72
1-19	33	0.60	2.4	18	22	0	0	0	30	0.60	3.2	12	26	0.33	3.4	15

Note: 1 mm = 0.039 in.

time can take the form of a loss in friction values as the angularity of the stone projections is reduced and the microtexture is lost because of polishing of the aggregate particles. This appears to be a relatively slow process and is most noticeable in the coarse, open-graded mixes. An increase in skid resistance can result from differential wear between the stone particles and the matrix; that is, parameters A, B, and D increase. This phenomenon appears to be continuing in some of the project HL1 and modified HL1 mixes where low-abrasion, hard, coarse-aggregate particles and somewhat softer, fine-aggregate materials are blended together. Aggregate polishing and differential wear continue simultaneously and, for a given traffic condition, the properties of the aggregate largely control whether the net change in skid resistance is positive or negative.

HL1 and Modified HL1 Mixes

The most striking feature of skid-resistance characteristics in the Toronto By-Pass project is the excellent performance of the bituminous mixes that contain crushed traprock or slag screenings as the fine aggregate and the poor performance of the mixes in which the fine aggregate consists of natural sand or limestone screenings. The traprock and slag screenings initially produced higher skid numbers and deeper textures, and the sections have maintained adequate friction characteristics during the first four years of service.

Under the standard test conditions for the ASTM trailer, test section 7 (steel-slag coarse and fine aggregates) and test section 9 (blast-furnace-slag coarse and fine aggregates) in each of the three pavement lanes have maintained skid values in excess of the target value of 31. Macroprojection height exceeds 0.4 mm (0.016 in) in the driving lane (Table 3), and the matrix and stone microtexture have not polished to a significant extent.

In comparison, mix 8 (steel-slag coarse aggregate and a blend of natural sand and limestone screenings as the fine aggregate) and mix 10 (similar fine aggregate and blast-furnace-slag coarse aggregate) exhibit significantly lower skid resistance. Except for the passing lane of section 10, the mixes have not maintained the desired level of skid resistance. The effect on skid resistance of the fine-aggregate component is strikingly illustrated in Table 3 for sections 9 and 10, the two test sections that contain blast-furnace slag. In less than a year, the macroprojection height (parameter A) and the density of stone projections (parameter D) for mix 10 declined to zero, whereas mix 9, the mix that contains the blast-furnace-slag screenings, has maintained a well-developed macrotexture. The skid resistance of section 9 increased during the first few months, and in the passing lane a significant improvement in friction properties has occurred during the past two winters.

In comparing the performance of the two slag aggregates, it is evident that the vesicular nature of the blast-furnace-slag coarse aggregate provides the harshest microtexture to the stone projections and that this roughness is maintained, or regenerated, under heavy traffic. The steel slag produces better microtexture in the matrix. A combination of steel-slag fine aggregate and blast-furnace-slag coarse aggregate might therefore represent the best use of the slag materials provided the blast-furnace-slag coarse particles do not exhibit undue wear under traffic.

The type of fine aggregate has a similar influence on the skid resistance of the HL1 mixes that contain traprock coarse aggregate (mixes 1 to 6), particularly in the driving lane. Mixes 1, 2, 4, and 5, in which a large proportion of the fine aggregate is natural sand, have skid numbers between 6 and 10 points below the desired

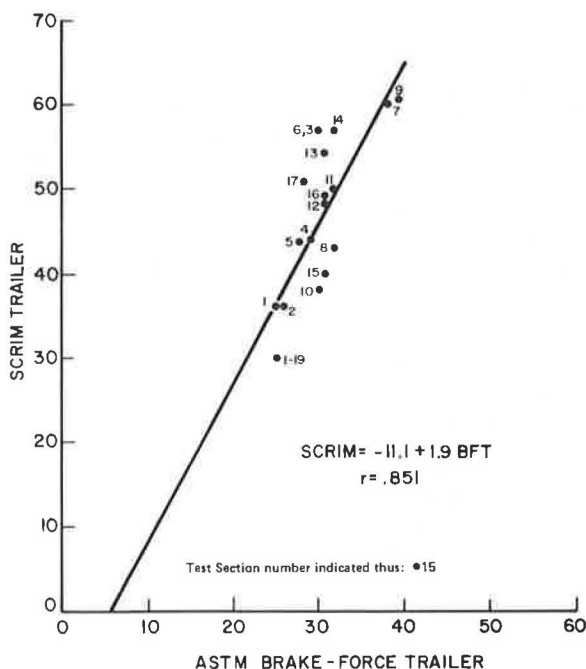
level at 100 km/h (60 mph), and the macrotexture parameters have significantly declined. Although the performance of these mixes is better in the passing lane, they do not provide satisfactory levels of skid resistance under heavy truck volumes in the driving and center lanes. Test sections 3 and 6, which used traprock screenings as the fine aggregate, have maintained satisfactory macrotexture (Table 3), but polishing of the fine-grained traprock particles in the driving and passing lanes has reduced the skid numbers measured by the brake-force trailer to slightly below the desired levels (Figure 4).

The addition of asbestos filler to mixes 5 and 6 reduced initial high-speed skid resistance somewhat, but little difference is apparent after four years.

The Mu-meter tests (Figure 5), which measured friction properties of the pavement sections under a variety of weather conditions, provide impressive additional evidence of the benefits of using crushed traprock or slag screenings in the bituminous mixes. Whereas mix 3 (traprock fine aggregate) maintained high skid resistance for all conditions up to heavy slush, mix 1 showed a significant decline in friction under conditions of moderate and heavy rain and light snow. In fact, in the driving lane the HL1 mix of test section 1 is little better in terms of skid resistance than the existing smooth, polished concrete of the Toronto By-Pass although the SNs measured by the ASTM brake-force trailer are significantly greater. These data clearly indicate the need for well-developed macrotextures for surfaces that carry traffic traveling at normal freeway speeds, a characteristic not necessarily measured by the standard brake-force skid trailer.

Side-force coefficients measured by SCRIM (see Figure 7) confirm the better skid resistance of the higher-stability mixes—i.e., those that contain traprock or slag screenings as the fine aggregate. Mixes 1, 2, 4, 5, 8, and 10, which contain a large proportion of natural sand, are characterized by skid coefficients between 36 and 44, which are below the levels proposed in Britain. In contrast, sections 3 and 6, which use traprock screenings as the fine aggregate and have skid coefficients in the

Figure 7. Comparison of test results for SCRIM and brake-force trailer at 60 km/h.



high 50s, and the all-slag mixes 7 and 9, which have coefficients of 60 and 61, respectively, are substantially in excess of the minimum skid-resistance values.

Open-Graded Mixes

Based on tests with the brake-force trailer, test sections 13 and 14, which consist of open-graded mixes that contain traprock coarse and fine aggregate, have maintained adequate levels of skid resistance. The visual appearance of such mixes is impressive because of their high stone content and the well-developed macrotexture of the surface. Even though the skid numbers measured for these mixes by the standard trailer are slightly lower than those of the slag mixes (test sections 7 and 9), Mu-meter measurements indicate that these mixes maintain a high level of skid resistance in conditions of moderate or heavy rain and light snow.

The SCRIM tests on sections 13 and 14 indicate friction levels in the same high range as those for sections 3 and 6, which contain similar types of material—i.e., traprock coarse and fine aggregate.

In comparison with the dense-graded mixes, the open-graded mixes appear to have some additional advantages that are not measured by standard test methods. In wet conditions, the pavement surface is comparatively dry and there is noticeably less splash and spray than there is on the other test sections. After the cessation of rain, the pavement surface dries out somewhat more rapidly.

Test sections 15 and 16, which contain a reduced fraction of coarse aggregate, initially had satisfactory skid resistance at high vehicle speeds, but in the driving and center lanes skid resistance has declined to less-than-desirable levels. As the data in Table 3 indicate, the mixes for these sections have a low proportion of stone projections (parameter D), which results in little macrotexture.

The performance of the open-graded mixes—particularly sections 13 and 14—is impressive. The interconnected voids in the mix are clearly very efficient in moving bulk water away from the tire-pavement interface. The excellent durability of the pavement during the first four years of service has overcome some of the initial skepticism about the performance of these high-void-content mixes.

Other Mixes

The two sand mixes (sections 11 and 12) that contain traprock screenings plus small amounts of 6-mm (0.25-in) traprock chips have relatively good skid resistance as measured by the brake-force trailer and SCRIM. After the first six months of service, little change in skid resistance has occurred. The matrix has excellent microtexture characteristics but, because of the lack of coarse aggregate in the bituminous mix, macrotexture is non-existent. As the Mu-meter tests (Figure 5) indicate, this lack of coarse texture results in a significant reduction in skid resistance as rainfall intensity increases. Such mixes are not considered suitable for high-speed free-way traffic.

The mastic mix (section 17) had the lowest initial skid resistance of all the test sections, and after four years the values are somewhat less than desired. The high stone content has resulted in good surface macrotexture, but most stone projections are covered with a film of asphalt cement and mineral filler.

Comparison of Testing Devices

Since the Mu-meter was not used to test the pavement

sections under the standard conditions imposed by a truck watering system, correlation with the brake-force trailer is poor. The best correlation was obtained when the Mu-meter was operated under conditions of light rain. Good correlation was obtained between measurements taken by SCRIM and the brake-force trailer (Figure 6).

In general terms, SCRIM and Mu-meter measurements correlate well with macrotexture measurements determined by photo-interpretation, i.e., parameters A, B, and D. In contrast, the brake-force-trailer tests carried out at the same time as the SCRIM tests correlated well with the microtexture of the surface, i.e., parameters D, E, and F. It appears, then, that the coefficients of side-force friction are more influenced by the harshness of the macrotexture (capability for drainage of bulk water) and that brake-force-trailer values are more dependent on the harshness of the microtexture (abrasive qualities of the pavement surface).

In considering these and previous observations, it becomes apparent that one must be cautious about using either brake-force-trailer or side-force measurements without considering other parameters to determine the adequacy of pavement skid resistance. The brake-force trailer does not provide a totally satisfactory measurement of pavement skid resistance; to ensure adequate friction at higher speeds and in adverse weather conditions such as heavy rain, sufficient texture depth (defined by stone projections above the matrix) must be achieved. Similarly, side-force friction is not by itself a totally satisfactory measurement of pavement skid resistance; to ensure adequate friction in areas of heavy traffic demand, aggregates with harsh, durable microtexture must be used.

PAVEMENT CORE SAMPLES

Core samples were taken from the wheel paths of the driving lane of each test section at 3 months and 21 months after construction. The samples were subjected to the usual control tests and, in addition, the pavement voids were determined. These results were compared with the voids in the recompacted mix, and the percentage of compaction was determined. Since each test section was represented by samples taken at only one location and since many variables affect the determination of compaction, the data are useful only as a general comparison of how the various materials and mix proportions affect the degree of achieved compaction and the increase of pavement density under heavy traffic in the driving lane.

The standard requirement of the Ontario Ministry of Transportation and Communications for the field compaction of bituminous mixes other than sand mixes—i.e., not less than 97 percent of the density of the laboratory compaction for layers 38 mm (1.5 in) thick and 93.5 percent for layers 25 mm (1 in) thick—was not achieved in almost all of the test sections. The lowest densities occurred on sections 3, 6, 7, 9, and 13-16, which represent (a) normal or modified HL1 mixes that contain crushed rock or slag material as both the coarse and fine aggregates and (b) open-graded mixes. In these mixes, between 89 and 94 percent compaction was achieved. It appears that the field packing properties of a bituminous mix that contains all crushed aggregates, in either the continuously graded or the gap-graded mode, make it more difficult to attain the traditional required density.

Of the four open-graded test sections, mixes 15 and 16, with 30 percent coarse aggregate, had initial void contents of 7 percent, which is far lower than the generally specified void content for such mixes. Increasing the stone content to 67 percent in test sections 13 and 14

resulted in a pavement void content of 12.2 percent. The HL1 and modified HL1 mixes that contain crushed trap-rock, blast-furnace slag, or steel slag as both the fine and coarse aggregates had initial pavement void contents that ranged from 11.3 to 15.2 percent, i.e., similar to those desired for the open-graded mixes. The particle shape of the fine aggregate as well as the combined aggregate grading has a marked influence on the void content in the compacted pavement.

As anticipated, all mixes exhibited reduced voids and increased compaction between 3 and 21 months of service; some HL1 and modified HL1 mixes that contain natural sand and limestone screenings approached 100 percent of laboratory compaction. Mixes with initial void contents in excess of 10 percent showed a reduction during this 18-month period of about 1.5 to 4.5 percent; the exception was mix 13, which declined from 12.2 to 4.9 percent. The large decrease in void content in the open-graded mix is attributable in part to sand and dirt that infiltrated the matrix of the pavement layer from the roadway surface.

A further coring program carried out in the summer of 1978 produced significantly different data for the open-graded mix in section 13. The pavement void content of 15 cores varied between 7.1 and 9.5 percent and averaged 8.5 percent (this does not include the one sample taken from a flushed area of the roadway). There was no significant difference in results for cores taken from the wheel paths and the center of the lane. The mean compaction of the same core samples was 94.4 percent; compaction was 2 percent higher in the driving-lane than in the passing-lane wheel paths. Most core specimens were contaminated with fine material near the surface.

PERMEABILITY TESTS

Permeability tests were conducted after two and four years of service in the driving-lane wheel path of each test section. The test method, which is based on equipment developed by the Johns-Manville Company, requires the use of a head of water contained in a vessel that has a sealed perimeter joint with the pavement surface. Permeability is defined as the change in the head of water with time as the water is permitted to drain into the pavement layer. The method is not entirely satisfactory for measuring permeability in the upper range since such mixes exhibit little resistance to the passage of water.

After two years of service, open-graded test sections 13 and 14 showed high permeability. During the next two years, the mixes became much less permeable: Three of nine locations were defined as impermeable. Tests on section 13 after four years showed that the passing lane tended to retain the characteristics of high permeability better than the center and driving lanes. The HL1 and modified HL1 mixes, with initial void contents in excess of 10 percent, were permeable after two years but to a somewhat lesser degree than the open-graded mixes. After four years, these mixes were impermeable.

All other bituminous mixes in the project were impermeable to the penetration of water after two years.

TEXTURE DEPTH

Satisfactory skid resistance at high vehicle speeds requires adequate macrotexture or drainage of bulk water. Based on skid measurements of the 18 test sections with the brake-force trailer and the Mu-meter and the measurement of the texture parameters by photo-interpretation, desirable textures to achieve adequate surface drainage for conditions more adverse than light rain are defined as follows (1 mm = 0.039 in):

Parameter	Measurement	Minimum Amount
A	Height of macroprojections (mm)	0.5
B	Width of macroprojections (mm)	2.0
D	Density of distribution of macroprojections (%)	25

CONSTRUCTION PROGRAM

As part of the first phase of the pavement improvement program on the Toronto By-Pass, 58 lane-km (36 lane miles) in the center section were rehabilitated with bituminous overlays in 1976, 1977, and 1978. The surface course was a 25-mm (1-in) thick open-graded mix in which traprock aggregates and a mix composition similar to that of section 13 of the 1974 experimental test sections were used. A binder course 38 or 51 mm (1.5 or 2 in) in thickness was placed on the concrete.

Mean test results for the open-graded mix were as follows (1 mm = 0.039 in):

Item	1976	1977	1978
Asphalt cement content (%)	4.9	5.1	4.6
Material retained on 4.75-mm sieve (%)	60	65	62
Voids in pavement samples (%)	10.9	7.8	10.0

Skid Resistance

Average skid numbers [SN_{100} km/h (60 mph)] for the 1976 resurfacing program were initially 39 and, after two years of traffic, 34. These values are slightly less than the equivalent figures for section 13.

Noise

Changes in community noise levels attributable to resurfacing the existing concrete pavement with the open-graded bituminous mixes are difficult to determine with precision because of variations in total traffic flow. In addition, the "staged" nature of the overlay construction program resulted in not all of the 12 pavement lanes being treated in one year.

May and Osman (8) have described a near-tire procedure of noise measurement and a test program on various freeway pavement surfaces in southern Ontario, including the Toronto By-Pass. This technique uses a microphone mounted near the tire of an automobile 152 mm (6 in) from the road surface. A 1974 Ford LTD sedan equipped with summer radial tires was operated at 100 km/h (60 mph). The open-graded mix (1976 construction program) was 3 dB(A) quieter than adjacent smooth concrete and 4-5 dB(A) quieter than a typical HL1 bituminous mix.

Favorable community reaction to the open-graded mix appears to confirm the low-noise properties of the new pavement.

Summary of Results

The general effect of the use of an open-graded-mix bituminous overlay on the driving quality of the Toronto By-Pass pavement has been to double skid resistance and decrease tire-pavement noise.

CONCLUSIONS

To provide acceptable levels of skid resistance at high vehicle speeds so as to minimize the number of wet-pavement skidding accidents, a pavement surface must

have sufficient roughness or macrotexture to provide for the drainage of bulk water from the contact area between the tire and the road surface and sufficient harshness or microtexture to facilitate the breakup of the remaining thin water film on the roadway surface. These characteristics can be provided by selecting aggregates that do not wear and polish rapidly and thus retain angularity and microtexture and by using fine aggregate and a mix composition that produce a stable matrix microtexture and a well-defined surface macrotexture. The choice of materials and mix types must reflect the speed and volume of traffic and the number of commercial vehicles.

The performance of 18 pavement test sections on the Toronto By-Pass portion of Highway 401 during the first four years of service has provided useful data on the skid resistance of bituminous mixes under very heavy traffic volumes. The testing and evaluation reported in this paper have led to the following conclusions:

1. Almost all of the bituminous mixes tested provide substantially better skid resistance than the existing smooth, polished concrete.

2. Most bituminous mixes provided adequate skid resistance immediately after construction, but all mixes were characterized by a decline in skid resistance during the first four years of service. Initial target skid numbers must therefore be substantially higher than the required minimum level.

3. The early decline in skid resistance was caused by a reduction in the depth of the macrotexture as the coarse-aggregate particles were pressed into the matrix under wheel loads. This decline in skid resistance was most pronounced in the driving lane, where the majority of commercial vehicles travel, and least pronounced in the passing lane, which carries few trucks. There is an indication that some of the third- and fourth-year decline is attributable to wear and polishing of the coarse-aggregate particles.

4. In the driving lane, which carries 3700 commercial vehicles/day, the bituminous mixes that provide skid values close to or above the recommended minimum figures are (a) dense-graded mixes with both coarse and fine aggregates that consist of traprock, steel slag, or blast-furnace slag and (b) open-graded mixes that contain traprock coarse and fine aggregates with high stone contents. These mixes have also retained a high level of skid resistance during particularly adverse pavement conditions, such as heavy rain and slush from light snow.

5. In the passing lane, which carries few commercial vehicles, most bituminous mixes provide adequate skid resistance. The least skid resistance is provided by those that contain fine aggregates that consist of natural sand blended with limestone screenings.

6. Sand mixes that contain traprock screenings that produce good microtexture but little macrotexture have provided a reasonably good level of skid resistance when they were tested under standard conditions with the brake-force trailer but have shown a significant decline in skid resistance under conditions of moderate or heavy rain. Such mixes would provide a satisfactory surface texture only for low-speed traffic.

7. The characteristics of the fine aggregate in dense-graded bituminous mixes affect the depth of the macrotexture (the protrusion of coarse-aggregate particles from the matrix). Mixes that contain traprock or slag screenings have much better macrotexture than mixes that contain sand. This mechanism is not completely understood, and additional research is necessary to develop mix design methods and procedures of aggregate selection that will ensure adequate macrotexture in dense-graded bituminous mixes.

8. The ASTM brake-force trailer widely used in

North America to measure skid resistance is useful in assessing friction values under standard conditions that approximate the thin water film that occurs in light rain on a typical pavement. Whether a pavement texture provides adequate skid resistance for high-speed traffic under a variety of adverse conditions depends on the attainment of both microtexture and macrotexture. The photo-interpretation test is a satisfactory method for the study of these two important parameters. For high-speed freeway traffic, adequate pavement macrotexture is achieved when the average projection of stone particles above the matrix is not less than 0.5 mm (0.02 in).

9. Blast-furnace-slag and steel-slag aggregates appear to provide somewhat better skid resistance in dense-graded bituminous mixes than the traprock aggregate widely used in the past on main highways in Ontario.

10. The new open-graded surface-course-mix pavement on the Toronto By-Pass is noticeably quieter under traffic than adjacent sections of smooth, polished concrete.

11. The main thrust of the project is to develop bituminous surface-course mixes that will provide adequate, long-lasting skid resistance for the heavy traffic volumes encountered on the Toronto By-Pass portion of Highway 401. Some of the conclusions on the unsatisfactory performance of bituminous mixes will obviously not apply to highways that carry less traffic or have a lower maximum speed limit.

ACKNOWLEDGMENT

Special thanks go to F. B. Holt of the Ontario Ministry of Transportation and Communications, who carried out the photo-interpretation of the pavement textures, and to P. DeMontigny of the Quebec Ministry of Transport for the SCRIM testing program.

REFERENCES

1. J. T. Corkill. Construction of 17 Test Sections of Special Bituminous Mixes. Presented at the Annual Conference of the Canadian Technical Asphalt Association, Toronto, Nov. 1975.
2. H. J. Fromm and J. T. Corkill. An Evaluation of Surface Course Mixes Designed to Resist Studded Tire Wear. Research and Development Division, Ontario Ministry of Transportation and Communications, Downsview, Rept. RR 171, Feb. 1971.
3. R. W. Smith, J. M. Rice, and S. R. Spelman. Design of Open-Graded Asphalt Friction Courses. Federal Highway Administration, U.S. Department of Transportation, Rept. FHWA-RD-74-2, Jan. 1974.
4. V. P. Puzinauskas. Gussasphalt of Pourable Asphaltic Mixtures. Asphalt Institute, College Park, MD, Res. Rept. 70-2, Feb. 1970.
5. F. Copple and A. P. Chritz. An Evaluation of Mastic-Type Paving Mixtures for Resurfacing a Roadway and a Bridge Deck. Michigan Department of State Highways and Transportation, Lansing, Rept. R-861, June 1973.
6. H. W. Kummer and W. E. Meyer. Tentative Skid-Resistance Requirements for Main Rural Highways. NCHRP, Rept. 14, 1967.
7. R. Schonfeld. Photo-Interpretation of Pavement Skid Resistance. Research and Development Division, Ontario Ministry of Transportation and Communications, Downsview, Rept. RR 188, June 1974.
8. D. N. May and M. M. Osman. Noise from Re-textured and New Concrete and Asphalt Road Surfaces. Presented at Inter-Noise 78, San Francisco, May 1978.
9. J. Ryell, J. J. Hajek, and G. R. Musgrove. Con-

crete Pavement Surface Textures in Ontario: Development, Testing and Performance. Presented at the 55th Annual Meeting, TRB, 1976.

10. G. F. Salt. Research on Skid-Resistance at the Transport and Road Research Laboratory (1927-1977). Presented at the 2nd International Skid Prevention Conference, Columbus, OH, May 1977.

11. G. F. Salt and W. S. Szatkowski. A Guide to Levels of Skidding Resistance for Roads. Transport and Road Research Laboratory, Crowthorne, Berkshire, England, Rept. LR 510, 1973.

Publication of this paper sponsored by Committee on Characteristics of Bituminous-Aggregate Combinations to Meet Surface Requirements.

Synthetic Aggregates for Skid-Resistant Surface Courses

D. A. Anderson and J. J. Henry, Pennsylvania State University, University Park

Synthetic aggregates are produced by the thermal or chemical processing of natural or manmade materials. The physical properties of these aggregates vary considerably, depending on raw material and method of processing, and their properties are often considerably different from those of the natural aggregates on which current test methods and specifications are based. Skid resistance is primarily a function of the microtexture and macrotexture of the pavement surface. The physical properties of the individual aggregate particles determine level of microtexture and resistance to wear and polishing, which are important properties in the retention of skid resistance. Various methods of producing synthetic aggregates for skid-resistant surfaces are reviewed. Emphasis is placed on processing methods, available raw materials, and properties of the processed aggregate. The mechanisms by which different classes of aggregates develop microtexture and resistance to wear and polishing are discussed. It is concluded that each of these materials develops skid resistance and resistance to wear and polishing in a different way and that this should be reflected in designs and specifications. Many potentially acceptable synthetic aggregates are energy and capital intensive.

Synthetic aggregates are produced by the thermal or chemical processing of either natural or manmade raw materials and include waste materials as well as aggregates that are produced specifically for construction applications. The physical characteristics of synthetic aggregates vary depending on the raw material and the method of processing. In many cases, the physical characteristics and engineering behavior of synthetic aggregates are considerably different from those of the natural aggregates on which current specifications and test methods are based.

As supplies of readily available natural aggregate become depleted and the demand for skid-resistant pavements increases, synthetic aggregates will of necessity become more important as an aggregate source. In this paper, potential sources of synthetic aggregates are reviewed with respect to existing technology, and the aggregates are differentiated as to aggregates that are "tailor-made" as skid-resistant aggregates and those that are "non-tailor-made", such as lightweight aggregates, slags, and industrial by-products.

SKID-RESISTANCE REQUIREMENTS

The skid resistance of a pavement is primarily a function of its surface texture. It is convenient to divide texture into two components: microtexture with asperities smaller than 0.5 mm (0.02 in) and macrotexture with asperities larger than 0.5 mm. Microtexture is generated by the surface texture of the

individual aggregate particles, whereas macrotexture is generated by the gradation and maximum size of the coarse aggregate. Low-speed skid resistance is developed from microtexture. Both macrotexture and microtexture are required for high-speed skid resistance (1).

A relation between pavement texture and skid number at any speed V was developed by Leu and Henry (2):

$$SN_v = ae^{-bv} \quad (1)$$

In this relation, coefficient a can be predicted from microtexture data (BPN or profile data) and becomes smaller as the aggregate is polished. The parameter b becomes larger as aggregate particles wear away and can be predicted from macrotexture data (i. e., sand-patch texture depth or profile analysis). It should be noted in Equation 1 that a particular skid number can be produced by different combinations of macrotexture and microtexture.

Although initial as-constructed skid resistance is an important requirement, it is also important that adequate skid resistance be maintained under the action of traffic. A loss in skid resistance can be produced by polishing (loss of microtexture) or by wear and abrasion (loss of macrotexture). Many aggregates, such as some sandstones, renew their microtexture as they wear away by exposing new, unpolished grains. Resistance to polishing is thus often gained at the expense of wear or abrasion.

To perform satisfactorily as a surface aggregate, an aggregate must

1. Be graded so that it can provide adequate initial macrotexture;
2. Provide adequate resistance to environmental exposure, abrasion, and impact (retain its macrotexture);
3. Provide adequate initial microtexture; and
4. Provide adequate resistance to polishing (retain its microtexture).

TYPES OF AGGREGATE

Different aggregates achieve microtexture and resistance to polishing through different mechanisms. James (3) has developed the following aggregate groups for purposes of classification:

Group	Material
1	Very hard materials
2	Conglomerations of small, hard particles
3	Dispersions of hard particles in a softer matrix
4	Materials that fracture during wear, leaving irregular fracture surfaces
5	Vesicular materials

Experience has shown that hard materials by themselves, without the features of groups 2 through 5, are not satisfactory in terms of resistance to polishing. Group 2 materials rely on the angularity of the mineral grains and sacrificial wear to provide microtexture and resistance to polishing. The group 3 materials require hard, sharp, angular grains that stand out above the soft matrix as wear proceeds. Microtexture in the group 4 materials depends on anisotropic, angular, sharp mineral grains that yield a rough fracture surface. Sacrificial wear or abrasion is necessary for resistance to polishing. Finally, the group 5 materials retain their microtexture as they wear by exposing new, sharp cell walls.

CERAMIC PROCESSING

The ceramics industry has developed highly specialized processing techniques to meet a wide variety of product requirements. Depending on the processing technique and product requirements, materials with a wide range in properties can be produced (4).

Processes

Ceramic processes that are potentially useful in the manufacture of paving aggregates are given in Table 1. The table is arranged according to the nature of the

finished product, e.g., sintered, bloated, or glassy. The range of properties of synthetic aggregates is much greater than that of conventional aggregates, and this must be taken into account in their use, particularly in the development of test methods and specification criteria.

With the exception of some forms of thermal-chemical processing, the potential techniques for processing ceramic aggregates are energy intensive and will become more expensive as energy becomes more costly. Exact energy requirements depend on the chemical composition of the raw material, the processing method, and the number of processing steps required.

For example, the extended thermal treatment needed to produce ceramic is more energy demanding than the sintering process in which the raw material is brought to a temperature below melting. Another consideration is the energy content of the raw feedstock. For example, coal-mine refuse, incinerator refuse, and other waste materials contain some unburnt carbon, and this can be used to feed the ceramic processing. If the feedstock is a molten slag, the cost of initial melting can be eliminated. Considerable energy could be saved if certain industrial slags, such as boiler slag, coal-gassification wastes, and pyrolysis slags, were tied directly to the production of aggregate rather than disposed of in the most convenient manner and later reclaimed as aggregate. For example, the energy required to sinter fly ash is about 1163 MJ/Mg (1 million Btu/ton), whereas energy requirements for sintered clay may be in the range of 3490-4650 MJ/Mg (3-4 million Btu/ton) because of the carbon content of the fly ash.

Energy requirements for a number of ceramic processes are given in Table 2 (5). The energy requirements and kiln efficiencies vary considerably, according to the load on the kiln, the quantity of heat, and the temperature required.

Table 1. Potential sources of synthetic aggregate by method of manufacture.

Process	Description	Example	Current Pavement Use	Comments
Sintering	Heating (to below melting point) of agglomerate fines into larger, tougher particles	Brick making; sintered shales, clays; molarite, refractories; fly-ash lightweight aggregate	Texas ("Red Rock")	Agglomerate fine material (e.g., wastes, clays) into hard, large-sized particles; blend ingredients to control differential hardness; properties vary
Sintering with bloating	Heating as in sintering, but bloating gives "expanded" particle	Expanded shale, clay, coal-mine refuse	Expanded shale, clay, coal-mine refuse	Good skid resistance, doubtful durability and wear resistance; control of wear and skid resistance by bubble size, density, and wall thickness
Glass ceramics	Controlled thermal processing of glass to give appreciable crystal growth	Processed blast-furnace slag; Synopal	Extensive use; blast-furnace slag; excellent skid resistance	Development of crystalline phase controlled by processing and composition; desired process waste slags
Glass ceramics with bloating or expansion	Melted glass expanded by internal gas or injected air or steam; appreciable crystal growth on cooling	Expanded blast-furnace slag	May not be advantageous in cost if glass-ceramics process gives adequate differential wear	Expanded blast-furnace slag currently used in block manufacture; no advantage reported over normal blast-furnace slag; cost and environmental disadvantages
Calcining	Heating in solid phase to effect crystal change and drive off water or carbon dioxide	Calcined bauxite	Limited because of expense	Potential as "high-class" material; cost-effectiveness needs to be improved
Chemical processing	Hydraulic cement or other chemical reaction at ambient temperature	Pozzopac, sulfate-fly-ash waste	None	Questionable; low energy input implies material without hardness and wear resistance
Thermochemical processing	Hydraulic cement or other chemical reaction at elevated temperature	None known	None	Inclusion of hard particles in softer matrix suggested; process represents low-energy agglomeration of fines
Glassmaking	Heating to above melting temperature; rapid cooling without crystal growth	Water-quenched boiler slag, steel and blast-furnace slags, slags from incinerators, etc.	Boiler slag; controversial for skid resistance	Marginal as skid-resistant aggregates; modify to glass-ceramics process if possible; vesicularity may extend usefulness
Glassmaking with bloating	Melted slag expanded with gasses produced in process or with injected air or steam; no appreciable crystal growth on cooling	None	None	Vesicularity may improve skid resistance; probably not preferred process but may be necessary with some waste-slag compositions that do not readily crystallize
Recycling	Recycling of portland cement concrete or asphaltic pavements	None	None; ongoing demonstration projects	Alteration of future construction to allow aggregate recycling should be considered; crushed portland cement concrete may give good differential wear
Coatings	Thermally or chemically applied thin surface coatings	None known	None	Limited application unless coating is thick as in composite material; expensive processing

Table 2. Energy requirements for various ceramic processes.

Process	Temperature (°C)	Energy (MJ/kg)	Efficiency (%)
Structural products and refractories			
Kettle calcining, gypsum to plaster	151	1.28	51
Tunnel kiln, fireclay brick	1426	5.23	35
Rotary kiln			
Calcining kaolin	1649	6.97	32
Dead-burning dolomite	1749	10.23	53
Glass containers			
Gas-fired regenerator furnace	1426	6.56	39
Electric furnace	1426	3.95	64
Tunnel-kiln whitewares			
Porcelain	1410	41.86	5
Tableware	1226	6.97	27
Abrasives			
Arc fusion of alumina	2093	5.58	64
Reduction to silicon carbide	1982	29.07	71
Reduction to boron carbide	2399	116.28	52
Synthetic aggregates ^a			
Sintered shale or clay	1204	5.81	-
Sintered coal-mine refuse	-	1.39	-
Sintered fly ash	-	1.16	-
Fusion of municipal waste	2204	5.81	-

Note: °C = (°F - 32)/1.8; 1 MJ/kg = 430 Btu/lb.

^aEstimated values.

Table 3. Laboratory test data for various aggregates.

Material	PSV	AAV	Water Absorption (%)	Los Angeles Abrasion
Synopal	50	35.0	-	23
Calcined bauxite				
RASC	75	3.0	3.6	-
RSG-F	79	5.3	4.3	-
RSG-G	54	3.7	1.1	-
Brick				
Fireclay	63	19.0	-	-
Bauxite	88	38.0	-	-
Silica	58	8.0	-	-
Flint				
Crushed	35	1.0	1.0	-
Calcined	53	0	1.3	-
Expanded shale	60-75	High	-	-
Slag				
Blast furnace	40-63	7-29	-	-
With heat treatment	62	7.7	-	-
With foaming	69	6.2	-	-
Steel	44-67	3	-	-
Limestone	48	-	0.3	18
Expanded glass	45	-	2.4	23
Granite	54	-	0.3	36
Arkosic sandstone	62	-	2.6	-

Use of Existing Ceramic Products as Paving Aggregates

It should be emphasized that, since ceramic products are produced for a specific purpose, their attendant materials specification criteria may have to be re-evaluated in any consideration of existing ceramic products for use as paving aggregates. For example, paving aggregates do not have to be refractory. This means that processing requirements as well as raw-material requirements may be less restrictive for paving applications than for the original application. In turn, a considerable cost saving may be realized or a new supply of raw materials may become available. For example, low-grade bauxite that cannot be used as a refractory brick makes an excellent paving aggregate, one that is superior to an aggregate made with a purer grade of bauxite. Thus, a much wider source of raw materials becomes available at a lower cost (6). On the other hand, certain requirements that are not significant for refractory brick—such as resistance to freezing and thawing and impact resistance—are critical for pavement aggregates.

With the exception of lightweight aggregates from shale and clay, there are almost no examples of manu-

factured synthetic aggregates that are used as skid-resistant aggregates in significant quantities. Blast-furnace slag is an industrial by-product widely used as an aggregate, but neither it nor ordinary lightweight aggregate is produced specifically for skid-resistant purposes. In 1972, Marek and others (7) noted that since 1964 there had been few significant additions to the list of available or potentially available synthetic aggregates. This is still the case. Increased energy costs and environmental restrictions and the shortage of money for capital expenditures have placed additional constraints on the development of synthetic aggregate.

TAILOR-MADE CERAMIC AGGREGATES

Tailor-made ceramic aggregates are materials specially processed for use as skid-resistant aggregates. Processed Synopal and calcined bauxite are perhaps the best-known, best-documented of these materials.

Synopal

Synopal is a silicate-glass ceramic produced by first solidifying the melted raw material to a glass and then heat-treating it to induce crystal growth (method 2 in Table 1). The result is a hard, fine-grained (low-porosity) calcium silicate mineral with an amorphous (glass) matrix. Its high compressive strength [620 MPa (90 000 lbf/in²)], hardness (7.5 Mohs), and reflectivity under night illumination are its favorable properties. Synopal has been little used in the United States, principally because of its high cost [\$55/Mg (\$50/ton)] and marginal skid-resistance performance (3). The marginal skid resistance is caused by the fine-grained, dense texture, which provides little differential wear and microtexture. A laboratory polished-stone value (PSV) of 50 is reported for Synopal (Table 3). Although it is no longer produced in the United States, Synopal has been used in test roads in Michigan, West Virginia, Illinois, and other states.

The use of calcined bauxite as a skid-resistant aggregate has been studied extensively in England (6). In these studies, raw bauxite that ranged up to 7 mm (0.28 in) in diameter was calcined in the laboratory at 1500°C to 1750°C (2730°F to 3180°F) in a rotating drum. Cooling rates were essentially furnace rates. The calcining (temperature) schedule was critical: A 30-min hold at temperature resulted in large crystals being tightly bound in an unbloated, glassy matrix. Too little matrix gave a friable aggregate; too much sintering lowered the PSV.

Certain special qualities of calcined bauxite make it an excellent skid-resistant aggregate. Polycrystalline α -alumina is an anisotropic, tough, hard, strong material. Pure sintered α -alumina has a Mohs hardness of 9, and its tensile strength ranges from 410 to 690 MPa (65 000 to 100 000 lbf/in²). Differential wear and microtexture are obtained by the random orientation of the grains of α -alumina, which tend to retain a blocky structure under wear by traffic. Optimal skid resistance has been obtained by using α -alumina crystals 15-70 μ m (0.000 59-0.0028 in) in size bonded by a moderate quantity of glassy matrix. Water absorption of up to 5 percent was characteristic of calcined bauxites that had better polishing resistance. The porosity and glassy matrix and the tendency of the alumina to retain sharp corners on its cleavage planes all contribute to its high PSV. In addition to being very skid resistant, calcined bauxites are highly wear resistant.

PSVs (British pendulum tester values retained after polishing) for a variety of calcined bauxites are given in Table 3. The values range from 54 to 79 and show

a strong dependence on porosity. In contrast, pure α -alumina, an industrial abrasive, has a PSV of 62.

Obviously, calcined bauxite, deposits of which exist in Arkansas, represents an excellent source of skid-resistant aggregate, and its use should be pursued in the United States. Bauxite with clay is also a possible source. The high cost of calcined bauxite [\\$33-\$55/Mg (\$30-\$50/ton)] reflects costs for shipping, raw material, and energy for processing. Conventional rotary kilns could, however, be adapted to its manufacture.

Bricks

Limiting its study to materials currently in production, the Transport and Road Research Laboratory (TRRL) has investigated various types of bricks for use as skid-resistant aggregates (6). Brick is a sintered or liquid-phase sintered material that must be pressed to shape before the firing process. Its PSVs range from 58 to 88 and do not show a good correlation with crushing strength or abrasion resistance (Table 3). Common brick is not satisfactory as a skid-resistant aggregate. Generally, brick of a quality acceptable for skid-resistance purposes is refractory and hard fired. This requires a relatively high temperature, which allows considerable crystal growth beyond the initial sintering. Refractory qualities are not necessary in brick that is to be used as aggregate, but the hard firing is necessary to give adequate crystal growth for good resistance to polishing.

As part of a TRRL study of synthetic aggregates of controlled porosity, a refractory brick called mossite was prepared at various porosities. The PSV increased from 53 to 89, and porosity increased from 18 to 43 percent (8). Although excellent correlation was obtained between PSV and porosity, some of the higher PSV values were associated with weak material that had unacceptable aggregate abrasion values (AAVs). An acceptable AAV and PSV were obtained at a porosity of 43 percent and a firing temperature of 1300°C (2370°F) when firing and composition were carefully controlled.

Other Possible Tailor-Made Aggregates

The concept of materials specially tailored for use as skid-resistant synthetic aggregates has been studied in detail by Roy (4). These materials are typified by molochite, which is currently produced as a refractory by firing a China clay to give mullite crystals dispersed in an amorphous phase (44 percent amorphous and 56 percent mullite). Whereas molochite requires a high firing temperature and can be energy intensive to produce, compositions may be made more cost effective by

1. Varying the raw materials,
2. Neglecting the refractory requirement,
3. Fluxing to reduce firing temperature,
4. Bloating to give vesicularity and thereby improve polish resistance, and
5. Blending hard and soft components to give a multiphase aggregate, e. g., using a low-temperature flux to "cement" together a harder high-melting-temperature phase.

A more comprehensive approach to developing tailor-made synthetic aggregates would be to study the phase diagrams that represent compositional ranges within which the most plausible ceramic aggregates could be produced—that is, to include most of the abundant raw materials that would not be out of the cost range. Clearly, many ceramic systems could potentially be

used to produce skid-resistant aggregates. With proper research, it should be possible to identify systems that provide appropriate aggregate properties and are cost effective.

NON-TAILOR-MADE SYNTHETIC AGGREGATES

There are a number of potential non-tailor-made sources of skid-resistant aggregates. In some cases, these materials have been used as aggregates (e. g., blast-furnace slag or lightweight aggregate); in other cases, they are yet to be developed as aggregate sources (e. g., taconite tailings, steel slags, and pyrolysis slag). In view of the energy savings, environmental advantages, and potential skid resistance of many of these materials, they should be more fully evaluated as sources of skid-resistant aggregate.

Lightweight Aggregate from Shale and Clay

Lightweight aggregate includes expanded shale, slate, clay, and sintered fly ash. The majority of the lightweight aggregate used in the United States is made from crushed shale fired in rotary kilns. The firing is a sintering process accompanied by bloating (Table 1) in which the bloating is caused by the interlayer water released by the clay particles in the shale (9). If clay is the raw material, it must first be agglomerated by a pelletizing or extrusion process. Most of the lightweight aggregate used for skid-resistance purposes has been used in bituminous pavements in Texas and Louisiana (10). In some instances, it has been used as the sole aggregate; in others, it has been blended with natural aggregates.

The skid-resistant properties of lightweight aggregates are derived from their vesicular nature and their ability to maintain sharp, exposed edges (cell walls) as they wear. The vesicular nature provides the differential hardness and, as wear progresses, the newly exposed bubbles (cell walls) preclude polishing. Consequently, properly designed and constructed lightweight-aggregate surfaces can maintain a high level of skid resistance throughout their service life.

Lightweight aggregates are generally produced as structural aggregate, and the properties of the fired aggregate are adjusted to meet this use. Little research has been done on the properties that optimize both skid resistance and wear resistance. It is likely that the optimal properties of aggregate to be used as skid-resistant aggregate are different from those of aggregate that is to be used in structural concrete. Additional research is needed to better define the properties of lightweight aggregate (such as porosity, cell wall thickness, and bubble size) that optimize both wear resistance and skid resistance, particularly in northern climates.

In addition, field data are needed—particularly data that relate the characteristics of field performance, such as wear and polishability, to aggregate properties. Comparative skid data for lightweight-aggregate pavements are generally scattered in the literature along with data for other aggregates, and data on wear resistance are generally not available. The wear resistance of lightweight aggregate is questionable in northern climates and is perhaps best dealt with by using blended aggregate. Test procedures such as those used in Texas need to be verified for the wear and skid resistance of lightweight aggregates produced nationally.

Lightweight Aggregates Other than Shale and Clay

Lightweight aggregate can also be produced by sintering fly ash. The ash does not bloat during firing but remains at a nearly constant volume. Currently, only two plants produce sintered-fly-ash aggregate, and the production from these plants is consigned to lightweight block and concrete construction. Because of the carbon content of the ash, fly-ash aggregate is less energy intensive than expanded shale [1163 MJ/Mg (1 000 000 Btu/ton) compared with 4650-5814 MJ/Mg (4 000 000-5 000 000 Btu/ton)] and therefore potentially less expensive. Because it does not bloat or skin over during firing and because it has an open bubble structure, fly-ash lightweight aggregate is very porous and potentially very absorptive of asphalt. The wall structure is very thin; on the basis of a visual examination of the particles, it does not appear to be useful as a skid-resistant aggregate because of its potentially poor resistance to wear. Additional developmental work would be required to improve the pore structure to increase wear resistance and reduce absorptivity. This may be a worthwhile effort in view of the hardness of the high silica-alumina fly-ash compositions (7.5-8.0 Mohs).

Another technique for producing lightweight aggregate is the sintering of refuse from coal-preparation plants (11). Two plants currently produce sintered refuse: the By-Lite Corporation of Pennsylvania and a pilot plant at the University of Kentucky. One potential advantage in using this material is its fuel content. Although some supplemental fuel is required for ignition, it is less than 10-25 percent of the total energy required for sintering. Because of high sulfur content and related emissions problems during firing, not all refuse is equally suited for sintering. The bloating of pure refuse is not controllable (i. e., the process is self-determining); however, the addition of clay or sand may control bloating (11). This would also offer the opportunity to dope the refuse with a more skid-resistant additive such as calcined bauxite.

Sintered refuse is reported to be a skid-resistant and durable aggregate. Soundness values are high—40-50 percent—but this is said to be counteracted by asphalt absorbed into the aggregate pores. Wear data are not available, and the potential wear resistance is suspect. More attention should be given to this material, particularly if pore structure can be controlled or if other materials can be blended with the refuse to increase the wear resistance of the sintered product.

Blast-Furnace and Steel-Furnace Slags

Slags make up a large family of nonmetallic by-products from the refining of metals from metallic ores. Blast-furnace slag is the most widely used slag in pavement construction, especially in surfacing mixtures. The demand for blast-furnace slag has resulted in full use of this material, mainly as a construction aggregate.

The composition of blast-furnace slag varies from furnace to furnace, depending on operating practice, raw materials, and the grade of steel being produced (12). The parameters that optimize the production of steel also optimize the properties of the slag for paving purposes. Average chemical composition has been given as 36 percent SiO₂, 12 percent Al₂O₃, 42 percent CaCO₃, 6 percent MgO, and lesser amounts of FeO, MnO, and S. The various crystalline phases are bound together with a softer glassy matrix. Blast-furnace slags are alkaline in nature.

Mineralogical composition is controlled by rate of

cooling and chemical composition; a more rapid rate of cooling and a higher silica content give a finer crystal size. Water-quenched or granulated slag is amorphous and is preferred in cement manufacture. Air-cooled slag is predominantly crystalline and is preferred for use as an aggregate in portland cement and construction of bituminous concrete pavement. Blast-furnace slag may also be expanded by using steam or a jet of water. Expanded slag is used principally in block construction and lightweight concrete.

There are few references in the literature to the mechanism by which slags develop their skid-resistant properties. Not all blast-furnace slags have good resistance to polishing. Undoubtedly, the vesicular and hard nature of the slags plays a major role, but the presence of differential wear is less firmly established.

A British study examined the mineralogical and physiographic properties that influence the PSV of blast-furnace slag (13). The study found that the slag was heterogeneous and that different crystalline compounds predominated in the slags that had different PSVs. Increasing both porosity and crystalline size improved the PSV of the slag, but large porosities gave poor resistance to wear. Increased crystalline size did not alter wear resistance. Typical data for slags and processed slags are given in Table 3 (14).

Steel slag is quite different (14). To its advantage, it is a dense, hard, polycrystalline material. It must be aged in stockpiles, however, to allow the hydration of the calcium and magnesium oxides if it is to be used in a confined situation or in an alkaline environment. To stabilize this potential expansion, steel slags can also be treated by using spent pickling liquors. Steel slag contains varying quantities of iron; recycling it to a blast furnace for additional iron recovery will further affect its variability.

The properties and mineralogy of steel slag are quite varied because of plant-to-plant and within-plant variation. This variation can become an important factor in the use of the material, affecting its expansion potential, mixture design, and skid-resistance potential. Steel slags have reportedly provided surfaces with adequate skid resistance and should be more fully evaluated. But, as the range of PSV values in Table 3 shows, not all steel slags give good resistance to polishing.

Industrial and Mining Wastes

Various waste materials have been proposed as alternative sources of aggregate (15). Most of the feasible ones are either the result of the crushing of rock, mine tailings, refining, or incineration. Examples are metallurgical slags (14), incinerator refuse (16), smelter waste (17), and spent oil shale (18). Laboratory data for some miscellaneous materials are given in Table 3. Many of the industrial slags are glassy whereas others are at least partially crystalline. The as-processed glassy slags, in spite of their hardness, are poor candidates for skid-resistant materials because they lack differential hardness and microtexture. Increased vesicularity through controlled processing may improve their microtexture and provide adequate skid resistance. Many are relatively small in size as a result of being quenched in water [minus 9.5- to 2.36-mm (³/₈-in to no. 8) sieve]. They often suffer in toughness because they are glassy and also because they are homogeneous. In the pavement they tend to produce cleavage planes parallel to the pavement surface so that texture is lost with wear. The result is a flat, glassy road surface.

The hard, glassy slags might serve as excellent aggregates if they could be processed to produce crystal-

line rather than glassy particles. Both heat treatment and fluxing would probably be required. Additional research is needed on the processing of glassy industrial slags to improve their properties if they are to become strong candidates for skid-resistant aggregates. Bloating procedures and thermal processing with fluxes to give compositions that crystallize more readily and/or result in vesicularity would appear to be viable research approaches. The limited availability of these slags may preclude any significant expenditure of research and development funding.

A method of producing a "bubble aggregate" has been reported (19). Briefly, organic waste or nonsintering mineral waste is pelletized and then coated with a clay or some other flux. The result is an expanded bubble that has many of the properties of an ordinary lightweight aggregate. In another approach, a composite aggregate has been made on a laboratory scale by fusing a siliceous mining waste with a glass that has a lower melting temperature. This multiphase aggregate gave good skid resistance after being polished on a circular test track (20).

The coal-burning power plant is a major source of industrial waste (21). Boiler slag is produced by water quenching molten slag drawn from a slag tap furnace. The slag is one size—typically 1.18- to 2.36-mm (no. 16-no. 8) mesh—angular, glassy, and lacking in microtexture. In this regard, it is similar to many other glassy industrial slags that lack microtexture and differential hardness. Its sharp corners fracture under traffic and offer poor resistance to polishing. Boiler slag is no longer in widespread use as a skid-resistant aggregate, and there are varied reports as to its effectiveness. Boiler slag has been used in sand mixes, slurry seals, and surface treatments, but little use is reported in the literature.

Bottom ash can be produced in various forms, as a fine sand or as agglomerated or poorly sintered fly-ash particles, and it may even contain some slaglike particles. Most bottom ashes range in size from 0.075-mm mesh to 3 cm (no. 200 mesh to 1.2 in). Bottom ash has not been used to any extent as a surfacing aggregate except in West Virginia. Although it does have excellent differential hardness and microtexture because of its vesicularity, bottom ash does not generally have the toughness required of a surfacing aggregate. When it is used as the sole aggregate, it breaks down under the action of traffic to form a very fine-textured surface that is high in microtexture but lacks macrotexture. Bottom ash may have potential as the fine aggregate in surfacing mixtures if it is crushed before use to control breakdown or if it is blended with conventional aggregates (21).

A host of other mining wastes are potential candidates as skid-resistant aggregates (15). Many of the mining wastes are merely waste rock and can be treated as conventional aggregates. In other instances—uranium tailings for example—there are serious environmental problems to be considered.

AGGREGATE BENEFICIATION FOR SKID RESISTANCE

Aggregates that require beneficiation can be divided into two groups: those that possess adequate durability but inadequate skid resistance and, conversely, those that possess acceptable polishing characteristics but inadequate durability. Beneficiation should therefore be approached from two viewpoints: (a) improving durability for resistance to wear and abrasion and (b) improving polish resistance. Both approaches may be valid for upgrading otherwise marginal or unacceptable aggregates.

Ceramic Processing

Heat treatment is a potential method for beneficiating marginal materials; however, the composition of the material must be such that crystal growth or a phase change occurs during heating (e.g., Synopal, bauxite, slag ceram). Glassy industrial slags that can be worked in the molten state can be improved by the injection of steam or air to create vesicularity. Further improvement can also be achieved by adding fluxing agents and controlling the rate of cooling to improve crystallinity and control grain size. The molten slag can be modified further by doping it with harder mineral particles to provide differential hardness. Examples of ceramic beneficiation given in Table 3 are the calcining of flint (a PSV of 53 versus a PSV of 35 for crushed flint) and the heat treatment of blast-furnace slag (a PSV of 62 and 69 versus a PSV of 52). Other examples include sintered silt and bauxite (a PSV from 68 to 73), fly ash and magnesia (PSV of 67) and rock fines (PSV of 72) (14). In each case, the beneficiation requires calcining or sintering at temperatures of 1100°C-1600°C (2000°F-3000°F) and an energy consumption of 4650-9302 MJ/Mg (4 000 000-8 000 000 Btu/ton).

Coatings and Penetrants

Another approach to beneficiation for improving the skid resistance of a marginal aggregate is the addition of a hard coating to a softer aggregate. For example, alumina might be added to a soft limestone. To be successful, the added material would probably have to be crystalline; a low-temperature, glassy coating would be too soft. More exotic procedures, such as flame spraying, do not seem to be economically feasible. Thick coatings or, more correctly, composite aggregates appear promising from a cost standpoint. Denis and Massieu (22) have prepared a polymer-sand aggregate from various sand-sized and smaller materials by using only 10 percent epoxy.

The use of coatings and penetrants also appears promising for improving aggregates that are deficient in durability or exhibit excessive asphalt absorption. Several organic coatings have been evaluated by using absorptive limestone (23). Both water absorption and asphalt content were reduced. The cost-effectiveness of the combinations reported might be questioned, but there may well be instances in which polymer impregnation would substantially improve durability. Gneiss, for example, which is resistant to polishing, might show adequate durability if it were impregnated with polymethylmethacrylate. Research is currently under way at various agencies to upgrade aggregates that are marginal in both skid resistance and durability. This research is directed at coatings and penetrants that can be used to improve freeze-thaw resistance, the effect of water (stripping), mechanical degradation, and resistance to polishing and wear. A disadvantage of organic coatings is that they are expensive and require considerable handling (24).

SUMMARY AND CONCLUSIONS

Skid resistance is controlled by both the microtexture and the macrotexture of the pavement surface. Macrotexture is controlled principally by the gradation of the aggregate, whereas microtexture is controlled by the properties of the individual aggregate particles. The combined effect of microtexture and macrotexture in determining SN_v at various speeds has been defined in previous research and can be used to estimate the

potential skid resistance of new or untried aggregates before their design or manufacture.

Skid-resistant aggregates must also be resistant to wear and polishing. Differential hardness in the aggregate particles can provide resistance to polishing, but the aggregate must be sufficiently tough and consolidated so that it does not exhibit excessive wear. The designer or engineer is limited with regard to resistance to wear and polishing in that neither test methods nor specification criteria are available that can be universally used to control the wear and polishing potential of different aggregates.

Aggregates provide skid resistance and resistance to wear and polishing by means of a variety of mechanisms. Simply producing a synthetic aggregate that is hard and dense will not result in a skid-resistant aggregate, as the marginal performance of Synopal shows. The same ceramic process may be used to produce aggregates of different classes. For example, it is possible to successfully use sintering (a) to consolidate a hard material, as long as sufficient porosity remains for resistance to polishing, and (b) to produce dispersions of hard particles in a soft matrix so that resistance to polishing is provided by differential wear.

The following conclusions can be stated in relation to the design, manufacture, and specification of skid-resistant aggregates:

1. The processes required to produce or modify aggregates for skid-resistance applications are energy and capital intensive, and these factors must be considered in future aggregate development.
2. Different classes of synthetic aggregate achieve their macrotecture and their resistance to wear and polishing by different mechanisms, and this should be recognized during their development and in their specifications.
3. Materials that are hard and dense are not necessarily good aggregates; differential hardness is required to resist polishing.
4. Industrial waste materials are potential sources of raw materials for aggregate production, but they must generally be reprocessed, especially if they are produced as glassy slags.
5. Sintered alumina-bearing clays or low-grade calcined bauxite, which are potentially excellent aggregates and are amenable to current manufacturing equipment, should be investigated further.
6. A test method is needed for the prediction of wear, particularly for vesicular and friable materials.
7. Required levels of microtexture and macrotecture need to be defined for the various classes of synthetic aggregates; i. e., the a and b parameters in Equation 1 need to be defined for various classes and mixtures of aggregate.
8. Aggregates of controlled vesicularity—intermediate between normal and lightweight aggregate—should be considered since they may offer improved resistance to wear and polishing.
9. Exotic processing techniques tend to be more energy intensive than simpler processes such as sintering; they may also be difficult to adapt to the manufacture of aggregate.
10. Production of aggregate from waste materials should be considered part of the primary process rather than an afterthought of the reclamation process.
11. Composite aggregates, such as low-temperature-melting clays doped with hard fines, are promising, particularly if they can be fired in existing kilns.

ACKNOWLEDGMENT

This paper is based on research sponsored by the Federal Highway Administration, the Pennsylvania Department of Transportation, and other agencies. The work was conducted at the Pennsylvania Transportation Institute, Pennsylvania State University. Many valuable suggestions were contributed during the conduct of the research by J. M. Rice of the Office of Research, Federal Highway Administration, U.S. Department of Transportation, and staff members of the Pennsylvania Transportation Institute. The contents of this paper reflect our views, and we are responsible for the facts and accuracy of the data presented. The contents do not necessarily reflect the official views or policies of the Federal Highway Administration. This paper does not constitute a standard, specification, or regulation.

REFERENCES

1. H. W. Kummer and W. E. Meyer. Tentative Skid Resistance Requirements for Main Rural Highways. NCHRP, Rept. 37, 1967.
2. M. C. Leu and J. J. Henry. Prediction of Skid Resistance as a Function of Speed from Pavement Texture Measurements. TRB, Transportation Research Record 666, 1978, pp. 7-11.
3. J. G. James. Calcined Bauxite and Other Artificial Polish-Resistant Roadstones. British Road Research Laboratory, Crowthorne, Berkshire, England, Rept. LR 84, 1968.
4. D. M. Roy. Advanced Technology Materials Applied to Guideways, Highways, and Airport Runways. Program of University Research, U.S. Department of Transportation, Project DOT-05-40009, Feb. 1976.
5. D. J. Whittemore. Energy Consumption in Ceramic Processes. Ceramic Bulletin, Vol. 53, No. 5, 1974, pp. 456-457.
6. L. W. Tubey and J. R. Hosking. Synthetic Aggregates of High Resistance to Polishing: Part 2—Corundum-High Aggregates. Transport and Road Research Laboratory, Crowthorne, Berkshire, England, Rept. LR 467, 1974.
7. C. R. Marek and others. Promising Replacements for Conventional Aggregates for Highway Use. NCHRP, Rept. 135, 1972.
8. J. K. Hosking. Synthetic Aggregates of High Resistance to Polishing: Part 3—Porous Aggregates. Transport and Road Research Laboratory, Crowthorne, Berkshire, England, Rept. LR 655, 1974.
9. B. M. Gallaway and W. J. Harper. A Manual on the Use of Lightweight Aggregate in Flexible Pavement Systems. Expanded Shale, Clay, and Slate Institute, Washington, DC, 1969.
10. Open-Graded Friction Courses for Highways. NCHRP, Synthesis of Highway Practice 49, 1978.
11. J. G. Rose and D. S. Decker. Sintered Coal Refuse Lightweight Aggregate for High-Friction Bituminous Surface Courses. Paper presented at Annual Meeting, AAPT, San Antonio, TX, Feb. 1977.
12. A. R. Lee. Blast Furnace and Steel Slag: Production, Properties and Uses. Halsted Press, New York, 1975.
13. W. H. Gutt and B. Hinkins. Improvement of the Polished Stone Value of Slag Roadstone by Heat Treatment. Journal of Institute of Highway Engineers, Vol. 4, No. 4, 1972.
14. S. H. Dahir and others; Pennsylvania Transportation Institute. Alternatives for Optimization of Aggregate and Pavement Properties Related to

- Friction and Wear Resistance. Federal Highway Administration, U.S. Department of Transportation, 1978.
15. R. J. Collins and R. H. Miller. Availability of Mining Wastes and Their Potential for Use as Highway Material: Volume 1—Classification and Technical and Environmental Analysis. Federal Highway Administration, U.S. Department of Transportation, Rept. FHWA-RD-76-106, May 1976.
 16. D. Pindzola and R. C. Chou. Synthetic Aggregate from Incinerator Residue by a Continuous Fusion Process. Federal Highway Administration, U.S. Department of Transportation, Rept. FHWA-RD-74-23, April 1974.
 17. M. L. Hughes and T. A. Haliburton. Use of Zinc Smelter Waste as Highway Construction Material. HRB, Highway Research Record 430, 1973, pp. 16-25.
 18. G. J. Gromko. A Preliminary Investigation of the Feasibility of Spent Oil Shale as Road Construction Material. TRB, Transportation Research Record 549, 1975, pp. 47-54.
 19. P. C. Aitcin and C. Poulin. Bubble Aggregates. Proc., 4th Mineral Waste Symposium, U.S. Bureau of Mines and Illinois Institute of Technology, Chicago, 1974.
 20. D. E. Ramsay and R. F. Davis. Fabrication of Ceramic Articles from Mining Waste Materials. Ceramic Bulletin, Vol. 54, No. 3, 1975.
 21. D. A. Anderson, M. Usman, and L. K. Moulton. Use of Power Plant Aggregate in Bituminous Construction. TRB, Transportation Research Record 595, 1976, pp. 18-24.
 22. A. Denis and E. Massieu. Sand Resin Mortars for Road Surfacing. Bulletin de Liaison des Laboratoires des Ponts et Chaussées, Supplement 80, Nov.-Dec. 1975.
 23. R. N. Dutt and D. Lee. Upgrading Absorptive Aggregates by Chemical Treatments. HRB, Highway Research Record 353, 1971, pp. 43-46.
 24. P. D. Cady and others; Pennsylvania Transportation Institute. Upgrading of Poor or Marginal Aggregates for PCC and Bituminous Pavements. NCHRP Project 4-12, draft final rept., 1978.

Publication of this paper sponsored by Committee on Characteristics of Bituminous-Aggregate Combinations to Meet Surface Requirements and Committee on Mineral Aggregates.